12-1997

Biodegradable staple fiber nonwovens calendered with the assistance of an aqueous solvent : $btheir fabrication, properties, and structural characteristics

Greta Marie Heismeyer
University of Tennessee

To the Graduate Council:

I am submitting herewith a thesis written by Greta Marie Heismeyer entitled "Biodegradable staple fiber nonwovens calendered with the assistance of an aqueous solvent : $btheir fabrication, properties, and structural characteristics." I have examined the final electronic copy of this thesis for form and content and recommend that it be accepted in partial fulfillment of the requirements for the degree of Master of Science, with a major in Human Ecology.

Kermit E. Duckett, Major Professor

We have read this thesis and recommend its acceptance:

Accepted for the Council:
Carolyn R. Hodges

Vice Provost and Dean of the Graduate School

(Original signatures are on file with official student records.)

To the Graduate Council:

I am submitting herewith a thesis written by Greta Marie Heismeyer entitled "Biodegradable Staple Fiber Nonwovens Calendered with the Assistance of an Aqueous Solvent: Their Fabrication, Properties, and Structural Characteristics." I have examined the final copy of this thesis for form and content and recommend that it be accepted in partial fulfillment of the requirements for the degree of Master of Science, with a major in Human Ecology.

Kermit E. Duckett

Kermit E. Duckett, Major Professor

We have read this thesis
and recommend its acceptance:

Accepted for the Council:

Associate Vice Chancellor and
Dean of The Graduate School

BIODEGRADABLE STAPLE FIBER NONWOVENS CALENDERED WITH THE ASSISTANCE OF AN AQUEOUS SOLVENT: THEIR FABRICATION, PROPERTIES, AND STRUCTURAL CHARACTERISTICS

A Thesis Presented for the Master of Science Degree
The University of Tennessee, Knoxville

Greta Marie Heismeyer
December 1997

DEDICATION

This thesis is dedicated to my younger siblings, Eric Jon Heismeyer and Amy Lynn Heismeyer; the former for his courage in overcoming two life-threatening illnesses, and the latter for her open-mindedness and emotional support.

ACKNOWLEDGEMENTS

The completion of this thesis marks the end of another of life's little chapters, one that I should like to largely forget, for it has been a substantial assault to my pocketbook and to my self-esteem. This chapter was excessively long, and nothing short of miserable; however, two very important conclusions came about as a result. The first being that common sense will always continue to preclude the value of an advanced degree; and, secondly, common sense still continues to elude some of the most highly educated professionals in our society. More importantly, these last four years have been a time of self-revelation and metamorphosis. The moral ambiguity of academia was too much of an insult to my often naive notions about the goodness of people. Furthermore, any preconceived notions and ideals I held about the elevation of intellectual capacities achieved with an advanced degree are now largely cerebral residue. Despite these misgivings, I am almost grateful for their occurrence, because they saved me from a wretched life as a laboratory rat and allowed me to acknowledge my gratefulness for my Midwest agricultural experiences, arriving at the realization that one can remove the girl from the farm, but the farm can never be taken from the girl. This realization has allowed me to capitalize on interests and experiences that I might never have cared to acknowledge prior to this experience.

There were many editors and contributing authors to this chapter of my life. I would like to thank my Editor-In-Chief, Dr. Kermit E. Duckett, and his assistants, Dr. Gajanan S. Bhat and Dr. Larry C. Wadsworth, for their guidance and valuable input in

the completion of this research. I am most grateful to Dr. Duckett for taking me on as his student in the midst of my studies. I am greatly appreciative for the technical advice and support offered me by Richard Meade, Larry Spires and Scott Strawn in the fabrication of these fabrics. I am most grateful to Dr. Charles Hassenboehler, mentor and friend, whose coined phrase "widespread interaction" has forever changed my outlook on my life. I am also most appreciative of the Midwest work ethic, unrelenting perfectionism, and stamina instilled by my parents, Willard Waldo and Gail Marie Heismeyer, that permitted me to overcome the obstacles placed before me during the completion of my studies. The person who has inspired me the most, and has fostered my pursuit of knowledge throughout my life has been my uncle, Dr. William Patrick Rahilly, whose brilliance and moral integrity in theoretical physics, in my opinion, remains unsurpassed. I am most grateful for his unmatched emotional and moral support throughout some most troubling times. I would like to thank my employer at the University of Tennessee College of Veterinary Medicine, Carloyn Wilson, whose kindness, sincerity, and respect have remained unmatched in my duration as an employee of this university. I am most grateful for the opportunity she provided me to work as a large animal caretaker because it provided reaffirmation that I could still function effectively in the real world, and provided a significant boost to a badly bruised self-esteem. I am most appreciative of Barry Gordon, DVM, who has reassured me that it is not to late to have a rewarding career as a large animal veterinarian, and for the abundant experience and knowledge I have already gained from him - for every day that I made calls with him gave me the stamina to finish this work and forever be done with textiles.

Lastly, the two most important contributors to this chapter and every subsequent chapter in my life, my canine companion, Krunches, and my significant other, David Scott Krafsur, deserve unequaled gratefulness. I am most thankful for David's incredible faith, understanding, and patience during the period of writing this document, which just happened to be during the early stages of our courtship and later engagement. To be continued in another chapter .

ABSTRACT

Biodegradable cotton/cellulose acetate thermal calendered webs were consolidated with the assistance of an aqueous acetone solvent. Existing patent literature cited lower acetate binder softening temperatures could be achieved because of the plasticization, hence microstructural changes brought on by the localized interruption of hydrogen bonds between adjacent molecular chains in the acetate fibers associated with acetone treatment. Acetate fibers softened at temperatures far below their typical 230°C melting temperature, fiber coalescence could be achieved between 177 and 191°C. Microstructural responses to solvent modification include solvent induced crystallization, surface and internal cavitation and shrinkage, that ultimately cause suppression of the fiber second order glass transition and softening temperatures.

Two different blend systems were treated with 20 and 40% acetone and consolidated at 150, 170 and 190°C using thermal calendering rolls. Fabric mechanical integrity, web dimensional stability and fabric hand were evaluated, the performance of the different fabric combinations was compared statistically using the General Linear Model.

The control fabrics that were not subjected to solvent modification had no mechanical integrity, regardless of consolidation temperature, illustrating the ability of the solvent to lower the softening temperature of the acetate binder. Statistically speaking, those fabrics treated with the higher acetone concentration were significantly stronger than those treated with less acetone, however from a practical standpoint it was

difficult to embrace the additional benefits associated with more acetone because of its environmental toxicity. The mechanical integrity of those webs consolidated at the lowest consolidation temperature, 150°C was very negligible compared to those consolidated at the higher temperatures. This behavior suggests that the solvent did not suppress the acetate binder softening temperature in the vicinity of the 150°C consolidation temperature. Those webs that contained less cotton and more acetate binder exhibited superior mechanical and hand properties compared to those webs comprised of more cotton and less acetate binder. Because this study sought to select the process variables that would optimize web performance and preserve commercial acceptability, the researcher concluded that 60/40 webs treated with 20% acetone and consolidated at 190°C would achieve the ultimate mechanical and hand properties desired.

TABLE OF CONTENTS

TABLE OF CONTENTS (CONT.)

CHAPTER **PAGE**

TABLE OF CONTENTS (CONT.)

CHAPTER **PAGE**

LIST OF TABLES

TABLE NO. **PAGE**

LIST OF TABLES (CONT.)

TABLE NO. **PAGE**

LIST OF FIGURES

LIST OF FIGURES (CONT.)

LIST OF FIGURES (CONT.)

1. INTRODUCTION

Nonwovens usage spans the continuum of ordinary, everyday-use products such as disposable diapers, feminine sanitary napkins and premoistened wipes to high performance applications including surgical face masks and gowns, filtration media and automotive airbags. These products are limited-use, disposables that generate excessive non-biodegradable waste because the fibrous components are largely synthetic [1,2].

The nonwovens industry can expect to grow 8 to 10% annually in the coming years [1]. The largest end-use application for nonwoven fabrics is the absorbent personal care products market. In 1994, this market accounted for 26% (by weight) of the worldwide nonwovens consumption [1]. Disposable baby diapers are very popular absorbent products that have replaced their cloth counterparts because of their convenience, reflecting the changing lifestyles of modern parents [2]. Parental acceptability of disposable baby diapers is reflected by their growing contribution to municipal solid waste in recent decades. In 1960, disposable baby diaper presence in municipal solid waste was negligible; however, by 1993 disposable baby diapers contributed 2,700,000 tons of solid waste to our country's municipal solid waste management programs [3]. Disposable baby diapers represent approximately 1.3% of total U.S. municipal solid waste [3].

While this figure (1.3%) may seem minimal relative to the municipal solid waste generated by paper, packaging, glass soft drink bottles and food storage containers, public concern for the burden exerted by disposable baby diapers on the nation's landfill space would prove otherwise [2,3]. This is a legitimate concern given that the most

common waste management program for soiled disposable baby diapers is landfilling [2]. The landfill volume consumed by disposable baby diapers is 1.1% of which 0.5% is the actual diaper materials [3].

Although 90% of a soiled baby diaper is biodegradable because its major constituents are the degradable fluff pulp absorbent core and the urine/feces, the polymeric components are the solid waste culprits . The polypropylene or polyester coversheet, the polyethylene backsheet intended to act as a moisture barrier, and the elastic, glues and tapes providing fit and shape are essentially non-biodegradable (**Table 1**) .

TABLE 1

COMPOSITION OF A TYPICAL BABY DIAPER

COMPONENTS	GRAM/DIAPER	% OF DIAPER
PULP		
(Core, Tissues)	39	72
POLYMERS		
(BS, SA, CS)	14	26
OTHERS		
(Glue, Elastics, Tapes)	1	2
TOTAL DRY WEIGHT	54	100
[1]**BS** = Backsheet	[2]**SA** = Superabsorber	[3] **CS** = Coversheet

Furthermore, the landfill entombment of solid wastes intended to minimize harmful leachates and biogas generation creates unfavorable conditions for biodegradation of those diaper materials that are degradable because of denied air and water access [2].

Alternative methods of soiled baby diaper waste management include incineration and composting. Composting reduces the landfill contribution of soiled disposable baby diapers while producing a safe, useful endproduct that finds application as a soil additive or organic fertilizer in the agricultural and horticultural industries [2]. Procter and Gamble, a major player in the disposable baby diaper sector has sponsored diaper compostability studies in the U.S. and Europe using rotating drum and box technologies [2]. Both technologies create a biocell reactor with stringent temperature, air and moisture controls to produce the ideal environment for organic waste transformation and sanitization through temperatures of 65-70°C that kill the infectious organisms and provide a safe endproduct [2]. Included in this transformation are the soiled diaper urine/feces and the absorbent core. The nuisance diaper coversheet and backsheet remain and are screened out from the compost [2]. The elimination of these remaining nuisance materials requires a working relationship between the key players in the personal care absorbents market and the nonwoven roll goods suppliers to develop and introduce a disposable baby diaper that is entirely biodegradable.

Cotton fibers impart softness, absorbency, breathability and biodegradability to personal care products. A major endorsement for cotton fiber use in personal care products has been the recent introduction of the Tampax Naturals tampon, the first 100% cotton tampon made with U.S. cotton [4]. Nonwoven roll goods producers, however,

have shown a reluctance to introduce cotton-based nonwoven fabrics because of fiber cost, variability and bleaching limitations [4,5,6].

Insect manifestations in China, India and Pakistan and increased demand for U.S. cotton on the domestic and international markets created price pressures that caused prices to soar to levels not seen since the post-Civil War era, escalating to $1.00/lb in 1995 [4,5]. Roll goods producers responded by overlooking the inclusion of cotton in their fabrics or reducing their 70% cotton/30% synthetic to 60% cotton/40% synthetic blends [4,5]. Recent price stabilization to approximately 75 cents/lb is creating hope for renewed interest for the inclusion of bleached cotton in nonwoven fabrics [4,5,7]. Furthermore, long-term budget plans and price locking using the futures market can be employed to overcome anticipated price variations [5].

Producers of roll goods have also shown reluctance to elect to use cotton in their fabrics due to perceived variations in quality and the misconception that cotton fibers can not run on nonwovens machinery [4,5]. The implementation of a USDA cotton bale classing system, improved bleaching techniques, and lubrication and antistat finishes are all intended to reduce variation and improve cotton processability. Luxicot Ultraclean (Edward Hall, U.K.), High Q and Ultrawhite (Barnhardt, Charlotte, NC) are commercially-available cotton fibers that are more open and cleaner than standard bleached cotton, making the production of uniform weight, aesthetically-pleasing, lightweight cotton-based nonwoven fabrics a reality [4,5].

While 90% of domestic cotton bleaching is accomplished using the batch keir bleaching process, resultant fibers have been labeled unacceptable for nonwovens fabrication [6]. However, advances in mechanical cleaning and high-speed (up to 500

lbs./hour) course wire carding of the bleached fibers prior to baling reduce nep content, improve card web appearance and make kier bleached cotton fibers more acceptable for nonwovens fabrication [6]. Continuous bleaching such as the proprietary process introduced by Cotton Incorporated produces very high quality open, bleached fibers that will greatly improve the utilization of cotton fibers in the fabrication of nonwovens. High speed output is achieved with the use of a "Cottonmaster" cleaning card that can produce 840 lbs. of mechanically cleaned fiber per hour. Scouring and bleaching efficiency are improved by the use of a patented steam purge system that permits more uniform application of the scouring and bleaching agents. Previous impregnated batts exhibited wet out of the top and bottom surfaces while the batt core was dry, air-saturated fibers. Steam applied to the top batt surface and a slight vacuum on the batt underside purge the air from the batt so when the dry batt is immersed in the cold scouring solution, the steam condensation permits the scouring solution to penetrate the batt without air interference.

Bleaching is accomplished using the same purge system where steam application purges the residual rinse, permitting uniform penetration of the hydrogen peroxide (H_2O_2) bleaching agent. Following this wet-on-wet impregnation, a second steaming elevates the temperature and thereby increases the reaction rate so that completion of bleaching can be accomplished in 15 minutes, compared to 30 minutes required for completion of the scouring process. Bleaching removes the natural finish so that resultant cotton fibers become highly texturized, creating fiber friction. To make bleached cotton fibers suitable for future processing operations, a lubricant and antistat agent are required. Historically, stearic and oleic acid soaps were used but the chemical of choice for both continuous and

kier operations is butoxyethyl stearate (BES) because of its environmental soundness and inability to inhibit fiber absorption capabilities [6].

The alleviation of price pressure, quality variations and bleaching problems should assist in the decision to utilize more cotton fibers in nonwovens fabrication, especially in the development of biodegradable disposable baby diapers. Cotton fiber brittleness with temperature elevations imposes limitations on the possibilities for a 100% cotton coverstock fabric for disposable baby diapers given the most prevalent bonding technique used in the coverstock industry is thermal bonding. Because cotton is a nonthermoplastic, it requires the addition of a low melting point thermoplastic binder fiber that permits lower temperature bonding by the fusion of the binder fibers with the adjacent cotton fibers, eliminating harsh fabric handle associated with higher bonding temperatures. Polyproyplene and cellulose acetate are binder fibers with melting temperatures of 165°C and 230°C, respectively that make the possibility of soft, supple cotton-based nonwoven fabrics a reality [8].

Biodegradation evaluations of cotton-based nonwovens bonded with the assistance of polypropylene or cellulose acetate binder fibers have been made using evaluative measures such as fungal growth rating, tensile strength loss, scanning electron microscopy and carbon dioxide evolution.

The presence of cellulose is necessary to propagate fungal growth in cotton-based nonwoven fabrics; however, regardless of cotton percentages in the fiber blend, no appreciable differences in fungal growth were noted for various cotton/polypropylene blends after 14 days. Increasing polypropylene percentages preserved the tensile integrity of the fabrics, 100% polypropylene thermal calendered fabrics showed no

evidence of fungal growth or strength loss after 98 days of microbial exposure. SEM analysis of 70/30 cotton/polypropylene fabrics following 56-day exposure showed that cotton fiber disappearance caused cracking of remaining thermoplastic polypropylene fibers because the bound cotton fibers were no longer there to support the spaces within. The 70/30 blend exhibited negligible strength loss after 7 days, however a significant transition occurred in the 80/20 cotton/polypropylene blend. After 7-day microbial exposure, the increased cotton content contributed to a 46% loss in breaking strength [9,10].

Because cellulose acetate fibers are suitable binder fibers, the biodegradability of cotton/cellulose acetate fiber blends has been studied at the University of Tennessee using strength loss and carbon dioxide (CO_2) evolution measurements. Unlike 100% polypropylene fabrics evaluated in other studies, 100% acetate fabrics exhibited a 27% loss in peak breaking load following twelve-week deposition in a soil bed. Microbial attack of cellulose acetate fibers was also confirmed by the evolution of CO_2. The CO_2 evolution of 100% cotton, 100% cellulose acetate and various blends thereof confirmed the synergistic activity between the cellulase and esterase enzymes responsible for the catalyzed microbial degradation of cotton and cellulose acetate fibers. Total CO_2 evolution and the rate of degradation was greater for the blended fibers than that of the 100% cotton fibers alone. Total CO_2 evolution over 45-days for 100% cellulose acetate fibers was 9.18 and 27.0% for 100% cotton fibers. However, 50/50 cotton/cellulose acetate fiber blends showed 46.5% CO_2 evolution for the same time frame, supporting the proposed synergistic activities of the enzymatic catalysts. The CO_2 evolution was 55.5, 41.7 and 30.5%, respectively for the 75/25, 50/50 and 25/75 acetate blends. The

increased cotton content would imply the favorable inducement of cellulase over esterase enzymes [11].

The potential for environmentally sound cotton-based nonwoven fabrics precipitated research into the use of plasticizers to lower the softening temperature of the cellulose acetate binder fibers, thereby lowering thermal bonding temperatures. Plasticizing agents readily penetrate amorphic proximities, spreading apart the neighboring polymeric chains, thereby increasing chain flexibility. Consequently, the fiber glass transition temperature is lowered [8]. Improved binder flow enhances adhesion between the acetate binder and cotton base fibers. The improved bonding should be reflected by enhanced tensile strengths. Cellulose acetate is soluble in common solvents such as acetone and other low boiling point ketones, and methylene chloride.

Acetone, a common solvent for cellulose acetate that readily vaporizes at room temperature was selected to modify the cellulose acetate fibers. Acetone was poured into a container containing perforated racks that supported the 75/25 cotton/cellulose acetate carded webs, prohibiting liquid-fiber contact. The container was made air tight, creating a saturated acetone vapor atmosphere. The carded webs were exposed for various specified saturation times and then removed for immediate thermal calendaring at temperatures of 100, 170, and 180°C. Solvent modification indeed enhanced fabric tensile properties, as 30-minute acetone vapor exposure permits the vapor to penetrate the acetate amorphic regions and ultimately lower the fiber softening temperature. Tensile strengths exceeding 10 mN/tex for fabrics bonded at much lower bonding temperatures (170,180°C) than untreated fabrics bonded at 230°C with similar strengths were realized [11].

Solvent modification of cellulose acetate fibers can also be achieved using an aqueous solution. Enhanced tensile properties were the outcome of a 40% aqueous acetone solution application to blended fibrous webs before web consolidation using heated calender rolls operating at 170°C at 10 m/min. Strengths exceeding 10 mN/tex were reported, similar to strength values for previously reported vapor-modified fabrics [12].

Tensile performance relative to increased solvent concentration was evaluated on 60/40 cotton/cellulose acetate blends bonded at 170°C at a bonding speed of 10 m/min. Solvent concentrations exceeding 50% enhanced web consolidation, and tensile strengths greater than 18.0 mN/tex were observed (**Figure 1**). However, fabric hand was sacrificed with the enhanced tensile performance at higher solvent concentrations. The fabrics were stiff and boardy because the dissolved cellulose acetate was redeposited on the web surface before thermal web consolidation (**Figure 2**). A 40% solvent concentration appeared to be the upper limit for the realization of improved fabric tenacity [13]. A substantial improvement in fabric tenacity was achieved with as little as 10% aqueous acetone solution, with specific stress jumping from less than 1 mN/tex for untreated fabrics to almost 8 mN/tex [13]. Strength continued to improve when the solvent concentration increased from 20 to 50% (**Figure 1**) [13].

The remarkable strength and soft, supple hand that could be attained using this technology on thermal calendered staple fiber webs and their environmental friendliness were the precipitate for an intense processing parameter optimization study. Nip-line pressure and contact time were held constant while blend ratio, basis weight, solvent concentration and bonding temperature were manipulated. Solvent concentrations (20

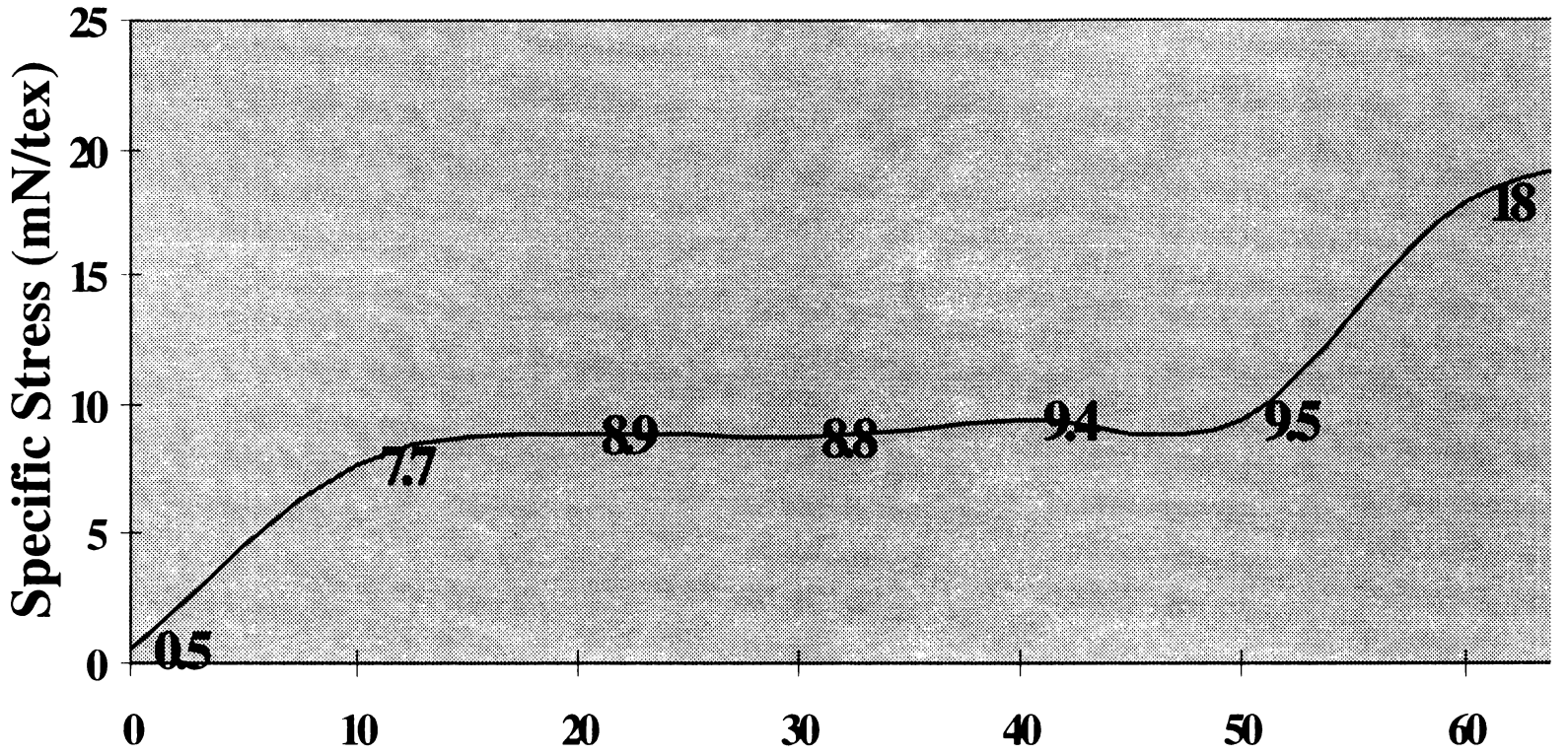

Figure 1: Solvent Concentration Effects on Fabric Specific Stress for 60/40 Blend Systems Consolidated at 170 C

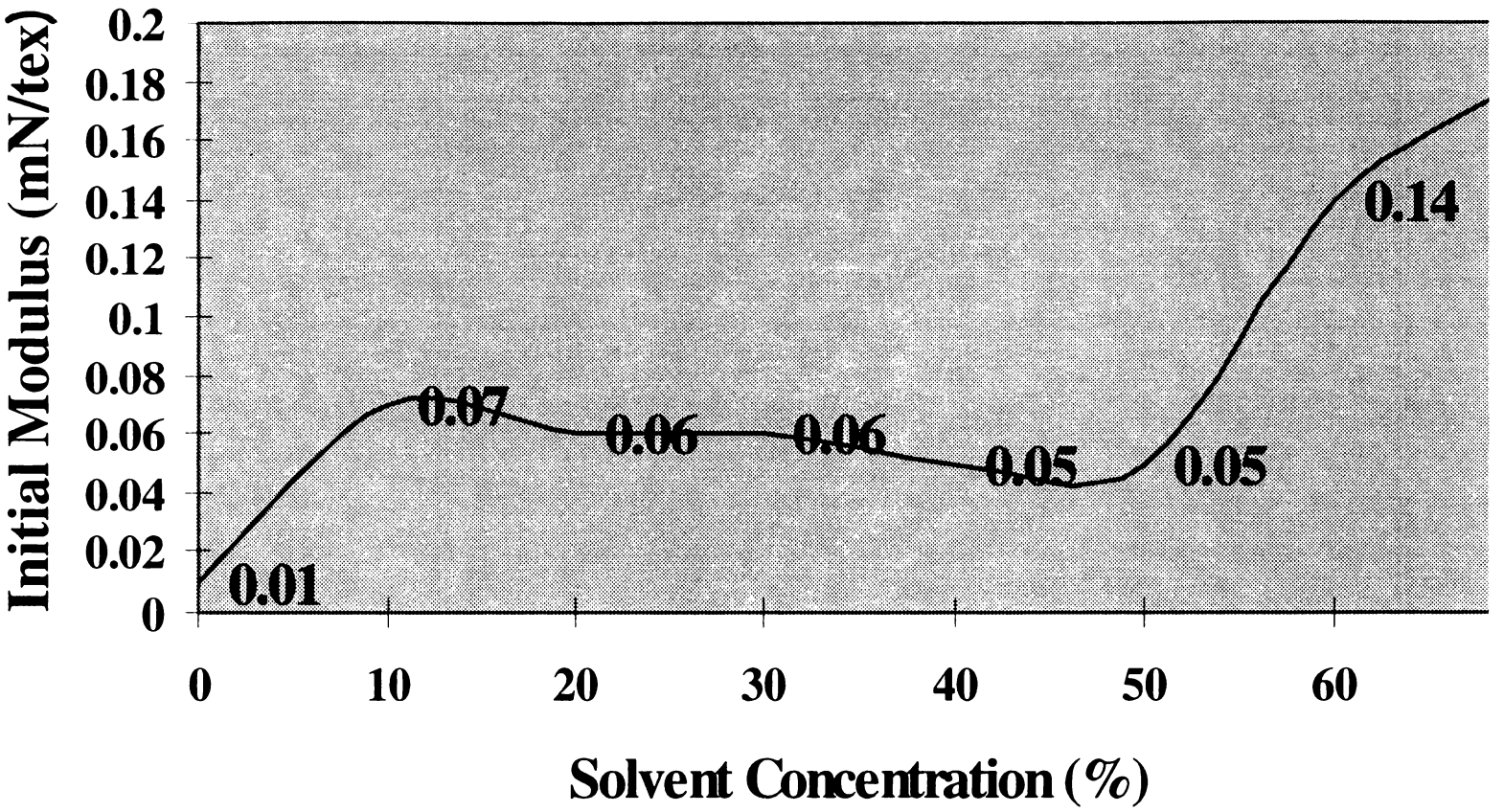

Figure 2: Solvent Concentration Effects on Fabric Initial Modulus for 60/40 Blend Systems Consolidated at 170 C

and 40%) were selected based on the early work that clearly demonstrated the substantial tenacity improvement that could be achieved with 20% concentration and the further improvement that was noted with 40% aqueous acetone solution [13]. The latter concentration was the upper limit for the study because solubility studies have shown cellulose acetate fibers to fully dissolve at concentrations exceeding 50% and the aforementioned strength-solvent concentration evaluation indicated that no further benefit could be attained by increasing the solvent concentration from 40 to 50% [14]. Statistical analysis was used to identify the optimum processing conditions that would produce the desired strength and hand properties. Microstuctural analysis was performed as further confirmation of the processing condition effects on fabric physical properties.

2. BACKGROUND

DEFINITION OF NONWOVENS

Although the nonwovens sector of the textiles industry is relatively young, the technology for nonwovens fabrication in its most rudimentary form has long existed with the mechanical interlocking of wool fibers that occurs with fiber moistening and agitation to produce wool felt. Nonwoven roll goods producers have either borrowed or manipulated much of the processing equipment and technology used for conventional textile assemblies manufacture. The carding machines used for the mechanical processing of staple length cotton, wool and synthetic fibers into sliver form for yarn spinning are used for the fiber individualization, parallelization and web formation of dry laid nonwovens [15,16].

Early bonded fiber fabrics were introduced as a more economical alternative to existing conventional woven and paper constructions used for tea bags and other food and beverage infusers. These end-use products require porous fabric constructions for rapid infusion and effusion, yet not so porous as to permit substance leachate into the surrounding beverage and food media, and because of the one-time product usage, the container fabric construction must be inexpensive to fabricate. Existing paper infusers were poor infusers/effusers and were fabricated from water-soluble cellulose binders. Their dissolution adversely effects the character of beverages and foods. Furthermore, their low wet strengths necessitated additional treatment to stabilize them in the presence of liquids. Bonded fiber constructions comprised of binder/nonbinder fiber combinations consolidated with the addition of heat, pressure and possibly a plasticizing agent were

proposed. Fabric properties based on the fiber and binder selection, processing conditions and solvent modification could be balanced to meet the individual requirements of beverage, food and other end-use products [15,16].

Not all textile experts would identify wool felt as an example of a nonwoven fabric. This discretion is an example of the considerable disagreement that exists among nonwovens industry members regarding the constitution of nonwoven fabrics. The generally accepted definition for nonwoven fabrics given by the American Standard for Testing Materials (ASTM) is: *A structure produced by bonding or the interlocking of fibers, or both, accomplished by mechanical, chemical, thermal, or solvent means and the combination thereof. The term does not include paper or fabrics that are woven, knitted, tufted, or those made by wool or other felting processes* [8].

Unlike conventional fabrics, nonwoven fabrics are planar assemblages in which fibers, not yarns act as the basic structural element. Nonwoven fabrics become self-supporting, mechanically-stable structures by means of bonding at fiber intersections either by self-means or the addition of a bonding agent, replacing the conventional interlacing and interlooping used to build strength and elastic recovery in traditional fabrics.

Nonwovens manufacturing is an economical, high-speed continuous process that completely eliminates the intermittent conventional textile processing operations such as combing, roving and yarn spinning. Dry laid webs, for example, exit carding machines onto a collector conveyor belt as a single web structure in parallel laid systems where they are carried by a belt transfer to the calender rolls for thermal bonding.

Nonwoven fabrics have found many everyday, industrial and medical end-use applications. However, great reluctance among apparel designers and consumers has limited the acceptance of nonwoven fashion apparel. In the apparel textiles market, comfort, hand, aesthetics and strength still preclude economics. Nevertheless, nonwoven roll goods producers are attempting to fabricate nonwoven fabrics with the comfort, aesthetic and performance appeal of conventional woven and knitted apparel fabrics [8].

Four basic steps are involved in the production of nonwoven fabrics and products-fiber/raw material selection, web formation, web consolidation, web finishing and converting [8]. Elaboration of each of the steps will be limited to specific processes and technologies employed in the fabrication of nonwoven fabrics considered in this study. Web finishing and converting will not be discussed as no mechanical or chemical finishes were applied following web consolidation and no end-product conversion occurred.

FIBER/RAW MATERIAL SELECTION (COTTON)

The three hydroxyl groups (-OH) per anhydroglucopyranose residue and the 1-4 beta glycosidic ether linkage between two anhydroglucopyranose residues impart chemical and structural attributes responsible for the physical, chemical and thermal performance properties of cotton fibers (**Figure 3**).

A planar aldehyde can react with any alcohol to yield an unstable tetrahedral hemiacetal which can assume either of two steric arrangements (**Figure 4**). Glucose is a carbon-1 (C-1) aldehyde sugar that can react with the hydroxyl group at its fifth carbon atom (C-5) to form a six-membered anhydroglucopyranose ring that can assume either a "boat" or "chair" conformation (**Figure 5**). The chair conformation is favored because of less bond strain and thermodynamic stability (**Figure 6**). The aldehyde-alcohol reaction

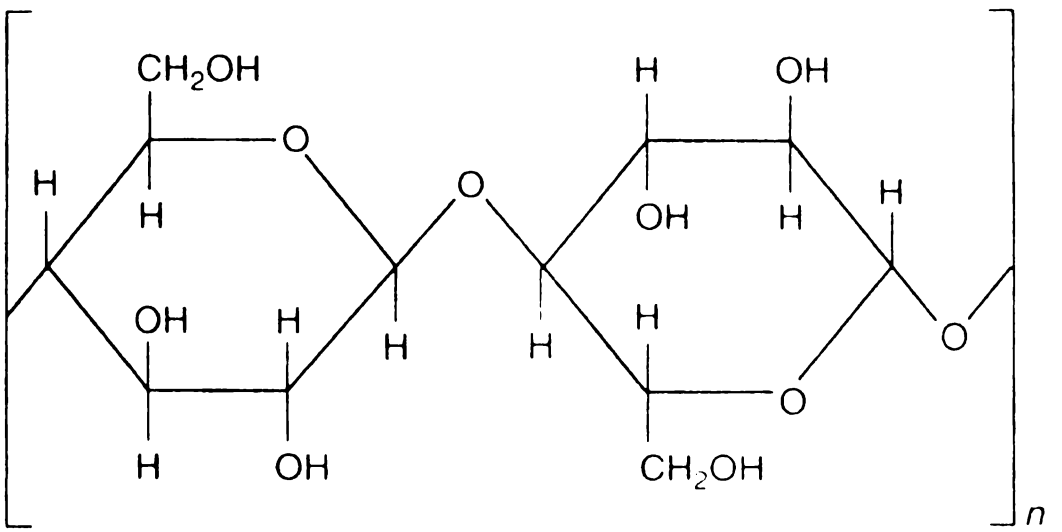

Figure 3. Chemical nature of cellulose.

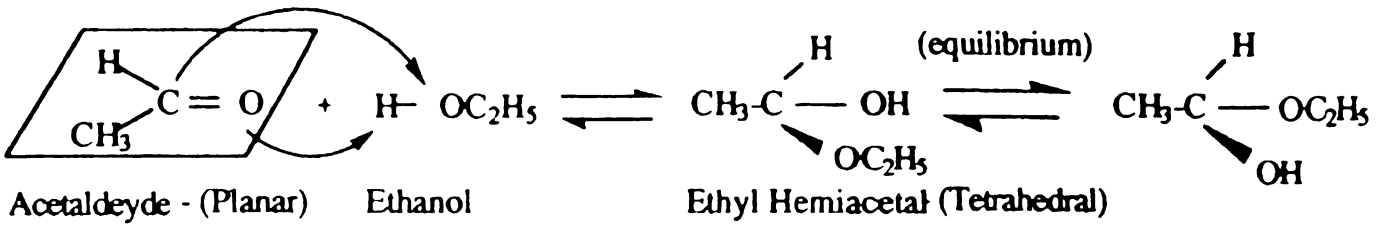
H
C = O
CH3
+
H– OC2H5
(equilibrium)
H
CH3-C — OH
OC2H5
H
CH3-C — OC2H5
OH
Acetaldeyde - (Planar)
Ethanol
Ethyl Hemiacetal (Tetrahedral)

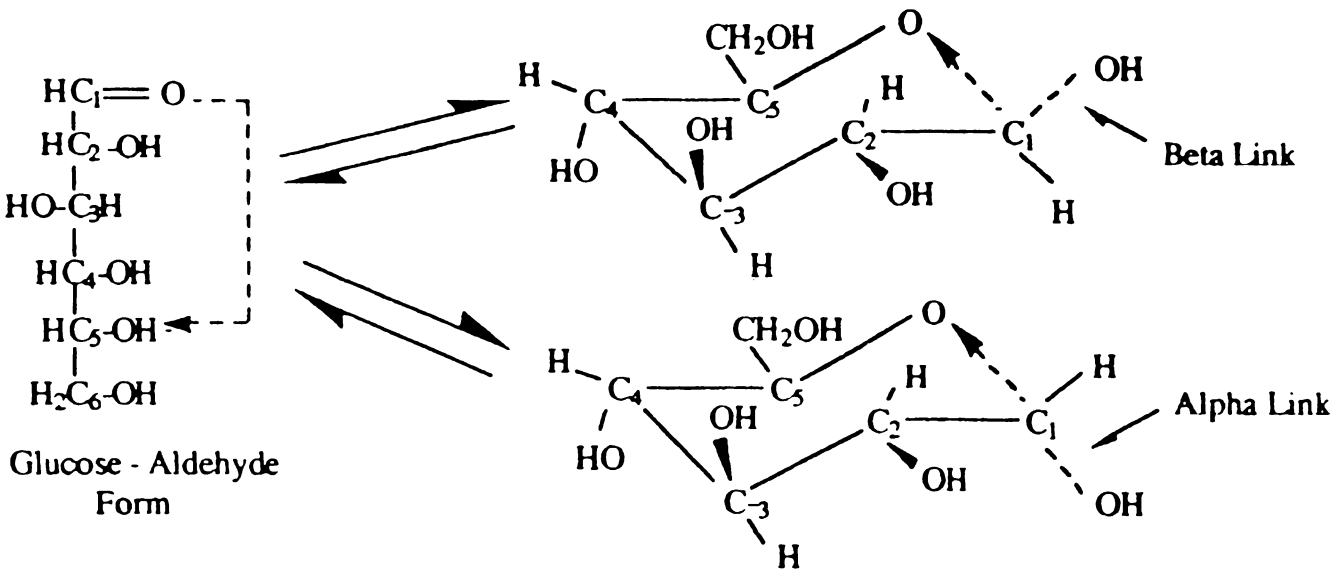
HC1═O
HC2-OH
HO-C3H
HC4-OH
HC5-OH
H2C6-OH
Glucose - Aldehyde Form
CH2OH
O
OH
H
C4
C5
H
OH
C2
C1
HO
C3
OH
H
H
Beta Link
CH2OH
O
H
C4
C5
H
H
OH
C2
C1
Alpha Link
HO
OH
C3
OH
H

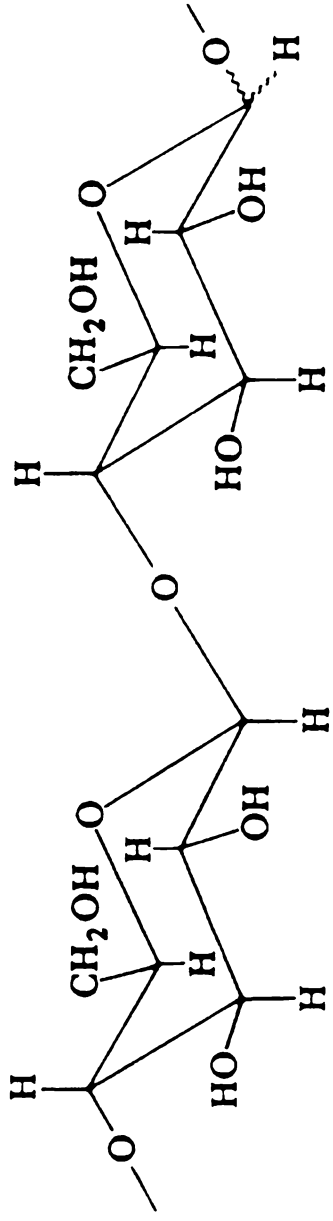
O
H
O
OH
H
CH2OH
H
H
HO
H
O
H
O
OH
H
CH2OH
H
H
HO
H
O

yields a hemiacetal hydroxyl group on the C-1 aldehyde carbon atom that can point up in a beta (β) steric arrangement or point down in an alpha (α) position (**Figure 7**) [8].

When two identical sugar monomers such as two anhydroglucopyranose residues combine, their condensation provides for the elimination of water (**Figure 8**) [8,17]. The anomeric conformation of the C-1 hydroxyl group gives rise to either α or β glycosidic linkages between the C-1 and C-4 carbon atoms of the two residues (**Figure 8**). While the same carbon atoms are involved in the ether linkage formation, two very different physical structures result, despite their chemical similarity depending upon which steric arrangement of the C-1 hydroxyl group is assumed [8,17]. Maltose results when the C-1 hydroxyl group points down, hence, a 1-4 alpha (α) ether linkage (**Figure 8**). This polymer when heated with water forms starch paste or gravy. A 1-4 beta (β) ether linkage, with the C-1 hydroxyl group pointing up gives cellulose, which is resistant to high temperatures and is the constituent of cotton fibers [8,17]. Because cellulose can withstand the temperature elevation of boiling water, cotton fibers can be greatly utilized in medical nonwovens subject to autoclave sterilization [8, 18]. The 1-4 alpha or beta ether linkage is very stable and most resistant to the harshest conditions, even hot alkali treatment. Consequently, cotton fibers are very resistant to alkali degradation [8, 18].

The molecular formula for cotton is $C_6H_{10}O_5$ or $C_6H_7O_2(OH_3)$, where the latter would indicate the presence of three hydroxyl (-OH) groups on each residue, identified as primary or secondary. The primary hydroxyl group is located on the sixth carbon atom (C-6) while secondary hydroxyls are located at the second and third carbon atoms (C-2 and C-3) (**Figure 8**) [18,19]. These hydroxyl groups contribute to weak inter-and intramolecular hydrogen bonds that collectively are very strong and account for the

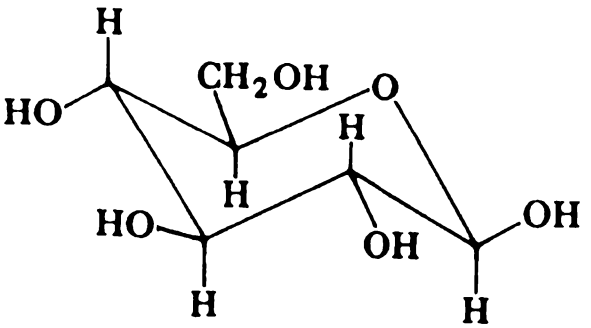

β-D-Glucose

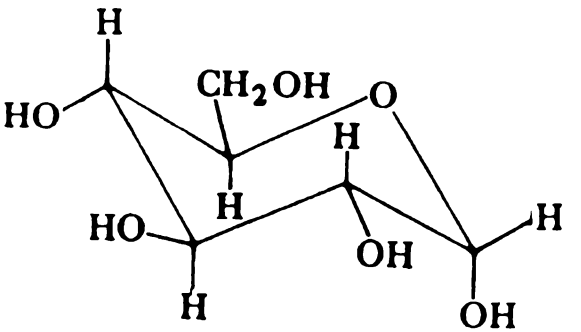

α-D-Glucose

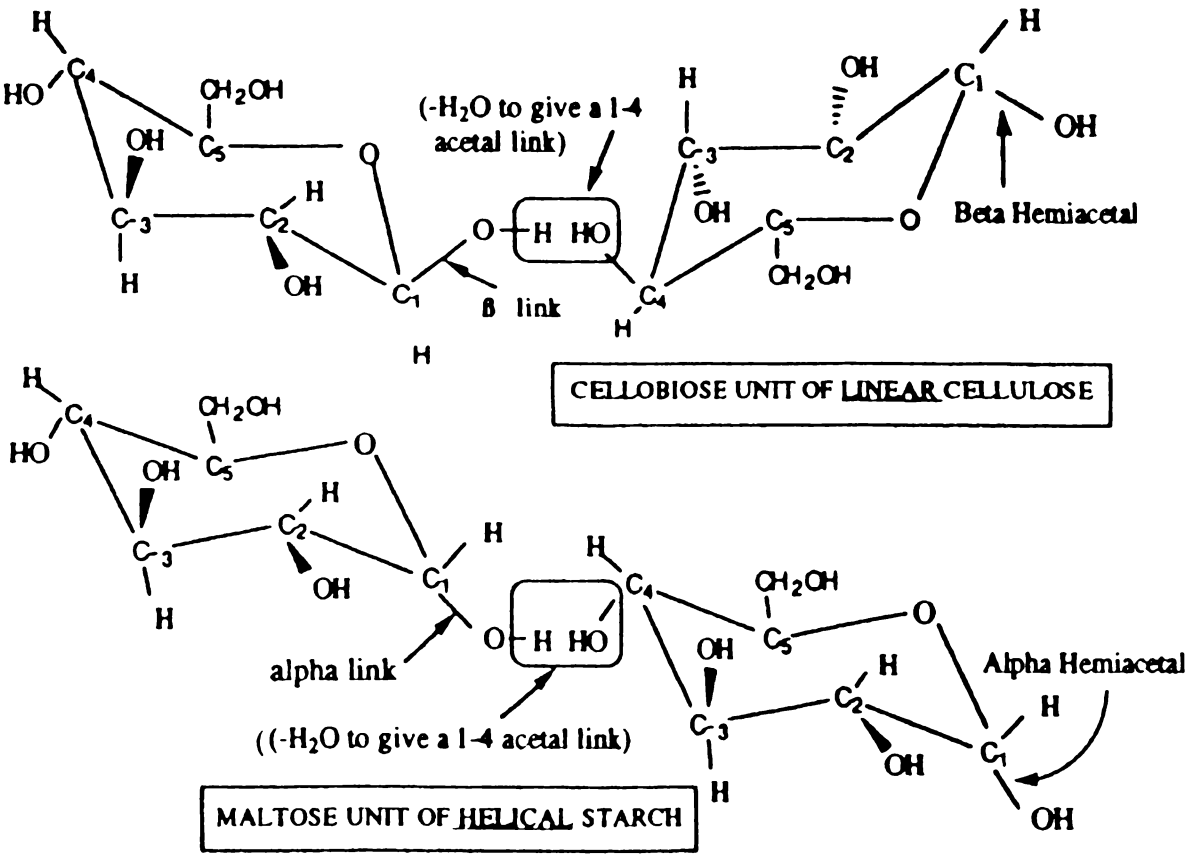

Figure 8. Carbohydrate acetal polymer formation.

crystallinity and orientation that determine cotton fiber performance [18,19]. Microstructural analysis using x-ray diffraction shows cotton to be 70% crystalline [20]. There exist four crystalline structures in cellulose, but the most important is Cellulose I, found in native cellulose (**Figure 9**) The cell dimensions are a = 8.35 Angstroms, b (fiber axis) = 10.3 Angstroms (length of unit cell equivalent to the length of one repeat unit; hence two combined glucose residues) and c = 7.9 Angstroms. The beta angle (β) is the angle between the a and c axes, both of which are perpendicular to axis b and is equal to 84° [19,20].

Hydrogen bonding is responsible for the moderate tenacity, 3.5-4.0 g/denier of cotton fibers [18]. Cotton fibers are not resilient and exhibit poor elastic recovery, and subsequent cotton fabrics exhibit very poor wrinkle recovery, especially in humid environments. Wear stress causes breakage of the hydrogen bonds, the atoms take up new positions, forming new intermolecular bonds such that removal of the stress still does not allow the atoms to recover their original positions [18,19].

Cotton fabrics are very comfortable apparel fabrics because of cotton fiber absorbency, soft hand, and excellent heat and electrical conductivity, again attributed to hydroxyl presence [18,19]. The tendency against static charge build-up facilitates the carding of cotton fibers. The fibers do not repel each other, cling to the apron, or spread upon their card exit, thereby preserving web integrity prior to entering the rotating collector drum [21].

Cotton is a seed hair fiber extracted from the boll of the cotton plant. The onset of fiber formation is marked by the full length establishment of a single epidermal cell, essentially a hollow cylinder which results in 13 to 20 days. A thin, primary wall covered

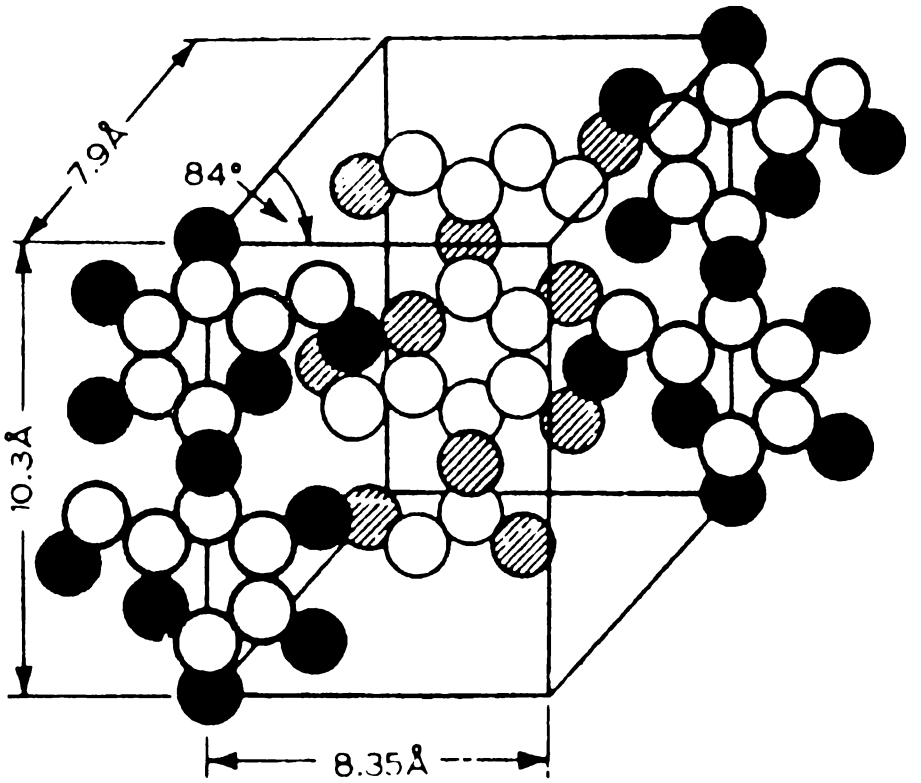

Figure 9. The unit cell of cellulose I[17].

by a waxy, cuticle layer is established. Cellulose is deposited to the inside of the primary wall over 20 to 30 days, largely occupying the hollow tube interior. The remaining space is occupied by a central feeding canal called the lumen [18,19].

The secondary wall formed by cellulose deposition assumes a fibrillar arrangement. The larger fibrils are in turn composed of microfibrils. These bundled cellulose chains assume a spiral arrangement, reversing direction, left to right at intermittent locations along the fiber axis. These points of reversal introduce weak spots (15 to 30%) weaker and are points of failure during the application of uniaxial tension [18,19]. Cotton is the only natural fiber to exhibit the helical arrangement, which has a 35° helical angle. Despite excessive crystallinity, these weak spots introduce some fiber extensibility-4 to 13% [18,19]. Upon fiber maturation, the lumen dries out and collapses, the reverse spirals introduce fiber twisting. These ribbon-like convolutions provide a natural crimp that enhances cotton processability, especially carding and yarn spinning. However, dirt collects in the twists, necessitating an intense washing [18,19].

FIBER/RAW MATERIAL SELECTION (CELLULOSE ACETATE)

Acetate is an ester of cellulose and therefore has a very dissimilar chemical, molecular, and superfine structural disposition than its parent cellulose (**Figure 10**). The substitution of approximately two hydroxyl (-OH) groups per anhydroglucopyranose unit with bulkier acetyl [$R_2C(OR')_2$] groups prohibits the ordered arrangement and sideways approach of neighboring molecular chains. This lack of physical chain proximity restricts the hydrogen bonding that facilitates crystallinity. The consequential amorphic nature of cellulose acetate determines fiber tensile, elongation, recovery, moisture regain and thermal attributes. Inefficient chain packing accounts for very low breaking

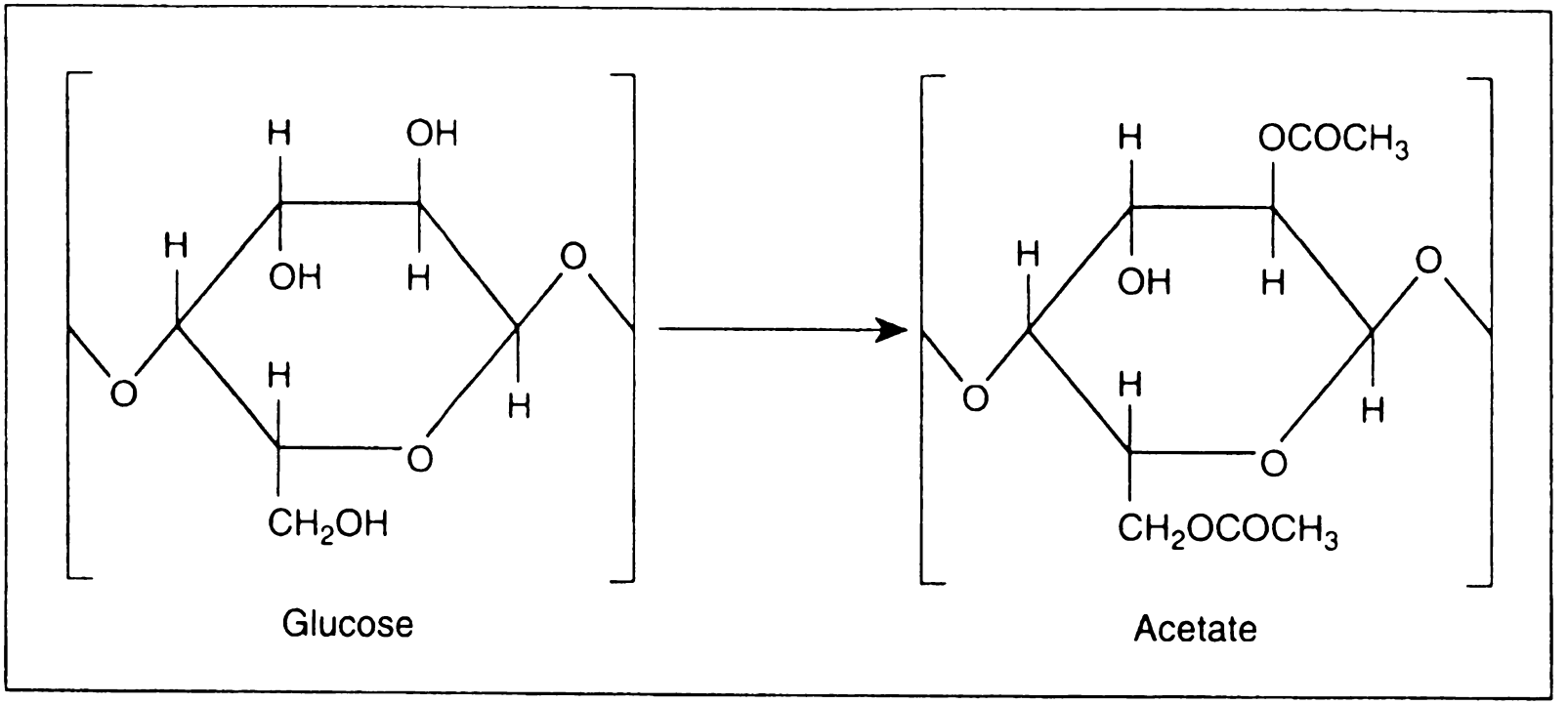

Figure 10. Chemical structure of acetate.

tenacities compared to those of the parent cotton, as low as 1.2-1.5 g/denier [18,19]. Low orientation introduced with the relatively little hydrogen bonding imparts chain flexibility, under uniaxial tension. Elongation ranges from 25-45% [18,19]. However, elastic recovery at 4% elongation is only 45-65% [18,19]. The diminished reactivity of the acetyl groups diminishes moisture regain to 6.3-6.5% from 7-8% for cotton, causing static buildup. The diminished reactivity of cellulose acetate makes it resistant to dry cleaning fluids. However, it is soluble in acetone and other organic solvents and swells or undergoes partial dissolution in acetic acid [18,19]. Acetate is thermoplastic and sticks at low temperatures of 177-191°C and melts at 230°C [18,19]. This relatively low softening temperature makes cellulose acetate fibers ideal binders of nonwoven fiber matrixes. Furthermore, their softening temperatures can be further reduced with solvent modification, reducing energy costs and improving fabric handle because of reduced bonding temperatures. Cellulose acetate is also a very low cost manufactured fiber [18,19].

Cellulose has three hydroxyl (-OH) groups per anhydroglucopyranose unit. In the presence of three mole acetic anhydride and sulfuric acid catalyst, the three hydroxyl groups can be reacted to form cellulose triacetate (**Figure 11**). The Federal Trade Commission defines cellulose triacetate *where not less than 92 percent of the groups are acetylated* [18,19]. It is difficult to spin triacetate fibers, requiring a highly toxic solvent, methylene chloride to reduce molecular weight sufficiently so that fiber spinning can proceed. Solvent toxicity concerns stimulated the Environmental Protection Agency to ban the solvent's usage, forcing domestic triacetate production to cease in 1986 [18,19]. Rather spinnability was more easily facilitated by partial hydrolyzation of the triacetate

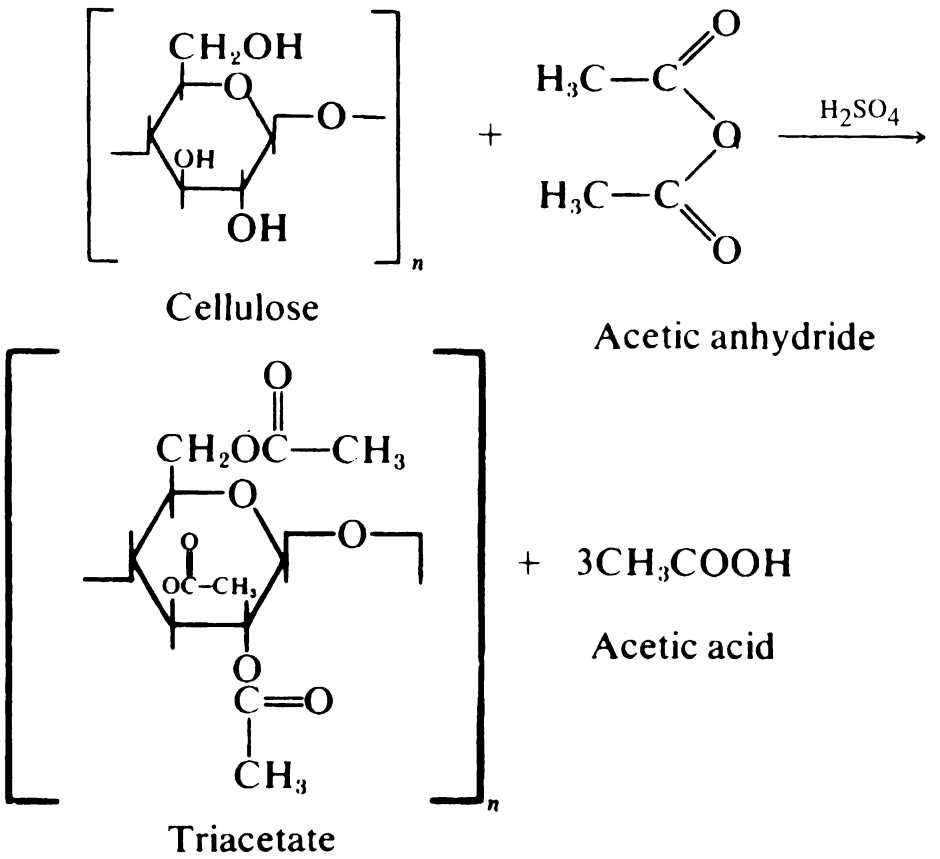

Figure 11. Acetylation to form triacetate.

derivative to a degree of substitution of 2.3 to 2.5 per anhydroglucopyranose unit. This degree of substitution permitted the ready dissolution of acetate in the less toxic acetone solvent [8,18,19]. Acetone solvent is combined with approximately 4% water to decrease solution viscosity. Twenty to thirty percent cellulose acetate is contained in the acetone solvent [8, 18]. Dope filtration and deaeration prior to dry spinning occur. The acetate-acetone dope is then extruded down a heated vertical column, countercurrent to the passage of hot air, quickly evaporating the solvent so that solidified cellulose acetate remains [8,18,19]. Fiber linear density and draw ratios are determined by the filament winder take-up speed relative to the pump speed. Speeds, temperature in the formation zone and proximate environment of the extrudate exit are ultimately responsible for subsequent fiber structure and properties [8,18,19].

Wood pulp is the primary acetylation starting material because of cost and availability. However cotton linters may be used, but both require purification and strict control of molecular weight and molecular weight distribution [18,19]. Complete esterification of the parent cellulose requires enhanced hydroxyl (-OH) accessibility achieved with starting material shredding and acetic acid swelling. Acetic anhydride, with sulfuric acid catalyst assistance, acetylates the hydroxyl groups in a random fashion initially, because of denied accessibility. The three hydroxyl groups ranked in order of decreasing reactivity in this acid-catalyzed acetylation reaction are C-6>C-2>C-3 [18,19]. Upon complete esterification, the addition of water allows controlled, partial hydrolysis to the desired 2.3 to 2.5 degree of substitution. The cellulose acetate is precipitated into dry flakes which are dissolved in acetone for subsequent dry spinning [8,18,19].

WEB FORMATION

Fibers are laid down to form a loosely held, weak fiber web during web formation. Dry laid web formation involves the mechanical opening and teasing of small fiber tufts to individualize and parallelize the fibers, forming a two-dimensional web with dominant machine direction orientation [8, 22,23]. Parallel webs have approximately 10 fibers in the machine direction for every 1 fiber in the cross direction (10:1 MD vs. CD ratio) [8]. Considerable disparity exists between subsequent machine direction and cross direction tensile strengths. The machine direction strength is generally 5 times the cross direction strength (5:1 MD vs. CD ratio) [23].

CARDING MACHINES

Metallic clothing covering the carding and stripping surfaces of the card machine rolls is responsible for the mechanical disentanglement of the fiber tufts. This clothing is a rigid, saw-tooth wire with height, pitch and angle points appropriate for the fiber type being processed [8]. Carding occurs between two metallic-clothed surfaces with opposing points because of differential surface velocities, one surface secures the fibers while the other combs them [8,22]. The partially disentangled fibers are stripped from one surface to another because of unidirectional metallic clothing points and differential surface velocities [8].

Two types of carding machines dominate the dry laid web process-roller-top card and the Cardmaster® stationary plate card. In roller-top models, tuft disentanglement occurs between the cylinder and worker roll point of contact because the rolls are clothed with opposing wire points. The slower worker roll transfers the partially disentangled fibers to the stripper because the metallic points do not oppose each other. The stripper

roll returns the fibers to the cylinder roll ahead of the carding plane for repeated reworking until complete fiber individualization has occurred. The Cardmaster® stationary carding plate machine has stationary carding surfaces unlike the roller-top models. Advances in metallic clothing design, its low profile and easy maintenance have made this machine the card of choice for the formation of webs ultimately used in baby diaper coverstock, adult incontinence pad covers and medical nonwovens [8].

The individualized and parallelized fibers are then condensed on a doffer roll to produce a web. The desired web weight is achieved by the successive layering of fiber webs either by the tandem arrangement of cards for parallel laying or by the successive layering of fibers in parallel on a revolving collector drum [8]. Because of equipment and space limitations at the University of Tennessee research facilities, the desired web weight was achieved by the parallel deposition of several fiber web layers on a revolving collector drum. A roller-top card was used for tuft disentanglement.

Conventional textile carding machines previously used to deliver slivers have been modified to deliver full-width webs. Since 1975, carding machines explicitly manufactured for nonwoven web formation have been designed to furnish up to 5 meter-width webs [8].

METALLIC CLOTHING/CARDING VARIABLES

Inherent fiber properties alone can significantly determine card performance and card quality. The fiber system (cotton/cellulose acetate) selected for this study presents specific examples of the fiber-card operation and quality relationship.

Foreign matter access to the card can have disastrous effects on card operation and card quality, the most severe card damage requires complete replacement of metallic

clothing. Caution must be exercised when cleaning the operating card using an air hose or a broom. Blasts of air can cause loose nuts, bolts and washers to enter the card. Broom handle entrance to the card can necessitate complete metallic clothing replacement, and worse yet can cause operator injury or even death. The presence of paper in the incoming fibers can have long-term effects unless the card is flushed with waste fibers. Otherwise the worker-stripper actions further reduce the paper to smaller entities that load up the wire clothing, with the end result being holes in the web. Trash in the form of leaves, stems and other foreign particulate present in cotton fibers challenges their carding performance. Natural fibers such as cotton, flax and wool arrive in highly compressed bales that require sufficient opening, cleaning and blending. The fibrous mass must be made into a lofty structure that eliminates the clumping and tufting of fibers that otherwise load up the roll wire clothing causing neps, holes and nonuniform fiber distribution throughout the card, prohibiting high speed production. Because of fiber variation within and between bales, blending is critical to achieve uniform distribution of fiber finish, crimp and other pertinent fiber attributes like length and denier so that fabric appearance is uniform throughout. Card machine integrity and web quality can be preserved using sensory metal detectors and other detector types that raise the worker and stripper rolls away from the adjacent main cylinder roll when foreign matter passes between them. Imaging equipment can be used to monitor web quality, detecting neps, fused fibers and other web shortcomings so that on-line maintenance and adjustments can be performed [24,25].

Crimped fibers are essential for roll interactions to proceed. The fiber must protrude above the wire clothing so the points of the mate roll can grab the fibers for

disentanglement, parallelization and fiber transfer. Working or stripping will depend upon the direction of the points between the mated rolls, the direction they are turning and their relative surface velocity [21,25]. The cotton/cellulose acetate fiber system selected for study presents optimum crimp conditions because cotton has a natural crimp introduced by fibril twisting upon fiber maturation and subsequent lumen collapse, while staple cellulose acetate is mechanically crimped for blending with natural fibers [18].

Crimp frequency can be expressed as the number of crimp per inch or centimeter of extended fiber length or as a percent using the following expression:

$$\textbf{CRIMP (\%)} = \textbf{(S-C/C) x 100}$$

where C is the crimped fiber length and S is the extended fiber length [21]. Excessively straight fibers inhibit roll interaction because they are caught between and below wire clothing, causing cylinder loading that ultimately leads to fiber dumping, weight variation, neps and holes [21].

Fiber processability often requires enhancement with the application of lubrication and antistat finishes. Lubricants assist in overcoming the frictional effects that cause fiber and machine damage as a result of their interaction, while still permitting adequate fiber coherence. Antistat finishes reduce fiber repelling, fibers clinging to the apron and web breakdown. Humidity can also dispel static charge accumulations. However, excessive moisture rusts machine parts and softens the apron varnish such that fibers stick. Static charge buildup can become a problem especially during winter months when heating installations reduce atmospheric moisture. Controlled humidification can be used to reintroduce atmospheric moisture and permit continued processing. The scouring and bleaching of cotton removes the natural waxes that

lubricate the fibers, and synthetic lubricants are generally applied as a replacement. Since cotton fibers are good conductors of heat and electricity, charge accumulation is not a concern. However cellulose acetate fibers are very subject to charge buildup, as was observed when carding the fibers for the study. The fibers often repelled each other upon exiting the card, causing web disintegration. The cellulose acetate fibers selected for this study had no special finishes because often these finishes are hydrophobic and can affect subsequent processing, particularly those operations involving aqueous systems. Spray and saturation bonding, solvent modification and even thermal bonding can be adversely affected by the hydrophobicity of finishes, introducing wet out problems and inhibiting binder/nonbinder adhesion [21,24].

The trend for lightweight nonwoven coverstock fibers challenges the card operator, as the fabrication of lightweight webs usually results in web holes and thick and thin lanes throughout the web length. Even coverage for lightweight webs requires finer fibers so the same number of fibers per unit area as heavier webs can be achieved [24,26].

Thirty-five percent of the web formation market is dry laid [26]. Modern carding technology permits the formation of webs using several fiber systems that can be formed into several web basis weights at higher production speeds with proper card maintenance and adjustments. Successful card manipulation and web formation, accompanying the web requirements and product diversity of the expanding nonwovens market will favor the dry laid industry [26].

WEB CONSOLIDATION

The loosely-held fiber web requires stabilization to impart structural integrity and strength. This stabilization can be applied by thermal bonding using calender rolls with

the appropriate temperature and nip line pressure that consolidates the fibrous mass into a bonded fabric. Depending upon the calender roll combination, area or point bonded fabrics can be produced. Combined smooth calender rolls produce area bonded fabrics that are stiff, paper-like, inextensible and very strong because all of the available bond sites are utilized [8,22,23,27]. Point bonded fabrics result when a combination of embossed (top) and smooth (calender) rolls are used because a very discrete portion of the fibers are exposed to the heat and pressure application [8,22,23,27]. Point bonding can be achieved with as little as 10% bonding area [8]. Point bonded fabrics can have a range of physical properties from thin, inelastic, strong and stiff to bulky, soft, flexible and elastic, depending upon the bond frequency, area and the calender roll surface [8,22,23,27]. Bonding temperature, pressure at the nip and bonding speed also play a role in the outcome of the fabric properties [27].

Of the gamut of web consolidation techniques, thermal bonding is preferred, especially among roll good producers of baby diaper and adult incontinence pad coverstock materials. Thermal bonding is a high-speed, low-energy, clean process compared to chemical web consolidation techniques such as latex bonding that require evaporation of water and residual disposal [23,27].

THERMOPLASTIC BINDERS

Thermal bonding requires the presence of a thermoplastic binder, that with sufficient heat and pressure, will flow within the compression sites to network fiber cross-over sites and adhere to the more stable, unaffected network fibers to form thermally-welded bonds that impart web dimensional stability. Thermoplastic binders can be in powder, granular, film, net or fiber form. Thermoplastic binder fibers can be

amorphous polymer binder fibers, sheath-core bicomponent fibers where the lower melting temperature sheath flows while the core remains unaffected and intact, or the outer surface of homogeneous carrier fibers. The latter is given preference because of their economic affordability [8,22,23,27].

AMORPHOUS POLYMER BINDER FIBERS

The 1937 introduction of synthetic, heat-sensitive vinyon textile fibers advanced bonded fabric process technology. Fibers (cotton, nylon, asbestos, and glass fibers, for example) insensitive to heat could now be coalesced with the addition of these thermoplastic binder fibers to produce thermoplastic fiber bonded fabrics. These fabric types were initially developed for the filtration of milk and for tea bags and other beverage infusers [28]. Vinyon, for example is a copolymer composed of 86% by weight of vinyl chloride units (-CH_2CHCL-) and 14% by weight vinyl acetate units (-$CH_2CHOCOCH_3$-) that is dissolved in acetone and dry spun into fibers. Vinyon's very low softening temperature, 66-77°C makes it very suitable for the coalescence of heat-resistant fibers. Vinyon fibers are hydrophobic and resistant to chemical, insect and biological attack, making them suitable for rigorous nonwovens applications. Their tenacity is approximately 0.7 to 1.0 g/d, with elongations ranging from 12 to 125% [18].

The early investigation of vinyon thermal bonded fabrics revealed that for a single fiber blend, materials with a wide range of physical properties could be realized by the selective manipulation of fabric weight and thickness. Furthermore, fabric thickness was determined by the heat and pressure applied to activate the latent adhesion of the vinyon binder fibers. Air permeability for example, decreased with increased fabric basis weight for a single blend and density because of the greater number of fibers present per unit

area [18]. Furthermore, air permeability decreased with increased density, a reflection of the bonding efficiency of the fiber system. Air permeability remained steady at fabric density maximums, this point reflected the maximum fiber compression attained for given bonding conditions (284 psi, 1 min at 150°C). Fabric physical properties were also largely determined by inherent fiber properties of the selected fiber system-fiber denier, length and surface characteristics which influenced bonding efficiency. The disparity in air permeability and tenacity for a given fabric basis weight between different fiber systems is an example of the significant relationship between fabric performance and fiber attributes. Fabrics containing cotton and asbestos were much stronger than nylon and glass fiber fabrics combined with equivalent quantities of vinyon. Cotton and asbestos fibers are finer and, therefore, offer greater surface area available for bonding. Furthermore, these two fiber types feature surface irregularities, *i.e.*, crimp that promote greater fiber compression for the stated bonding conditions than the coarser, smooth surface, cylindrical nylon and glass fibers. Furthermore, although individual glass fibers are stronger than cotton fibers, they do not exhibit softening until temperatures exceed 732°C. Thus the 150°C bonding temperature for the vinyon/glass fiber combination was severely inadequate for sufficient fiber coalescence. Those fabrics containing cotton and asbestos were less air permeable, again a reflection of the efficient bonding mechanism promoted by their inherent denier and surface properties that enhanced fiber compression for the stated bonding conditions [28]. However, maximum obtainable tensile properties and air permeability are not solely limited by the nature of the fiber system employed. These properties can still be improved for a given fiber system by the selective manipulation of the binder fiber quantity, bonding pressure and temperature [28].

Polypropylene binder fibers have played a prevalent role in the thermal bonding of nonwoven fabrics because of their low 165°C melting temperature and their low cost. Polypropylene-containing fabrics are soft and supple. The use of polyester fibers in thermal bonding was once very limited because of their very high 230°C melting temperatures that would require excessive thermal energy inputs and would introduce even more brittle qualities when blended with cotton base fibers [8,18,22,23]. However low-melting polyethylene terephthalate copolymer fibers, such as Kodel-438 manufactured by Eastman Chemical, have emerged to challenge polyproylene's dominance of the thermal binder fiber market for thermal bonded nonwovens. These copolymers flow and melt at substantially lower temperatures than conventional polyester fibers, 115°C (flow) and 130°C (T_m), respectively [29].

Polypropylene fiber acceptance is enhanced by its resistance to abrasion, microbial and chemical attack. The absence of active functional groups on its polymeric backbone is responsible for its hydrophobicity and low density. Polypropylene's limited microbial degradation capacity, attributed to its inactive chemical composition, limits its application in the development of cotton-based biodegradable nonwovens, however. Polypropylene fiber strength combined with its negligible density permits the realization of polypropylene fabrics with high strength-to-weight ratios. More importantly, from a commercial standpoint, the low melting temperature of polypropylene fibers permits lower temperature thermal bonding, thus significant energy conservation [27].

Fiber/raw material physical properties, polymeric factors such as chemical composition, glass transtion and melting temperatures, and finishing agents affect the outcome of interfacial binder-base fiber bonding [27,28,29]. Fiber blend ratios also play

a role in the web structural integrity [9,29,30,31]. Fiber system selection complemented by optimization of process variables such as temperature, pressure, contact time and calender roll attributes govern the nonwoven fabric performance and structural properties [27,28,29,30,31,32,33]. Process optimization largely affects nonwoven strength, aesthetic, hand and extensibility characteristics. Of course, process commercialization is cost-sensitive [27].

FIBER/RAW MATERIAL SELECTION AND PROCESS VARIABLES OPTIMIZATION STUDIES

USDA Southern Regional Research Center research intended to promote the utilization of cotton in nonwovens investigated the effects of blend ratio, fabric basis weight and bonding temperature on the strength and stiffness properties of thermal bonded cotton/polypropylene nonwovens. Nip-line pressure and contact time were held constant. A range of temperatures for each blend/weight combination were selected, the temperature range reflected the fiber composition; that is, blends with higher cotton percentages had higher bonding temperature ranges [9].

A significant relationship between increased breaking strength and increased bonding temperatures existed for all blend/basis weight combinations [9]. Without exception, all fabrics bonded at 145°C lost strength as the presence of cotton increased [9]. The inverse relation between strength and cotton content has been observed in other cotton/thermoplastic blends. For cotton/Kodel-438 blends, fabric strength diminished significantly when cotton presence increased from 50 to 85%. Specific stress values plunged from 9287 to 1180 N.m/kg [29]. These effects are not unexpected since diminished binder availability would decrease the welding of the network cotton fibers. Breaking strength for the previously mentioned cotton/polypropylene blends improved

significantly between 40 and 60 g/m^2 fabrics bonded at 145°C. However, strength observations for 60 and 80 g/m^2 fabrics bonded at this temperature were statistically equivalent. This suggested that for the given equipment and fixed processing conditions, the basis weight should be limited to 80 g/m^2 [9].

Fabric stiffness increased significantly with increased basis weight. Stiffness was also greater in the machine direction than the opposing cross direction, reflecting excessive machine direction fiber orientation introduced during web formation. The stiffness for lower basis weight webs bonded at the high temperature extreme was still lower than the heavier weight web stiffness bonded at the low temperature extreme. The enhanced bonding attributed to increased polypropylene content increased fabric stiffness [9].

Linear regression was used to observe which of the independent variables- bonding temperature, blend ratio or basis weight, had the greatest influence on the dependent variables, breaking strength and stiffness:

LOG Y = BONDING TEMPERATURE + PERCENT COTTON + BASIS WEIGHT

Log Y represented the dependent variables, breaking strength and stiffness. The respective correlation coefficients for breaking strength were 0.96, -0.89, 0.42 and stiffness correlation coefficients were 0.66, -0.48 and 0.75, illustrating the extreme tensile sensitivity to bonding temperature and the large influence of basis weight on fabric stiffness. Negative coefficients for cotton percent indicate the inverse relation between the dependent variables strength and stiffness and the independent variable, cotton, suggesting the advantageous inclusion of polypropylene related to fabric strength. However, the biodegradable capacity measured by the presence of fungal growth and

strength loss for fabrics containing 30% or more polypropylene was severely limited. Even though fungal growth was detected in those polypropylene-containing fabrics, the cotton deteriorated while the polypropylene remained unaffected, preserving the tensile integrity of the fabrics. Although increased polypropylene percentages improved tensile performance, biodegradation of the nonwoven fabrics was sacrificed. Finally, the fiber orientation effects on strength introduced during mechanical web formation should not be overlooked. Generally machine direction strengths were two to three times greater than cross direction strengths. Directional strength disparity could be attributed to the web collection technique that involved the successive layering of fibrous webs on a revolving collector drum to produce the desired batt weight. Furthermore, mechanical web formation may be more important than basis weight in the manipulation of strength since lighter fabrics had higher machine direction strengths than heavier basis weight cross direction strength for the same bonding temperature [9].

The effects of mechanical cleaning, scouring, bleaching and finishing agents intended to enhance cotton processability in nonwoven formation have also been studied [29]. It is quite apparent that removal of the natural waxes is necessary to promote cotton-binder interfacial adhesion. This was especially obvious for two reasons. For those fabrics made from griege cotton and mechanically-cleaned fibers only, significant strength reductions occurred as the percent cotton increased. However those fabrics comprised of scoured, bleached cotton fibers for effective wax removal, exhibited the highest strengths, even as cotton percentage increased. Of the finishing agents selected to enhance cotton nonwoven processing, butoxyethyl stearate (BES)-treated cotton fiber fabrics had the best strengths. For 65/35 cotton/Kodel-438 blends, the BES strengths

were very comparable to scoured and bleached fabrics. However, as cotton content increased, BES strengths were significantly lower than comparable cotton content scoured and bleached fabrics, suggesting greater interaction between BES-altered fiber-binder solubility and cotton presence at higher cotton percentages [29].

Because web consolidation accomplished with heated calender rolls involves crushing the loosely-held fibrous web, thermal conduction is assumed to be the fundamental mode of heat transfer, convection and radiation effects are largely ineffective [19]. The heat transfer-contact time relationship involves comparison between thermoplastic melt completion time and bonding site thermal contact time [29]. Sufficient first order predictions of thermal bonding efficiency have been made based on assumed conduction heat transfer mechanisms, and equivalent specific heat and thermal conductivities of the two fiber types. This approximation was limited to momentary instant contact, however [29].

Conduction depends upon the temperature gradient in which the heat flux, the rate of heat transfer per unit area is determined by the relationship [29]:

$$\textbf{HEAT FLUX} = -K \frac{dT}{dL}$$

where dT/dl is the temperature gradient and K is the fiber thermal conductivity. Initial heat flux is high because of the large temperature gradient. However as the web temperature throughout ascends to the calender roll temperature, the heat flux diminishes to zero. The average heat flux for 100 μm thick cotton/Kodel-438 web (160g/m^2) using a value of k = 20 W/m/°K in which both roll temperatures were 422°K and a 300°K initial contact temperature was 50 (10^6) joules/sec/m^2 [29]. For total web thickness [29]:

$$\textbf{HEAT FLUX} = 100\ (10^6)\ \textbf{W/M}^2 = 100\ (10^6)\ \textbf{joules/sec/m}^2$$

Estimation of the heat required to produce sufficient fabric temperature elevation from 300°K to 403°K (binder T_m) to complete thermoplastic melting was based again on equivalent fiber type heat capacity, c_p = 2.4 J/g/°K [29]:

HEAT REQUIRED = 2.4 J/G/°KC_P (103°K TEMPERATURE INCREASE) X

(160 G/M^2 BASIS WEIGHT) = 39,552 JOULES/M^2

The heat required to reach melting divided by the heat flux yielded the required time to melt [29]:

39,522/100 (10^6) = 0.0004 SECONDS

It was determined that for the bonding speed of 10 m/min the time of thermal contact was sufficient for bonding to occur. This conclusion was based on momentary instant contact where the effective thermal length was determined based on the assumption of total point bond embossed-smooth roll contact and that the 1 mm point bond width was the effective thermal length. The time for thermal contact was 1 mm divided by 10 m/min, or 0.006 seconds. Hence, sufficient thermal contact between the point bond area and smooth roll was established to permit thermoplastic melt completion (thermal contact time 0.006 sec > 0.0004 sec time to melt) [29]. Blend ratio comparison showed that increased binder presence increased melt completion time and that increased web speeds could cause incomplete heat transfer. However, for all blend ratios under consideration, thermal contact times (10 m/min bonding speed) were judged sufficient for complete melting of thermoplastic Kodel-438 fibers [29].

The same researcher went on to establish thermal profiles for very similar fabrics under either static or dynamic conditions, again based on the fundamental mode of conduction heat transfer assumption [30,31]. At zero feed speed, calender roll

temperature was achieved throughout the web at approximately 1.5" before the nip roll entrance. Under the same processing conditions at a fixed feed speed, the region of uniform temperature throughout the web equivalent to roll temperature was very proximate to the nip indicating web diminished area with equivalent calender roll temperature and diminished availability of time for thermoplastic melt completion [30,31].

Empirical research for the previously mentioned fabrics also supports the need for sufficient thermal contact since strength was significantly reduced when bonding speed increased from 10 to 20 m/min, especially when the binder fiber presence increased from 25 to 50% [30,31]. Even when the embossed roll temperature (436°K) exceeded the 403°K thermoplastic melting temperature, specific stress decreased from 10,720 N.m/kg (10 m/min) to 7,996 N.m/kg (20 m/min) [30,31].

Web preheating has been suggested to improve thermoplastic fusion, but not without morphological transformations that produce undesirable web qualities, including diminished strength and toughness. Preheating has been found to increase fiber crystallinity thereby necessitating higher bonding temperatures which are responsible for excessive binder penetration of the web [27].

The minor influence of crush edge pressure along the nip of the paired calendar rolls and the significance of the roll temperature on the tensile properties of smooth-roll thermal calendared cotton/Kodel-438 webs was confirmed by the same researchers. At the lowest bonding temperature (408°K), exceeding the 403°K melting temperature of the polyester binder, increased crush edge pressures did little to improve fabric strength. It was obvious that the negligible fabric integrity was imparted by the mechanical

entanglement effects introduced during web formation. Roll temperature made a more significant contribution to fabric integrity. Only at the high temperature extreme was enhanced roll pressure participatory in improving fabric strength [32].

Tensile properties for any temperature and pressure combination did not vary greatly for two different percentage compositions of the selected fiber system. Because the selected roll temperatures exceeded the binder melt temperature, even in the presence of less binder, sufficient flow was achieved to promote adhesion and encapsulation of the cotton base fibers. Microscopic examination revealed minimal cotton fiber breakage; rather, cotton fibers were pulled apart from the thermal welds in response to tensile loading, confirming bond shear as the primary mode of failure [32].

The effects of dynamic heat transfer on tenacity as defined by web thickness, blend ratio and the calendering variables, pressure and temperature were observed. The selected bonding speed, 3.3 m/min implied that no portion of the web was in the nip roll maximum temperature vicinity for more than one second. Consequently the opportunity for the temperature throughout the web thickness to reach the maximum roll temperature was severely limited for the thicker webs. Generally, the specific stress of 85 g/m^2 basis weight fabrics exceeded those of the 170 g/m^2 for all temperature and pressure combinations for both blend compositions. At the maximum bonding temperature, the increased crush edge pressure greatly influenced lightweight web strength. The added pressure and the diminished thickness overcame the limitations imposed by the dynamic heat transfer. The added pressure increased binder-base fiber contacts for added binder adhesion and encapsulation of the cotton base fibers [32]. At the pressure and temperature combination extreme, the lightweight specific stress for 50/50 blends was

nearly twice that of the heavier webs. For 75/25 blends and the same calendering conditions, the lighter web tenacity again surpassed the tensile performance of its heavier counterparts, however, with less disparity. Although the higher cotton blends contained less available binder, there was more thermal energy available for each bond site, such the bonds that were formed were sufficiently strong. This would also account for the very negligible tensile performance differences for the lighter webs of the two blend compositions consolidated at the pressure and temperature extreme combination [32].

The same researchers experimented with embossed and smooth roll thermal calendering of cotton/Kodel-438 blends bonded at different crush edge pressures and temperatures exceeding the 403°K polyester binder melt temperature. The new calender roll combination permitted separate temperature control of the two rolls so that the embossed roll temperature exceeded the binder melt temperature and the smooth roll operated at a temperature just below the binder melt temperature (394°K smooth roll) so that the binder would not flow through the fabric thickness entirety. This calender system permitted manipulation and control of the delivery speed as well. The experimental fabrics were consequently bonded at two different delivery speeds, 10 and 20 m/min. Three different crush edge pressures were selected. However it was expected that given the embossed roll replacement of the smooth roll and the steel on steel rather than the previous steel on rubber roll combination, that the pressure would actually be greater than the stated operating pressures, especially at the points of pattern contact with the bottom steel roll in the pair. These pressure effects were expected to be introduced into the fabric tensile performance [33].

Unlike the previous smooth roll calendering studies, where the influence of pressure in contributing to improved tensile performance was noted at the pressure and temperature bonding extremes, this same trend was not noticed for this study. Tensile loading was independent of crush edge pressure. However, tensile loading was sensitive to bonding temperature, showing marked increases with temperature elevations [33].

Fabric tensile loading was extremely sensitive to delivery speeds, generally the fabrics bonded at slower delivery speeds were stronger for all blend ratios and processing conditions combinations. However, the tensile loading of those blend ratios with greater binder presence were far more sensitive to delivery speed than those with less binder. The specific stress data for the 75/25 blends at the two delivery speeds approached the line of equality. The fabric thickness for this study was held constant (160 g/m^2) so that variable thickness effects would not be introduced into the complex variable interaction. At the lower delivery speed, the specific stress for the 50/50 blend exceeded those of the 75/25 blends because there was more binder available at each bonding site However, at the highest bonding temperature (436°K), for all pressure levels, the breaking loads for the two blends at the 10m/min delivery speed were very comparable. Although less binder was available in the 75/25 blend, more thermal energy was available for each potential bond site such that sufficient bonding occurred and the strength was nearly identical to the high binder composition blend. These findings would also corroborate previous microscopic evaluation that revealed the source of bond failure was not individual cotton fiber breakage, but rather failure because of bond shear of the binder encapsulation of the cotton fibers. Therefore, the higher cotton percentage was not the culprit for diminished fabric integrity. However, at the higher delivery speed, the

strength within each blend ratio was diminished, especially for the 50/50 blend. This would reflect the restrictions imposed by the dynamic heat transfer. That is, there was insufficient time for complete melting of the binder to occur at the greater delivery speed because of insufficient contact time for which the entire web thickness could reach the maximum temperature of the calender roll combination. This effect was further magnified by the web thickness selected for the study and the increased binder presence. There was very little strength disparity for the 75/25 webs bonded at the two delivery speeds because there was less binder present, such that complete melting near the raised points of the embossed roll could occur [33].

The calender attributes are very important in determining the web textile-like characteristics, *i.e.*; strength and hand. The patents suggest that there should be 15.5 x 10^4-77.5 x 10^4 bonds/m^2- that is, covering 5-25% of the web area [27]. The height of the lands (raised surfaces) on the embossed roll is also very important; the greater the disparity between the land height and the web thickness, the greater the strength and fabric softness because of diminished intermediate bonding or fibers in the pattern proximity failing to undergo compression [27]. Research has shown a disparity in fabric flexural rigidity between the fabric face and the fabric back in embossed-smooth roll thermal calendered webs. The fabric face exhibits a convex embossed surface while the fabric back exhibits a concave embossed surface. The embossed roll produces a cavity in the fabric surface, especially prominent on the fabric face. The bond is at the cavity base and in the fabric surface proximate with the smooth roll. Thus the fabric face fibers undergo compression while those on the rear surface undergo readjustment in response to the pressure of the calendar raised point. The fabric is always more rigid when bending

occurs in a convex embossed surface- that is, the fabric face is stiffer than the fabric back. Since the fibers undergo expansion at the rear surface, the back of the fabric is always more flexible than the face of the fabric [33]. The lands of the patterned roll should be slightly rounded to minimize fiber damage during compression [27].

SOLVENT MODIFICATION

Solvent modification as a means of improving the consolidation of an unspun (natural) and latent adhesive fiber matrix for nonwoven fabrics was patented in the early 1940's [15,16]. However widespread industrial practice and acceptance of solvent modification is limited, most likely to the toxicity, flammability and costly recovery of the solvents used to develop the adhesive binder qualities [15, 34]. Web aggregation using latex impregnation produces stiff fabrics because surface coating locks the fibers into place. Thermoplastic powder and granule binders, discontinuous web aggregation materials reduce fabric uniformity because of the inability to control the particulate binder dispersion, with the particles failing to retain their original positions of dispersion upon bonding [15]. The efficient intermingling of nonbinder and discontinuous binder fibers during mixing, blending and web formation promotes uniform binder distribution throughout the fibrous mass so that a homogeneous bonded fabric is achieved [15]. Examples of fibers with latent adhesive properties include esters and ethers of cellulose, vinyl polymers such as polypropylene, polyethylene and polyester and the polyamides, including nylon and all the various types and copolymers of the aforementioned fiber types. Their selection is dependent upon the specific product requirements [15]. The relative quantity of the binder is also mandated by the fabric end-use requirements [15].

At ambient temperature, the binder fibers retain their fibrous qualities, their adhesive capacities are activated by heat alone, or with additional assistance from plasticizers. Plasticizers modify the binder microstructural attributes that govern polymeric chain flexibility and mobility, the increase of these properties lowers the binder's glass transition temperature (T_g) so that fiber coalescence is enhanced, at lower than normal processing temperatures. The fiber matrix is passed through heated rolls at a specific nip pressure. The pressure serves to bring the discontinuous binder fibers into contact with a greater number of contiguous nonbinder and binder fibers. The binder can then flow to a greater number of fiber intersections, but diminished softness and drapability are the price for strength improvement. Manipulation of the nature and quantitative composition of the fibrous blend is critical in the engineering of fabrics for specific end-products [15]. The application of heat and pressure permits economical, high speed fabric production. Sufficient mechanical engagement of fibers during carding and pressure-induced fiber contacts have reportedly caused stiffness in nonwoven fabrics with higher cotton percentages. However, the use of water as a plasticizing agent, when applied to such fabrics destroyed these mechanically-induced cotton-cotton bonds, leaving behind only those bonds introduced by the binder/nonbinder coalescence. Upon drying, fabric thickness increased and the fabric took on more soft, cloth-like attributes [15]. The nonbinder fibers in these types of consolidated fabrics retain their mobility between welds, unlike those fibers in latex and particulate-bonded fabrics [15]. Although heat alone can facilitate sufficient bonding, plasticizing agents can assist in the conservation of heat input, improving web aggregation at lower than expected bonding temperatures [15].

The selection of an appropriate solvent to act as a plasticizing agent on the binder fibers requires that the nonbinder fibers retain their original attributes in the presence of the modifier. One of the earliest patents describing such a fiber unification process for the fabrication of tea bag and other hot water infusion products for making beverages suggested the use of Santicizers such as Santicizer E-15 (ethyl-phthalyl-ethyl-glycolate). Other members of this class of compounds include those in which the first ethyl group is replaced with a methyl or butyl group [16]. Sixty-percent cotton/forty-percent cellulose acetate fibrous blends containing 30% of the aforementioned plasticizing agents exhibited sufficient acetate fiber softening so that unification with contiguous nonbinder and binder fibers could be achieved at temperatures of 177-191°C. The glass transition temperature of the acetate fibers well exceeded the boiling point of water (100°C) so that even upon their plasticization, the fabric integrity was preserved upon exposure to boiling water. Furthermore, plasticizer leachate in the presence of water was so minute and nontoxic, that beverage palatability was unaffected [16]. These fabrics also exhibited greater wet strengths, critical in their appointment for infuser applications [16].

The same patent suggested the use of acetone, vapor or liquid as a modifier for acetate fibers [16]. Acetone ($-CH_3COCH_3-$), also known as dimethyl ketone or propanone, is a volatile, colorless, odiforous liquid ketone, completely miscible in water. It readily vaporizes and has a low boiling point temperature of 56.5°C [35].

Understanding fiber-solvent interactions and subsequent polymer structural attributes that influence processing conditions and performance characteristics requires a thorough understanding of the chemical nature of the monomer, degree of polymerization and chain alignment that facilitate interaction between the fiber and solvent.

The chemical and physical nature of the side-chain substituents that influence interactions between adjacent molecular chains determine the efficiency of chain packing, that is the crystallinity of the polymer, reflected by the first and second order transition temperatures (T_m and T_g) and the solution behavior of a polymer.

Molecular interactions in nature are of two types, primary and secondary. Primary interactions are very strong bonding forces, in excess of 50 kcal/mol. There are three types of primary bonds-ionic, metallic and covalent. Ionic bonds result between an atom of a metal and another atom of a nonmetallic element. The metallic atom will completely relegate all of its outermost valence electrons to the more electronegative nonmetallic atom to attain the same electron configuration as the preceding noble gas, becoming a positively-charged cation. The nonmetallic atom seeks to attain all the necessary electrons to acquire the same electron configuration as the noble gas of the same period to become a negatively-charged ion called an anion. Thus these oppositely-charged particles are held together by strong electrostatic attraction, the result of significant electron-attracting disparities. Rarely are ionic bonds found in polymeric materials. Metallic bonds are formed between high molecular weight metallic atoms in which the outermost electrons are so distant from their parent positive ion cores that they are equally associated with neighboring positive ion cores. Again, these bonds are not typical of atoms in polymeric materials. The attractive forces between atoms comprising polymers are called covalent bonds and involve the sharing of electrons between the two adjoining nuclei. When two atoms of the same element combine, there is equal sharing of the bonding electrons and the bond is purely covalent or nonpolar. Such molecules are called diatomic. If there exists a disparity in electronegativities between the adjoining

atoms (slight compared to ionic bonds), the electrons are not shared equally and the bonding is directional or polar covalent. The bonding electrons are more closely associated with the more electronegative atom, this atom assuming a partial negative charge (δ-) which leaves the less electronegative atom with a partial positive charge (δ+). The bonding length of primary bonds is approximately 0.90-2.0 Angstroms with the carbon-carbon bond length typically 1.5-1.6 Angstroms [36,37]. The bond energies between carbon atoms in individual polymer molecules are on the order of 80 to 90 kcal/mol.

Secondary forces, collectively referred to as van derWaals forces span greater distances, their range of interactions is between 2.5 and 5 Angstroms. The force of these interactions is inversely proportional to some power of r, generally 2 or more [Force $\propto$ $1/(\text{distance}^r)$] and is obviously sensitive to the distance between the interacting molecular chains [35]. These are the intermolecular forces between substituent groups of adjacent molecular chains and within segments of the same chain that influence chemical and physical properties of polymeric materials such as textile fibers. The van derWaals attractive forces are further classified based on the source and the magnitude of the attraction between atoms. They include London dispersion forces, induced permanent forces and dipolar forces, including hydrogen bonding [35,37].

Polyethylene $(\text{-}CH_2CH_2\text{-})_n$ is a chain of nonpolar repeat units attracted to one another by very weak London dispersion forces that are the result of temporarily-induced dipoles associated with momentary electron cloud density fluctuations. The force is approximately 2 kcal/mol of interaction and remains insensitive to temperature fluctuations. Different nonpolar molecules assume different physical states at room

temperature because increased mass per molecule. Hence the degree of polymerization affords more opportunities for London dispersion forces along the growing chain length; thus, ethylene is gaseous at ambient conditions but a solid when polymerized. Polar molecules such as PVC, poly(vinyl chloride) $[-H_2CHCL-]_n$ are attracted to each other by weak dipole-dipole interactions resulting from the more electronegative chlorine atom seeking the less electronegative hydrogen atom in another molecule. These are permanently-induced dipoles with strengths on the order of 2 to 6 kcal/mol. Their strength of these interactions can be reduced with temperature elevations [35,37].

Neighboring cellulose molecules with their three polar hydroxyl groups per anhydroglucopyranose residue exhibit special dipole-dipole interactions called hydrogen bonds on the order of 10 kcal/mol of interaction. The very electronegative oxygen atom of each hydroxyl group exerts a strong attractive force on the hydrogen atom of the hydroxyl group of a nearby molecule. This attractive force also occurs between nitrogen and hydrogen atoms of neighboring molecules containing amine and amide substituent groups. Hydrogen bonding is exhibited between polymeric chains in close proximity in cotton, wool, silk, nylon and polyester textile fibers [35,37].

The presence of chain flexibilizing or stiffening groups in the parent chain also influences polymeric properties. The presence of methylene ($-CH_2-$) groups or oxygen atoms introduces flexibility to the parent backbone chain, facilitating chain segmental motion in the form of rotation about the single bonds. Stiffening groups in the backbone, including aromatic rings, amides or carbonyl groups prohibit rotation about the single bonds and introduce stiffness to the polymer [35].

Physical properties such as first and second-order transition temperatures are extremely sensitive to conformation (arrangement of chain substituents as determined by rotation about single bonds) and configurational arrangement. That is, the actual chemical bonding about a given atom dictates the proximity neighboring chains can assume. Glass transition temperature (T_g), a second-order transition is that temperature below which polymer chain segmental motion is restricted and the polymer assumes a brittle quality. Any dimensional change in the polymer is the consequence of strained primary valence bonds. Above the transition temperature, the polymer is ductile and has a tendency to flow because of increased segmental flow in the form of rotation about single bonds in the chains and segmental vibrations that are translated along the chain length entirety. Evidence of this increased segmental motion above the transition temperature is the accompanying specific volume increase required to accommodate the enhanced chain motion. At the glass transition there is a sharp increase in the polymer specific volume. Therefore an approximation of the transition temperature can be determined by plotting the change in specific volume with temperature. The melting point of a polymer is a first-order transition temperature and is typically 33 to 100% higher than the glass transition temperature for a given polymer [36].

The linear nature of cellulose molecules, molecular polarity and degree of polymerization ranging from 3,500 to 36,000 facilitate greater opportunity for sufficient chain proximity, promoting strong intermolecular hydrogen bonding along these adjacent long chains. Highly ordered, crystalline cellulose has a reported density as high as 1.63 g cm^{-3} [20]. Cotton fibers consequently become brittle when heated above 200°C. When subjected to temperatures above 200°C, the cotton fibers fail to exhibit any transitions,

rather they just decompose as a result of the anhydroglucopyranose residues within a single chain breaking apart at the flexible 1,4 beta-glycosidic ether linkages. Cellulose acetate (D.S. α 2.5) has a bulky acetyl pendent groups that prohibit neighboring chains from assuming close proximities such that chain packing is largely inefficient. Consequently, cellulose acetate is referred to as an amorphous polymer. At temperatures between 177-191°C, sufficient heat energy is supplied to overcome activation barriers, thus permitting rotation about the single bonds in the chains and interchain vibrational movements that break apart the neighboring chains in the amorphous regions, enabling the polymer to flow. Cellulose acetate fibers melt above 230°C [36].

PLASTICIZERS

Plasticizers are materials that, by ASTM definition, increase the workability and flexibility of a material. Their addition may lower the melt viscosity, elastic modulus or glass transition temperature [36]. Although plasticizers are a component of nearly every polymeric material and their annual worldwide production reportedly exceeds 3.2 million tons, their toxicity and leaching tendencies associated with their presence in long-term usage products such as tile flooring hinder their widespread usage and development [35,36]. The use of polychlorinated biphenyls (PCB's) as plasticizers, for example was banned because of their extreme toxicity [36].

Plasticizers can be internal or external. Internal plasticizers such as methylene (CH_2) groups or ether linkages act as chain flexibilizers in the parent chain that promote rotation about the single bond [36]. Examples of external plasticizers include water, glycol, Sanctizers and acetone. Most plasticizers are nonvolatile, high boiling point solvents [15,16,36]. In small amounts, plasticizers actually act as antiplasticizers,

increasing polymer hardness. Those less efficient plasticizers will require their presence in greater quantities to overcome this initial antiplasticization effect. An efficient plasticizer should improve chain segmental motion with as little as 10% plasticizer present [36]. The *Polymer Handbook* provides solubility parameters (δ) for solvents and polymeric materials so that potential plasticizers for a given material can be screened. The solubility parameter difference ($\Delta\delta$) between the solvent and the polymer should not exceed 1.8 for effective plasticization [36]. The solubility parameter for acetone $\delta = 9.9$ and for cellulose acetate $\delta = 10.0\text{-}14.5$ would indicate solvent-polymer compatibility [36].

THEORETICAL APPROACH TO UNDERSTANDING THE EFFECTS OF PLASTICIZERS

Three theories have been developed to explain the microstructural responses to the actions of plasticizing agents. The lubricity theory holds that the plasticizer serves to lubricate so that the chains slip past one another. The gel theory holds that the plasticizer penetrates amorphous regions and breaks apart the intermolecular attractions that serve to tie adjacent chains together. The free volume theory holds that the addition of a plasticizing agent increases the free volume of a polymer and that the free volume is identical for all polymers at T_g.

In practical terms, the polymeric behavioral response to the presence of a plasticizing agent is depressed melt and glass transition temperatures, reflections of increased chain mobility. The enhanced mobility can actually introduce crystallization, surface and internal cavitation, and shrinkage which permit manipulation of textile fiber mechanical properties.

A quantitative expression for the relationship between the melting point T_m of a semicrystalline polymer and the amount of plasticizer in the polymer amorphous phase was developed by Flory. Again, the assumption that no penetration of the crystalline phase by the modifying agent was employed [34]:

$$1/T_M - 1/T^\circ_M = RV_2/\Delta H_2 V_1 (\phi - X_1\phi_1^2)$$

T°_M = MELTING TEMPERATURE WITHOUT PLASTICIZER
V_1 AND V_2 = MOLAR VOLUMES OF PLASTICIZER AND POLYMER REPEAT UNIT
χ_1 = FLORY-HIGGINS INTERACTION PARAMETER
ϕ = VOLUME FRACTION OF PLASTICIZER
ΔH_2 = HEAT OF FUSION PER MOL OF REPEAT UNIT OF POLYMER

Gordon and Taylor developed a quantitative expression for the relationship between glass transition temperature depression and plasticizer uptake. Once again the assumption that only the polymer amorphous phase was sensitive to the plasticizing agent actions was held. The difference in the solubility parameters is negligible between the modifying agent and the polymer, their relative compatibility determining the equilibrium uptake of the solvent by the polymer. It is important to note that no term is included for the interaction of the solvent and polymer in the expression [36]:

$$T_G = KW_1T_{G1} + W_2T_{G2} / KW_1 + W_2$$

1,2 = PLASTICIZER, POLYMER RESPECTIVELY
W_1, W_2 = WEIGHT FRACTIONS OF TWO COMPONENTS

The parameter K is determined by the difference in the expansion coefficients of the melt and glass of the two components [36]:

$$K = \Delta\beta_2/\Delta\beta_1$$

MICROSTRUCTURAL RESPONSE TO SOLVENT MODIFICATION -SOLVENT INDUCED CRYSTALLIZATION (SINC)

Thermomechanical and solvent-induced structural modification of polyester fibers improves their uptake of high energy disperse dyes considerably compared to the dye uptake of similar, unmodified polyester fibers [38]. Conventional polyester fiber melt spinning and fiber extrusion is followed by subsequent drawing and heat-setting at temperature elevations that are responsible for structural nonuniformities responsible for the nonuniform dye penetration and distribution throughout the fiber that limit reproducibility and introduce a barre effect to fiber appearance [38].

Rapid quenching of the molten polyethylene terephthalate (PET) polymer produces an amorphous, glassy solid, the polymer cooling curve falling short of the 125 to 180°C crystallization endotherm [19]. Consequently, the as-spun PET fibers are amorphous, exhibiting limited molecular orientation. Subsequent drawing of the spun fibers at temperatures ranging from 180 to 200°C is useful in developing fiber tensile properties. Drawing brings the molecular chains in close proximity so that a highly oriented, crystalline structure emerges because of strong hydrogen bonding developed between adjacent ester functional groups [19]. SEM analysis reveals a complex heterogeneous fiber structure including a crust and an internal fibrillar matrix [19]. This would explain limited dye penetration into the fiber interior of experimental polyester fibers not subjected to further heat treatment [38].

Commercially drawn Dacron yarns immersed unrestrained in heated silicone oil at temperatures up to 240°C for 2, 15, 180-minute time intervals showed a moderate decrease in the relative dye uptake from 100°C, passing through a minimum at 160°C.

The dye uptake gradual recovery up to 200°C, followed by rapid ascent in relative dye uptake to the treatment temperature maximum [38]. The diminished dye uptake in the 100 to 180°C temperature range can be related to the microstructural response to these temperatures. Because crystallization emerges at temperatures between 125 and 180°C, rapid nucleation occurs, marked by the onset of numerous, small crystallites, their frequency diminishing the amorphous volume per crystallite. Accompanied diminishment of available sites for dye penetration thus occurs with decreased amorphic content. As temperatures exceed 180°C, sufficient thermal energy permits segmental mobility that causes the smaller, less perfect crystallites to undergo melting, permitting their recrystallization into larger, more perfect crystallites. While there is diminished crystallite presence, the amorphic volume per crystallite increases. A more open structure for dye penetration results [38].

Confirmation of melt/recrystallization behavior occurred in the form of critical dissolution time (CDT), density and crystallinity measurements [38]. CDT evaluation operates on the assumption that fiber solubilization is a reflection of its crystallinity and crystal morphology. Substantial increases in CDT (100 to 140 seconds) at temperatures in excess of 100°C were reached at different temperatures dependent upon the treatment time. At 180°C, CDT was independent of treatment time. Beyond 180°C, CDT values increased substantially, exceeding 3600 seconds (1 hr), occurring at a lower temperature for the longest treatment time (180 min at 180°) and at temperatures exceeding 200°C for the shorter treatment times [38]. This would corroborate with the substantial improvement in dye uptake for this temperature range [38].

Improved crystallinity for the same improved dye uptake temperature range was noted, as well. However density measurements for the same temperature elevations did not follow the discontinuity characteristic of dye uptake and CDT. A linear relationship between density and temperature at the lower temperatures reflected the diminished volume consumed by the growing crystallite frequency [38].

Polyester yarns were also treated with a strongly-interacting solvent, dimethyl-formamide (DMF) for the same treatment times at temperatures that approached the solvent's 152°C boiling point [38] for the purpose of dye uptake comparison in relation to proposed structural modification. DMF-treated yarns did not exhibit diminished dye uptake at all; however, increased dye uptake was more modest up to 100°C. At temperatures between 100°C and the most severe thermal treatment (approximately 150°C) dye uptake increased exponentially. At the most severe temperature and time combination, dye uptake was nearly 4 times greater than the dye uptake for thermal-modified yarns receiving the harshest possible treatment [38]. Furthermore, the DMF-yarn dye uptake ascended the thermal-modified yarn dye uptake maximum at significantly lower temperatures (100-120°C) compared to 240°C for the thermal-modified yarns [38].

Although both treatments improved polyester yarn dye uptake, dye penetration could be improved at much lower temperatures using solvent modification, thus conserving thermal energy inputs [38]. The second-order transition temperature of PET fibers is approximately 78-80°C [19]. Comparison of isothermal shrinkage in thermal and solvent-modified yarns revealed the effective solvent depression of the glass

transition temperature. No shrinkage was noted for the thermal-modified yarns until the treatment temperature surpassed the 80°C second-order transition temperature. Only at temperatures in excess of this transition point was there sufficient thermal energy input to overcome the activation barriers so that segmental vibrations and rotations throughout the chain length entirety could be supported. This motion permitted relaxation of the orientation strain introduced in the fiber structure during spinning and drawing. Above 200°C, discontinuous shrinkage of thermal-modified yarns was attributed to the proximity of the fiber melting temperature. A significant shift along the temperature axis was noted for DMF-treated yarns, providing evidence of depressed glass transition temperature in the presence of a solvent. At 40°C, DMF-yarns exhibited approximately 10% shrinkage. Extrapolation of the linear portion of the shrinkage-temperature curve showed zero shrinkage at approximately -70°C. DMF yarn shrinkage became discontinuous at a significantly lower 100°C temperature. Despite the shift along the temperature axis, the curves were remarkably similar for the two treatments, indicating that the morphological changes introduced by the two treatments were really quite similar. The disparity arose from the fact that the DMF system contained thermal and chemical inputs, and the fiber modification occurred in a swollen state.

At lower temperatures, DMF absorption remained stable. However at temperatures in excess of 120°C, 29% DMF absorption was recorded. Sufficient thermal and chemical inputs permitted adequate chain mobility such that the less stable, less perfect crystallites could melt and form larger, more perfect crystallites. Thus more amorphic solvent-containing sites were possible. Weight loss upon vacuum drying was

insignificant below 120°C; however, drastic weight changes were noted at temperatures in excess of 120°C, especially for the longest treatment duration. Solvent evaporation would leave a porous structure, facilitating dye penetration. At lower temperatures, dried solvent-modified fibers would collapse because the crystallites were too small to support the swollen structure. At the higher treatment temperatures, the larger crystallites were more capable of supporting the swollen structure upon solvent evacuation. This behavior would explain the significant improvement in dye penetration for an aqueous dye process conducted at 95°C over similar, untreated yarns dyed under the same conditions.

Initial density and crystallinity measurements were unbelievably high for DMF-yarns subjected to severe thermal treatments, supporting the proposed subsequent fiber porosity and void attributes. Carbon tetrachloride (CCL_4) and n-heptane (C_7H_{16}) were used for the density gradient column. The assumption was that the yarns exhibited preferential absorption of the heavier, non-interacting CCL_4 component. Furthermore, those yarns treated at less severe thermal conditions achieved equilibrium more quickly than those DMF-yarns treated at higher temperatures, some DMF-samples took up to 8 days to attain equilibrium. This would support the notion of enhanced porosity for solvent-modified fibers at higher temperatures as reflected by the improved dye uptake because of the greater amorphic localities created by recrystallization into larger, more perfect crystallites. When density measurements were made with a calcium nitrate ($CaNO_3$) solution, the unrealistic density values and crystallinities were not observed for the same conditions [38].

Under constant length conditions, dye penetration for both methods was considerably less than unrestrained conditions for both treatments intended to improve

the low temperature dyeing of polyester yarns. At the most severe temperature and time combination, dye uptake for thermal-modified yarns held under restraint fell considerably short compared to the dye penetration for unrestained yarns subjected to identical treatment conditions. Although dye uptake was limited for those DMF-treated yarns held under restraint, it was still sufficiently higher than restrained thermal yarns, again at much lower temperatures, 140°C to be approximate [38]. The restriction of molecular segmental motion (restrained yarns) was more pronounced for thermal-modified yarns because heat energy was the only input for increasing the segmental motion. However even under constraint, the introduction of a solvent permitted some chain motion so that recrytallization occurred, thus the superior dye penetration for the constrained DMF-yarns [38].

SURFACE AND INTERNAL CAVITATION

The development of fiber fine structure and morphology is attributed to stress, thermal or solvent-induced crystallization and the combinations thereof. Crystallization is temperature-dependent and occurs between first and second-order transition temperatures, its rate maximizes upon approaching the polymer melt temperature. Solvent depression of the second-order transition temperature (T_g) permits crystallization at lower temperatures. This solvent-induced crystallization (SINC) differs from purely thermal or stress-induced crystallization because it occurs in the swollen state. SINC has been shown to produce a porous, void structure in the case of DMF-modified polyester yarns [38]. The mechanical and thermal stresses introduced during conventional spinning and drawing of molten PET results in the evolution of a fibrillar fiber structure. These mechanical stresses are the result of differential take-up and delivery speeds. The

subsequent fiber physical properties are highly anistropic. Two completely different fiber fine structures and morphologies emerge, depending upon the nature of the induced crystallization.

Researchers have made attempts to produce a single fiber with both types of morphological attributes introduced by the different types of crystallization, solvent and thermal/stress-induced, sequentially. The proposed porous, cavitated structure achieved with SINC would provide a high surface area that would improve the absorption and diffusivity characteristics of the fiber and improve the fiber-matrix adhesion in composite materials. The fibrillar structure conferred by thermal/stress crystallization during subsequent drawing would impart desirable mechanical properties [39].

Researchers passed undrawn PET monofilament yarns into a solvent chamber that contained either DMF or methlyene chloride (CH_2CL_2) at ambient conditions for approximately 8 seconds. Solvent-induced crystallization occurred first and was limited to the surface. The fibers then passed over a ceramic hot pin at various temperatures and then onto a winder with a 4.0 draw ratio. At this point, thermal/stress induced crystallization resulting in a fibrillar internal structure occurred [39].

SEM analysis confirmed the proposed porous surface structure introduced by SINC, for the surface of as-spun fibers subjected to conventional thermal/stress drawing exhibited a smooth, uniform cylindrical surface. Only those fibers introduced to the solvents exhibited the proposed surface modification. The surface structure of the solvent-modified yarns was different upon subsequent drawing, however. The undrawn fibers showed undeformed spherulites; however, upon their drawing, there was evidence of spherulitic deformation. Some of the surface spherulitic deformation was attributed to

the shear stress introduced during passage of the molten polymer over the ceramic hot pin. SEM analysis also identified three distinct regions in the resultant fibers. The outer surface featured spherulites and cavitation, followed by another SINC region of strictly spherulites followed by a fibrillar structure. A clear interface existed between the combined spherulitic zones and the fibrillar zone. Approximately 40% of the fiber cross sectional area was spherulitic and the remaining cross sectional area was fibrillar [39].

While both DMF and CH_2CL_2 were effective solvents for inducing the surface crystallization, the liquid nature of the DMF interfered with the crystalline development during subsequent drawing, regardless of temperature elevation. Methylene chloride readily vaporized prior to hot pin entrance, while DMF required subsequent washing prior to thermal treatment. The subsequent surface cavitation introduced by solvent treatment caused solvent retention. In the case of DMF, subsequent water washing caused a great deal of water retention prior to thermal treatment. This presence of water reduced the nominal temperature experienced for thermal/stress crystallization in the DMF-filaments because of water evaporation in response to the temperature elevation-thus the low temperature dependence for the DMF filaments during drawing and crystallinity introduced during thermal/stress-activated crystallization.

Fiber tenacity studies of the different induced crystallization mechanisms were made, also. Those filaments with solvent-developed crystallization exhibited tensile properties similar to those filaments with thermal/stress crystallization development. The ultimate breaking load of the solvent-modified filaments was slightly lower and this attributed to their partial fibrillar structure. In any case, the effects of induced crystallization produced chain packing and orientation that produced high modulus, low

elongation filaments. Despite the fact that the evaporation of water required of DMF-treated filaments lowered their crystallinity, their moduli and breaking strengths were slightly higher than CH_2Cl_2-modified filaments. However, the DMF-treated filaments were considerably more extensible [39].

FIBER SHRINKAGE

Thermal or chemical-induced shrinkage of fibers is the result of the relaxation of built-in stress introduced during spinning/drawing operations and the recrystallization of the polymeric chains. Shrinkage causes more perfect crystalline structures and increased chain folding at temperatures in excess of the glass transition temperature. Thermal or chemical inputs disrupt localized intermolecular cohesive forces, thereby enhancing chain mobility and facilitating the evolution of a more thermodynamically-favorable configuration. Many textile industrial processes depend on the structural rearrangement at the molecular level with the addition of thermal or chemical inputs. One of the earliest examples would be the mercerization of cotton. Native cotton fibers in fabric form are held under tension and exposed to aqueous NaOH solutions. The cotton fibers undergo a transformation from a native crystalline configuration (Cellulose I) to a mercerized configuration (Cellulose II). Chain orientation parallel with the fiber axis is maintained, despite shrinkage [40].

This localized disruption of intermolecular cohesive forces can be brought about by either thermal or chemical means. Water and other plasticizing agents can cause shrinkage at lower temperatures and no shrinkage is noted for dry fibers at these lower temperatures. Chemically-induced shrinkage differs from thermal-induced shrinkage in that localized disruption of intermolecular attractions is facilitated by the formation of

solvated bonding sites. Therefore recrystallization can only occur with the chain dissociation and subsequent exclusion of the solvent molecules [40].

The evaluation of chemical-induced shrinkage kinetics identified three distinct regions along the time axis. The induction period was associated with solvent diffusion, in which virtually no shrinkage was observed. This was noted as the time required for a critical fraction of the fiber cross section to be penetrated by the solvent. The second region of the curve was defined as the maximum shrinkage rate, k_o. Extrapolation of the line defining k_o to the time axis defined the induction period. The final region of the shrinkage-time curve was marked by diminished shrinkage rate, an equilibrium was established [40]. When the temperature was increased, there was a shift in the curve along the time axis, the amount of time for critical cross section penetration by the solvent decreased. When the treatment temperature approached the polymer T_g, the induction time approached zero. This would correlate with the structural transformation that produced recrystallization into larger, more perfect crystals such that the amorphic content increased. Thus rapid solvent diffusion was facilitated. At treatment temperatures below the polymer T_g, the induction time was prolonged [40].

Activation energies for the various solvent employed were calculated based on the assumption that the induction period was defined by sufficient diffusion and activation of an Arrhenius type. The activation energies of the solvents were not the same and were apparently dependent upon their molar volume, suggesting simultaneous solvent diffusion and dissociation of the chain network. Furthermore, the shrinkage activation energies for all organic solvents, including water were higher than that observed for dry yarns. The ΔE_a was attributed to the larger molecular species that produced solvated

polymer structural segments with greater effective volume and the differences in the solvent-PET compatibility [40].

A linear relationship between equilibrium final shrinkage and temperature was observed for the experimental temperature range and all the solvents, except water. Extrapolation of the curve produced a zero shrinkage temperature, at which below no shrinkage was presumed to occur. This zero shrinkage temperature (T_o) was believed to be an approximation of the PET-solvent system T_g [40]. Suppressed second order transition temperatures were observed, the zero shrinkage temperatures shifted from the normal 80°C glass transition of untreated PET filaments [40]. Generally those solvents with lower energy activation barriers were most effective in second order transition temperature suppression [40].

EFFECTS OF SOLVENTS ON THE MECHANICAL PROPERTIES

The effects of nonaqueous solvents on the dimensional and mechanical properties on PET yarns was evaluated and compared to similar untreated yarns. The yarns were treated for sixteen hours at ambient conditions (21°C). The dimensional and mechanical properties of the yarns treated with water, primary alcohols, aliphatic and aromatic hydrocarbons remained relatively unaffected. This behavior was expected to be the result of the relative incompatibility between the polymer and the solvent, which would mean the T_g would remain largely unaffected by their presence, and because the experiment was carried out at a considerably lower temperature than the 80°C second order transition temperature of the PET filaments, impeding solvent diffusion [41]. The load-extension curves of the PET yarns were greatly affected by solvents such as DMF, methylene chloride (CH_2Cl_2), tetrachloroethane ($CHCL_2$-$CHCL_2$), and trichloroethylene

(CCl_2=CHCl) [41]. The rupture stress of yarns treated with these solvents, dried and reconditioned, actually improved. This was attributed to strain hardening that occurred in the post-yield region as a result of the increased chain mobility that permitted repacking and organization into a more perfect crystalline arrangement [41]. The initial modulus and yield point for yarns treated with these solvents were also drastically reduced. The region of initial elastic deformation completely disappeared for those yarns subjected to methlyene chloride and tetrachloroethane treatment, their yield stress approached zero [41]. Trichloroethlyene-treated yarns like DMF yarns still retained an elastic deformation region and a distinct region of flow, however their yield occurred at far lower stresses than similar dry yarns [41]. Considerable shrinkage was noted as well for those yarns treated with methlyene chloride and tetrachloroethane, as much as 17% [41]. The disparity in properties of those yarns treated with chlorinated solvents appeared to be the result of the presence of active hydrogen atoms on the parent chain, as the load-elongation curve for perchloroethylene-treated yarns (CCl_2=CCl_2) at 21°C was identical to the dry PET load-elongation curve [41].

More importantly, interactions between the solvent and polymer could be achieved at room temperature. The 80°C second-order transition temperature for the PET yarns did not have to be reached for permitted interaction to occur with these strongly interacting solvents [41]. Irreversible structural modification, hence shrinkage, occurred, evidence of glass transition temperature suppression well below room temperature [41]. The importance of consideration of the glass transition temperature for the polymer-solvent system- not just the polymer- was illustrated by the lack of appreciable interaction between solvents such as water, the primary alcohols, and the aliphatic and

aromatic hydrocarbons. The relative insensitivity of dimensional and mechanical properties of treated PET yarns to these solvents suggested that their interactions required temperatures in excess of room temperature, suggesting the addition of thermal input to facilitate irreversible structural modification. Because these solvents represent a range of polarity, hence hydrogen bonding capability, the segmental mobility required for second-order transtion temperature suppression required temperature elevation.

Approximation of solvent compatibility with the PET yarns was determined using the solubility parameter, δ. A solubility parameter of 10.7 $(cal/cm^3)^{1/2}$ was calculated for the PET yarns. The initial modulus decrease associated with the irreversible structural changes brought forth by suppressed glass transition temperature was plotted against the solubility parameter for each of the solvents selected for the study [41]. As expected, the diminished initial modulus was greatest for those solvents whose solubility parameters approached that of PET from either side. Two ranges of solubility parameter were identified, suggesting specific interactions between the solvent and PET. The first range of strong interaction was from 9 to 10, while the second range of strong interaction was for those solvents whose solubility parameters ranged from 11.5 to 13. The evidence of two ranges suggested interaction with aliphatic and aromatic members of the solvents, respectively [41]. Therefore those solvents whose solubilities approach that of PET or some segment of the parent PET chain will strongly react with the PET, as evidenced by the often irrecoverable physical properties of the PET yarns treated with such solvents [41].

The effects of the previously mentioned solvents on cellulose acetate yarns treated at room temperature (21°C) for 16 hours were observed [42]. Once again, comparison of

load-elongation curves for treated yarns to dry yarns illustrated the irreversible structural modifications that produced yarn mechanical property alterations, at room temperature. The initial modulus and breaking load were lowered by their presence. Clear demarcation of the elastic and inelastic deformation regions could be gleaned for most of the selected solvents compared to the load-elongation curves for similar dry yarns in which the identification of a clear yield point was more limited [42]. Load-elongation curves for carbon tetrachloride (CCL_4), propanol (C_3H_7OH) and water were nearly identical, suggesting both the hydrophobicity of cellulose acetate and the importance of hydrogen bonding in cellulose acetate structures [42]. Complete disappearance of elastic deformation was noted for mesityl oxides and nitrobenzene solvents, with considerable extension of the region of flow [42].

THERMODYNAMIC CONSIDERATIONS IN THE UNDERSTANDING OF FIBER-SOLVENT INTERACTIONS

Beyond polymer morphology, the extent of polymer-solvent interaction is defined by the source and intensity of the adjacent intermolecular attractive forces and the ability of the solvent to replace these polymer-polymer interactions with newly-formed polymer-solvent interactions. The intermolecular forces being referred to are the previously mentioned London dispersion forces, permanently induced forces and dipolar forces, including the exceedingly strong hydrogen bonding forces.

Before any further discussion on fiber-solvent interactions can be continued, a review of thermodynamic principles that govern reactions is mandated. The following equation is the Gibbs free energy equation for constant temperature [34,36,37]:

$$\Delta G = \Delta H - T\Delta S$$

ΔH is the enthalpy term. All systems in nature seek stability, and are willing to undergo the required processes to achieve this stability that ultimately lead to a decrease in the energy of the system. Solvent-solute interactions improve stability, more so than if the two components remain as separate entities. Historically, the spontaneity of a reaction was believed to be driven by exothermic release of energy during the reaction. Consequently, the enthalpy term was presumed to always be negative for reaction spontaneity [34,36,37]:

$$\Delta H^\circ_{RXN} = H^\circ_{(PRODUCTS)} - H^\circ_{(REACTANTS)} < 0$$

$$\textbf{THEREFORE, } -\Delta H^\circ_{RXN} = \textbf{SPONTANEOUS REACTION}$$

However not all spontaneous reactions are highly exothermic, sometimes the enthalpy term can approach or even exceed zero, indicating an endothermic reaction ($\Delta H^\circ_{rxn} \approx 0$ or $\Delta H^\circ_{rxn} > 0$). Therefore this enthalpy term is not the most suitable criterion for predicting the spontaneity of a reaction [34,36,37].

The driving force for polymer-solvent interactions, and the dissolution of polymer-polymer interactions is more related to the entropy term, ΔS. Entropy is an evaluation of the disorder or randomness of a system. There are two types of disorder, positional and thermal. Positional disorder describes the distribution of particles in space while thermal disorder describes the distribution of available energy among those particles. Any process that increases the particle randomness in space or a constant pressure process that increases the temperature of the system increases the system entropy. For a reaction to be spontaneous, the total entropy change must always be

positive ($\Delta S_{rxn} > 0$) and is an entropy-favored reaction in which the total entropy of the products is greater than the total entropy of the reactants:

$$\Delta S_{RXN} = S°_{(PRODUCTS)} - S°_{(REACTANTS)}$$

Nature acts to minimize the energy and maximize the entropy of all processes [34,36,37].

In simple terms, the old adage "like dissolves like" holds true. A polar solvent dissolves a polar solute and a nonpolar solute is more affected by a nonpolar solute. The penetration of amorphic localities accompanied by solute encasement in solvation spheres increases the positional disorder. Molar entropy of a solute is increased with incremental solvent addition because more polymer-polymer interactions are subject to interruption by the increased solvent presence. This increased positional disorder is accompanied by an increase in the specific volume of the solute. With respect to fiber-solvent interaction, the solvent penetrates the amorphic proximities, promoting separation of chains by the weakening and finally, breakage of the intermolecular attractions responsible for chain interactions. Solvation spheres around the chains emerge, with increased fiber-solvent interaction, subsequent solvation layers encase the chains and fewer liquid solvent molecules are "free". Therefore a solution viscosity increase is observed. Fewer solvent molecules are available to act as diluents. As solvation layers increase, the chains separate and expand, consuming more solution volume. Ineffective fiber-solvent interactions result in diminished chain straightening and expansion, the chains retaining a spherulitical arrangement. Since less solvent molecules are affected, less solution volume is consumed and the solution viscosity remains low. Again, solvent efficiency for a given polymer can be predicted with the assistance of solubility parameters for both components supplied by the *Polymer Handbook.*

System disorder increases with phase transitions and the entropy term is the greatest for vaporous transitions ($\Delta S_{vap} > \Delta S_{liq} > \Delta S_{sol}$) because of increased temperature that in turn increases particle disorder and, consequently, an accompanying volume increase is noted [8,34,36,37]:

MOLAR ENTROPY OF VAPORIZATION (ΔS_{VAP}): $\Delta S_{VAP} = \Delta H_{VAP} / T_B$ (K)

Gibbs free energy, G is a compromise between enthalpy and entropy changes. A reaction is energy favored if the energy of the products is less than the energy of the reactants. However, the energy term ΔH alone does not provide sufficient indication of the spontaneity of a reaction. This compromise between these two terms determines the sign of ΔG for the reaction, and thus whether or not it is spontaneous. At constant temperature and pressure, when $\Delta G_{rxn} < 0$, the reaction is thermodynamically-favorable- hence, spontaneous with the formation of additional products. When $\Delta G_{rxn} > 0$ the reaction is not favored thermodynamically and is not spontaneous. No additional products can form without additional energy input. When $\Delta G_{rxn} = 0$, the system is in equilibrium and no further changes are observed [8,34,36,37].

With respect to fiber-solvent interactions, the entropy term is always positive because the increased segment mobility caused by bond breakage unlocks the adjacent chains, permitting their dispersion and the consequential volume consumption in response to their growing randomness. Thus the negativity of the overall free energy change for the fiber-solvent system depends upon the magnitude of the energy (enthalpy) term, ΔH. Negative or minute values of ΔH permit solution to occur.

Hildebrand and Scott, and Scatchard are responsible for the development of the widely accepted expression for the development of this term [34,36]:

$$\Delta H_M = V_M[(\Delta E_1/V_1)^{1/2} - [(\Delta E_2/V_2)^{1/2}]^2 \phi_1 \phi_2$$

V_M = TOTAL VOLUME OF THE MIXTURE OF THE TWO COMPONENTS
ΔE = ENERGIES OF EVAPORATION
V = MOLAR VOLUMES
ϕ_1, ϕ_2 = VOLUME FRACTIONS OF THE TWO COMPOUNDS IN THE MIXTURE

The ratio $\Delta E/V$ has been called the cohesive energy density (CED) since it is a measure of the energy required to overcome all the molecular forces in 1 mol of the substance that is the molar energy of vaporization [34,36]. Hildebrand introduced the solubility parameter δ defined as the square root of the cohesive energy density:

$$\delta = (\Delta E/V)^{1/2}$$

The heat of mixing a solute and solvent ΔH_m is proportional to the square of the difference in solubility parameters [34,36]:

$$\Delta H_M = \phi_1 \phi_2 (\delta_1 - \delta_2)^2$$

The entropy term favors solution and the enthalpy term acts counter to solution. Therefore the solubility parameter difference should be small so that the reaction is favorable thermodynamically; that is, ΔH_m approaches 0 or is even less than zero [8,34,36,37].

3. EXPERIMENTAL PROCEDURES

FIBER SELECTION

Cotton fibers for the study were provided by Cotton Incorporated, Raleigh, N.C. while Hoechst-Celanese of Charlotte, N.C. provided the cellulose acetate binder fibers. Scoured and bleached cotton fibers were selected because removal of the natural wax surface coating facilitates improved bonding surfaces for binder fibers and bleached fibers enhance consumer aesthetic acceptability of respective end products.

The commodity cotton fibers had a reported moisture regain of 5.2%, a 5.4 micronaire value, and an upper-half-mean fiber length of 2.44 cm. Comparable denier and staple length cellulose acetate fibers had a degree of substitution (DS) of 2.5, an acetyl value of 55% and a moisture regain of 5.0%.

The two staple length fiber types were opened and blended at Cotton Incorporated facilities and sent to the University of Tennessee for continued processing. Two blend ratios, 60% cotton/40% cellulose acetate and 75% cotton/25% cellulose acetate were selected to observe potential physical property differences, namely how tensile properties were affected with increased binder fiber presence. The assumption was made that greater individual bond strengths would be achieved with increased binder content.

CARD FORMATION

The blended fibers were weighed to 0.1% of their gross weight using a precision balance. Prior experimentation determined that 13.5 g of the blended fiber input was required to achieve a final fabric with the desired target fabric basis weight of 40 g/m^2. Eventually interest was directed to the fabrication of ultralightweight fabrics with target

fabric basis weights of 25-30 g/m^2. To achieve this desired weight, 10 g of raw fiber input was required. After the required fiber mass was weighed, the fibers were pulled apart and placed in a feed tray for subsequent card formation.

A Saco-Lowell carding machine was used to form the carded webs. The feed tray was propped against the feed roll which secured the fibers, pulling them into the lickerin roll. The adjacent, large working roll revolved opposite to the lickerin, its quicker revolution permitted the working roll to draw the fibers away from the lickerin. Wire flats moving against the working roll removed trash and oriented the fibers parallel with one another. The fibers were collected in several successive layers on a revolving collector drum to produce a single carded web with excessive lengthwise fiber orientation. The collector drum circumference was 56" (142.2 cm) and the drum width 8.75" (22.2 cm). The carded web was then cut away from the drum and placed face up in a large brown paper storage envelope, awaiting further processing.

AQUEOUS SOLVENT TREATMENT

The carded web was cut in half to form two card half lengths, facilitating easier feeding during subsequent padding and thermal calendering operations. The first card half length was secured between two fine mesh screens face up so that subsequent padding operations would not harm the structural integrity of the card half length.

An H.W. Butterworth & Sons, Philadelphia, P.A. padding machine was used for the solvent application. Acetone was mixed with water to produce 20% and 40% v/v solutions. Then, 200 mL of the solution was poured into a tray and the first card half length was run through the padding machine at a nip pressure of 60 psi. The same 200 mL solution was recovered and the second card half was run through the padding

machine. The solution was then discarded and the tray was replenished with a fresh 200 mL solution for the next two card half lengths.

THERMAL CALENDERING

The saturated card half length was attached to a brown paper leader face up, using masking tape. This paper leader made feeding the card half length between the closed calendering rolls with a nip roll pressure of 160 KN and a feed roll speed of 10 m/min much easier. Thermal bonding was accomplished using a Ramisch Kleinewefers 23.6" (60 cm) wide five- roll calender. The top calender roll had an engraved diamond pattern resulting in 16.6% bonded area. The bottom roll was smooth. The rolls were heated by circulating oil, providing uniform heating across the width of both rolls Although both rolls were controlled by separate heaters, they were operated at the same temperature and were heated to 150, 170 and 190° C bonding temperatures, respectively. Card half lengths that did not receive the solvent treatment were calendered under the same conditions, serving as a control group.

ASTM/INDA STANDARD TEST METHODS

ASTM (American Society for Testing and Materials) is responsible for the development of standards pertaining to characteristics and performance of materials, products, systems and services. These standards are meant to provide a common language between the buyer and seller that leads to improved understanding of the needs of both parties, safe, consistent product quality and consumer confidence. Committee membership is covers virtually all industrial technology. The general committee D-13 and its ample subcommittees are responsible for the consensus development of test methods, specifications, definitions and practices relating to textiles. This material is

updated and published annually in two volumes, 07.01 and 07.02. This material has been developed with conventional textile and apparel structures in mind.

Standards and specifications developed specifically for nonwovens are the responsibility of INDA (International Nonwovens and Disposables Association). These test methods are referred to as *IST-INDA Standard Tests* and often are simply modifications of similar preceding ASTM standard protocol [8, 43,44,45].

CONDITIONING/STANDARD ATMOSPHERE FOR LABORATORY TESTING

Cotton and cellulose acetate fibers contain certain chemical reactive groups called hydroxyl groups (-OH) that give rise to their hydrophilic, moisture-loving nature. This necessitated that certain measures be taken to properly condition the test fabrics so that reproducible results would be achieved with test replications. Variations in results that could be attributed to temperature and humidity variations in the test environment housing the test fabrics and test equipment would be avoided.

The chemical reactive groups present in these two staple fibers are responsible for strong intermolecular forces called hydrogen bonds between the reactive groups and water vapor molecules in the surrounding atmosphere. Consequently, these fibers inherently contain a given amount of water in their molecular structures which varies with changes in the surrounding atmospheric relative humidity. Cotton and cellulose acetate fibers attain their equilibrium regains for a specific relative humidity more slowly than hydrophobic fibers and their mechanical and hand properties, especially, are sensitive to varied relative humidity. Equilibrium regain is described as the condition where a material no longer absorbs water vapor or undergoes water vapor desorption from its surrounding atmosphere. Therefore it is most crucial to bring all textile materials

subject to evaluation to their moisture equilibrium at the same relative humidity so meaningful comparison of the same material can be made.

The culling of assorted references concerning equilibrium regain for various fibers revealed that equilibrium regains for cotton and cellulose acetate are 8.5% and 6.0%, respectively in a standard atmosphere for textile testing in the United States of 65 ± 2% rh, 70 ± 2°F (21 ± 1°C) [43]. Consequently, the test fabrics were placed in a conditioning room which also housed the test equipment and allowed them to reach their temperature and moisture equilibriums at the previously stated conditions for at least 24 hours, a sufficient time elapse for all fiber types. Because the testing equipment was housed in the conditioning room, the actual testing occurred in the standard laboratory atmosphere for textile testing, eliminating temperature and humidity variations associated with an uncontrolled indoor test environment.

MASS PER UNIT AREA (FABRIC BASIS WEIGHT)

The fabric basis weight was determined as directed by INDA Standard Test Method 130.1-92 with reference to ASTM D-3776 Standard Test Method for Determining the Weight of Nonwoven Fabrics.

Because the carded webs were halved prior to bonding to facilitate calender roll feeding, Option C for determining the mass of small fabric swatches was selected. This option is an effective measure of the weight uniformity across the width of the cards produced with the particular carding machine employed. The fabric swatches (halved card lengths) served as the primary sampling unit from which one card length per replication was selected as the laboratory sample. Two 7" x 6" (17.78 cm x 15.24 cm)

test specimens were cut from each half length, excluding the fabric edges to eliminate the edge variation effects.

Each specimen was weighed to 0.1% of its gross weight using a precision balance. An average mass was calculated from the two observed test specimens and recorded in grams/meter^2 to three significant digits using the expression:

$$\text{G/M}^2 = \text{MASS (G)}/0.02709672\ \text{M}^2$$

The resultant basis weight values for each blend ratio, temperature and solvent concentration combination were used in subsequent flexural rigidity calculations for each of the fabric combinations and as a stress factor determinant in the tensile testing of each combination. The basis weight was measured five times for each combination, each time a different card half length was selected as the laboratory sample from which the two test specimens were cut.

FABRIC FLEXIBILITY (CANTILEVER METHOD)

Consumer acceptance of a fabric is largely determined by its hand, that is fabric characteristics which can be assessed by its touching and manipulation. Tactile characteristics including softness, smoothness, pliability and stiffness are deemed good indicators of garment comfort by consumers. ASTM has dissected the term into eight components, establishing preferred terminology to describe the range of each component [43].

The single most important component of hand is fabric flexibility, that is the ease with which a piece of material will bend, and bend repeatedly without rupture. Bending behavior is largely influenced by fabric construction, thickness, fiber type and denier, and

geometric shape, among other fabrication variables. Flexible fabrics are identified as pliable while more rigid fabric constructions are labeled stiff [43].

Fabric stiffness in bending for a single direction was evaluated for each fabric combination as directed by INDA Standard Test Method IST 90.1-92 Standard Test Method for Stiffness of Nonwoven Fabrics using the Cantilever Test. Four test specimens were cut from each of the remaining card half lengths previously used in assessing fabric basis weight for each replication of every blend ratio, temperature and solvent concentration combination. By sampling the same card half length for basis weight and fabric flexibility, the flexural rigidity calculation was a more truthful measure of the interaction between fabric weight and fabric stiffness as demonstrated by the way the fabric bent under its own weight. This occurs because the flexural rigidity calculation is based on the fabric basis weight and the cube of the bending length. The specimens were free of any abnormal distortions like wrinkles, creases and folds that would influence bending behavior. The test specimens were cut to 1" x 7" (2.54 cm x 17.78 cm) dimensions, the longer dimension being the dimension tested. Because this test is limited to single direction evaluation and because of expressed interest in cross direction stiffness in bending, specimens were cut from both the machine and cross directions. Machine direction stiffness in bending was repeated five times for each fabric combination while cross direction evaluation was limited to a one-time evaluation for the purpose of comparison between the two fabric directions, namely the conformation of orientation effects.

The F.R.L. Cantilever Bending Tester was used to evaluate fabric stiffness in bending. The fabric specimen was placed on top of the smooth horizontal platform and

slowly pushed over the platform edge by the movable slide until the tip of the fabric strip touched the knife edge of the bend angle indicator at an inclination angle of 41.5°. At that instant, the machine was turned off and the length of the fabric overhang was read from a linear scale and recorded in centimeters. At the 41.5° inclination angle, the bending length is exactly half the length of the fabric that overhangs the edge (overhang length, O) and bends under its own weight. Four readings were taken from each test specimen with each side up, first on one end and then on the other end. Although two overhang readings were made for the face of the fabric and two for the fabric back and recorded as face and back measurements, the four measurements were added together and an average overhang length was calculated for each test specimen. The overhang behavior for the two fabric sides was only noted as a reflection of the difference in stiffness resulting from the heat transfer effects associated with pattern/smooth calendar roll combinations.

The average length of overhang for each replication of every fabric combination was calculated from the overhang averages of the four test specimens. This average overhang length was divided by 2 (O/2) to give the bending length (c) expressed in cm. Flexural rigidity (G), a measure of the interaction between weight and stiffness was calculated using the expression:

$$G = W \times c^3$$

where W is the fabric mass per unit area in mg/cm^2. This figure was obtained by multiplying the previously determined basis weight in g/cm^2 by 0.1. The fabric mass was then multiplied by the cube of the bending length (c^3). Results were reported to three significant digits for each direction tested in mg . cm.

FABRIC TENSILE PROPERTIES

The two 7" x 6" (17.78 cm x 15.24 cm) test swatches used to determine the average fabric basis weight for each blend ratio/solvent concentration/temperature combination were used to assess fabric tensile properties because the basis weight value was an integral part of the specific stress calculation. The use of these swatches also permitted a representation of the variation that can occur across the fabric width or length, depending upon the direction of interest. The 7" x 6" swatches were cut into 1" x 7" (2.54 cm x 17.78 cm) test strips; thus, six test strips were obtained from each swatch. Two sets of test strips were obtained from the two basis weight test swatches for each fabric combination. Evaluation of machine direction tensile properties required that the test specimen long direction run parallel with the machine direction while cross direction specimens were cut with the long direction parallel to the fabric cross direction. The IST 110.1-92 Standard Test Method for Breaking Load and Percent Elongation of Nonwoven Fabrics mandates that five specimens in the machine direction and eight cross direction specimens per replication are evaluated. Therefore, five of the six test strips cut from each swatch were broken in the machine direction. The remaining test strip was reserved for SEM microstructural analysis so that visual observation of bonding behavior could be correlated with tensile measurements for each fabric combination. Ten test strips obtained from both basis weight fabric swatches for cross direction evaluation were ruptured. Ten replications of machine direction tensile properties were performed for each fabric combination. Cross direction analysis was limited to 60/40 blend ratio fabrics and was a one-time evaluation for the purpose of confirming preferential lengthwise fiber orientation introduced during card formation.

A United Tensile Tester, CRE type was used to make the tensile measurements. With this type of tensile testing machine, the increase in specimen length is uniform with time. The machine settings were followed as prescribed by ASTM D 1117-80 Standard Test Method for Tensile Testing of Nonwoven Fabrics. A QS5200 Load Cell S/N was attached to the lower stationary clamp. The specimen grips which held the test specimen in place featured smooth, metallic faces. The upper clamp attached to the horizontal crosshead extended the test specimen at a speed of 5.00"/min (12.7 cm/min). When the upper clamp attached to the crosshead traversed upward, its pull exerted on the lower stationary clamp excited an electrical transducer in the load cell. This signal was amplified, recorded on a computer monitor and transmitted to a computer. Peak breaking load, peak specific stress, elongation-at-break and yield point values were recorded.

The peak breaking load is the maximum load required to achieve fabric rupture-that is, the maximum deformation resistance of a fabric in a tensile test carried to rupture. The values were recorded in kg and converted to Newtons by their multiplication by 9.8. Peak specific stress expressed in mN/tex was based on stress (N/m^2) divided by fabric density. Fabric density was calculated by multiplying the fabric test strip width (m) by the fabric basis weight (g/m^2). Therefore, specific stress was determined by the following equation:

SPECIFIC STRESS = LOAD (N)/FABRIC WIDTH (M) X FABRIC BASIS WEIGHT (G/M^2)

Elongation-at-break is a ratio of the change in test specimen length in the direction in which the uniaxial tensile force is applied to the original fabric specimen gauge length. This original gauge length is the specimen length between the fabric grips that is actually

subjected to elongation. This unitless value multiplied by 100% gives the percent that the fabric elongated at break relative to the original specimen length:

$$\textbf{PERCENT ELONGATION} = \Delta L/L_O \times 100\%$$

Yield Point (mN/tex) is very important because it implies load resistance and ductility, hence fabric handle. Until attainment of the fabric yield point, the fabric undergoes elastic deformation, the interatomic and intermolecular bonds in the fibers are stretched. However, when the small force is removed these bonds resume their original positions. The thermal bonds introducing structural integrity to the fabric are stretched, but recover their original positions upon force removal, as well. When the fabric is strained beyond its yield point, some of the intermolecular bonds are broken. This displacement permits the formation of new bonds with newly adjacent chemical reactive groups between the fiber long chain molecules. The fabric thermal bonds are also broken, making recovery of original fabric dimensions impossible.

FABRIC THICKNESS

Fabric thickness, that is the distance between the fabric face and its opposing rear surface was measured according to IST 120.1-92 Standard Method for Measuring Thickness of Nonwoven Materials with reference to ASTM D-1777. Thickness measurements were read, to the nearest 0.02 mm directly from the digital display of a TMI Series 400 Model 49-70 Thickness Testing Machine. As mandated by the machine operating instructions, the machine was allowed to warm up for thirty minutes prior to making the measurements. The digital display was also corrected to read zero using the zero set button prior to specimen evaluation.

Because fabric thickness varies inversely with applied pressure, the same pressure (7.3 psi) was used in making the measurements. A short, fixed time elapse (5 seconds) for full load application by the cycling presser foot (diameter = 0.63") minimized thickness reductions associated with high impact loading. After the fixed time elapse, conditions were stable and suitable for making the readings.

Ten observations were made at random locations across and along a single card half length, free from any abnormal distortions for each replication of every fabric combination. An average thickness was calculated based on the ten observations made for each fabric combination.

FABRIC BURSTING STRENGTH

Fabric bursting strength, that is the pressure required to rupture the fabric by its distention with an rubber diaphragm inflated at right angles to the plane of the fabric was evaluated as directed by IST 30.1-1992 with reference to ASTM D-3786.

The Mullen Hydraulic Motor-Driven Bursting Tester was used to burst an approximate one inch diameter circle of fabric secured under the tension of an upper and lower ring clamp. Prior to specimen testing, a routine verification was performed by bursting five standard aluminum sheet specimens and comparing the average bursting strength to that marked on the pre-tested aluminum sheet package. The average was within the required $\pm$ 5% tolerance level, so testing continued as mandated in the standard.

The hydraulic diaphragm was inflated to cause fabric rupture. The force- that is the pressure in psi units required to rupture the specimen minus the tare pressure required for diaphragm inflation- revealed the actual fabric bursting strength. The card halves

previously evaluated for thickness were used to measure bursting strength. Ten individual observations were made across and along a single card half length for each fabric combination. Care was taken not to sample near the fabric edges or in areas of visual abnormal distortions. Based on the ten observations, an average bursting strength for each replication of every fabric combination was calculated in psi units. This value was converted to kilopascals by multiplying the value, in psi units, by 6.890 Kpa.

The appearance of the test specimens further supported the machine direction preferential orientation of the fibers introduced during carding operations, reflecting the unbalanced machine and cross direction breaking strengths. In unbalanced fabrics, the weaker fiber system fails; however, slit propagation is perpendicular to the failure direction [43]. In most instances, because of low cross direction fiber orientation, the cross direction fibers failed before the machine direction, and consequently the slit ran perpendicular to the cross direction fibers.

FABRIC AIR PERMEABILITY

The INDA standard test method for the direct determination of the air permeability of nonwoven fabrics, IST 70.1-1992 by the calibrated orifice method was used in the evaluation of fabric breathability. Air permeability is defined as the rate at which air flows through a material at a prescribed pressure differential between the two surfaces.

The Frazier Air Permeability Tester employs a suction fan drawing air through a known circular area of fabric, diameter = 2.75 in (70mm). Proper functioning of the test apparatus was established prior to actual specimen testing. This was accomplished by inserting a No. 4 orifice (air nozzle) in the large tank underneath the test apparatus table

and placing a No. 5 brass test plate on top of the opening of the large tank. The variable speed motor was slowly started, adjusting the position of the red oil in the inclined manometer with the assistance of the dial rheostat until a steady 12.7 mm prescribed pressure differential was achieved. The position of the red oil was read from the vertical manometer. This value represented the air flow rate through the test plate, which was converted to air permeability using the test plate conversion table. Because the air permeability was within ± 2% of the expected air permeability labeled on the test plate, testing proceeded. Trial testing determined that a 6 mm orifice was most appropriate for achieving the prescribed 12.7 mm pressure differential between the two fabric surfaces. During actual specimen testing, two operators were used to make the air flow measurements. One operator clamped the fabric over the large tank opening and slowly adjusted the dial rheostat until the oil level in the inclined manometer reached 12.7 mm while the other operator read the position of the red oil in the vertical manometer at the prescribed pressure differential.

One card half was used to conduct the testing for each replication of every fabric combination. Ten observations were made randomly across and along the length of each card half, no closer than one-tenth the fabric width near the edges and in areas free of abnormal distortions.

The air flow rate was then converted to air permeability using the "Results of Calibration of Fabric Air Permeability Machine Flow Nozzles" for a 6 mm orifice, supplied by the apparatus manufacturer. These values provided by the tables were in U.S. customary units of cubic feet of air per square foot of fabric a minute (ft^3/ft^2 . min). These values were converted to metric units (cm^3/cm^2 . s) by multiplication by the

conversion factor of 0.508. An average permeability value based on the ten observations for each fabric combination was calculated and reported to three significant digits at the stated pressure differential of 12.7 mm.

FABRIC TEAR RESISTANCE (ELMENDORF)

The average tear force required for the propagation of a single-rip tongue-type tear after an initial slit to a nonwoven fabric by means of a falling-pendulum (Elmendorf) apparatus was measured according to INDA Standard Test IST 100.1-92. An average tear force was obtained because of the force fluctuation incurred during the completion of the single-rip. During initial tear propagation the load was concentrated on a limited number of fibers which reached a maximum, representing the sum of the individual fiber tear strengths. Upon rupture the load was temporarily reduced to a minimum but ascended with continued elongation until the next set of fibers were affected, continuing this series of maxima/minima until the specimen tore into two separate pieces [43].

Tear deformation is unique from tensile and burst deformation mechanisms because of mobility and orientation effects on observed tear strengths [43]. The binding effects of the cellulose acetate fibers, combined with thermal calendering, locked the fibers into place, inhibiting the shifting and bunching of fibers in response to the applied load. Consequently the beneficial effects of mobility associated with woven fabric interlacings would not be appreciated with the experimental nonwoven fabrics [43]. Most assuredly the observed nonwoven tear strengths were considerably lower than those for a similar basis weight/fiber type woven construction. The experimental fabrics also refused to tear in the machine direction because of the excessive preferential machine direction fiber orientation introduced during carding. The excessive machine direction

fibers inevitably dissipated the tear force across the weaker cross direction, causing crosswise tearing [43]. Because the standard test method mandates that all tears that deviate 6 mm away from the original slit- indicating crosswise tearing of the system of fibers under test- be discarded, no machine direction tear strengths for all fabric combinations could be recorded. Thus tear strengths were only recorded for the cross direction test specimens.

Ten test specimens per replication were cut at intermittent locations along the length of a single card half for every fabric combination. They were cut away from the fabric edges to overcome edge variation effects, and their random placement was intended to reflect web variation in weight, fiber orientation and bond strength. The cross direction specimens were cut to specified dimensions of 2.5" x 4" (63 mm x 100 mm) with the short dimension parallel to the machine direction fibers. Care was taken to make sure that the fibers in the short dimension were parallel so that, during subsequent tear propagation, the tear would continue between these fibers, not across them. A 20 mm initial slit was made using the slitting knife that accompanied the tester. The falling pendulum Elmendorf Tester Model Cat 60-200, specially designed for lightweight-tissue type fabrics, was used. At its maximum potential energy, the falling pendulum was released and tore the test specimen through a fixed distance of 43.0 mm. The scale was read to the nearest whole scale division. Because the scale reflected the percent of the pendulum's original potential energy consumed in tearing the specimen, the scale reading was multiplied by a factor appropriate for the type and capacity of the particular tester used to obtain the average tearing force, in grams. The appropriate factor, 32, was obtained from the Annex Section A1.4 Table A1 of the standard test method. The

average tearing force, in grams was based on the ten observations made for each fabric combination.

SEM Microstructural Analysis

An Hitachi Model F-3200 N Scanning Electron Microscope was used to take both low and high magnification pictures of the fabric bond points for all of the 75/25 cotton/cellulose acetate blend fabric combinations. No metallic tapes or coatings were required to dispel charge buildup that typically occurs with beam penetration of textiles because this machine offers the convenience of variable gas pressure, thus creating a partial vacuum instead of a high pressure vacuum. The controlled presence of air allows the built up charges in the fabric specimen to be dispelled, eliminating the unnatural lighting effects that typically hinder the appearance of textile photomicrographs. Photomicrographs were made of each fabric combination for the selected blend ratio and the images were also saved as bitmap files to a computer disc so that paper copies could also be made using a high-resolution laser printer.

4. RESULTS AND DISCUSSION

GENERAL COMMENTARY

The ability of acetone to plasticize the cellulose acetate fibers at room temperature was clearly evident, as significant improvements in fabric performance properties were realized. The performance of control fabrics in which the web cellulose acetate fibers were not subjected to solvent modification fell drastically short of comparable treated fabrics, even at the harshest bonding temperature. It was difficult to ascertain any disparities in properties among the control fabrics for all three selected bonding temperatures. For the selected bonding temperatures, the role of plasticization in achieving sufficient chain segmental mobility for binder flow to occur, precluded any beneficial effects associated with additional thermal input brought on by bonding temperature elevation. These findings also suggest that the second-order transition temperature for the unmodified cellulose acetate fibers exceeded the harshest 190°C bonding temperature.

However, when the web cellulose acetate fibers were subjected to acetone modification prior to their consolidation, the role of temperature in enhancing the newly softened fiber flow became evident. For a given blend-solvent concentration combination, those webs consolidated at the low end of the temperature range (150°C) had considerably less mechanical integrity than those webs consolidated at the higher temperatures (**Figure 12,13**). Upon initial examination of the data, it was difficult to identify any additional benefits associated with increased temperature for a given blend system-solvent concentration, especially for 60/40 blends treated with the highest solvent

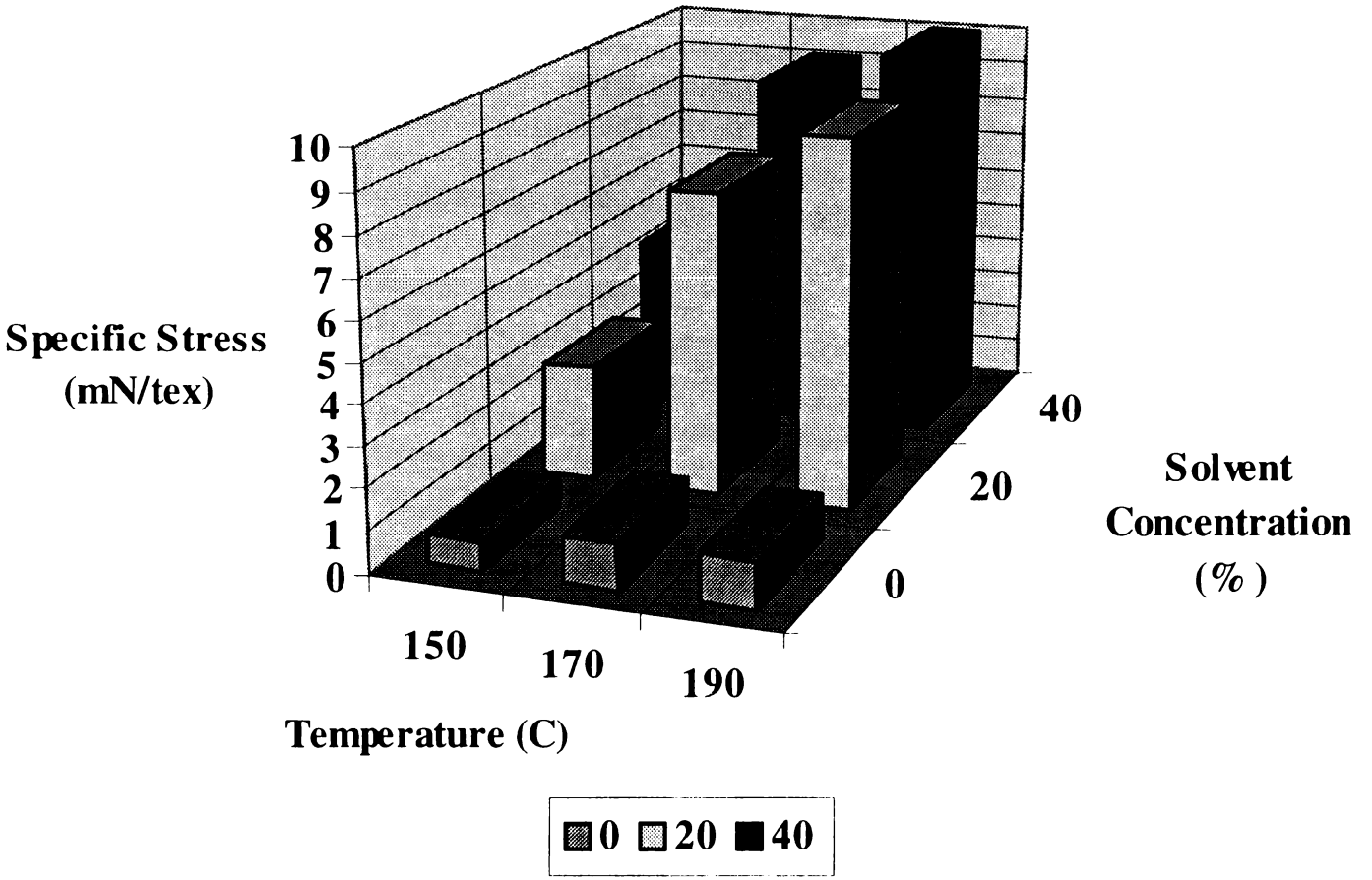

Figure 12: Temperature Effects on Fabric Specific Stress for 75/25 Blend Systems

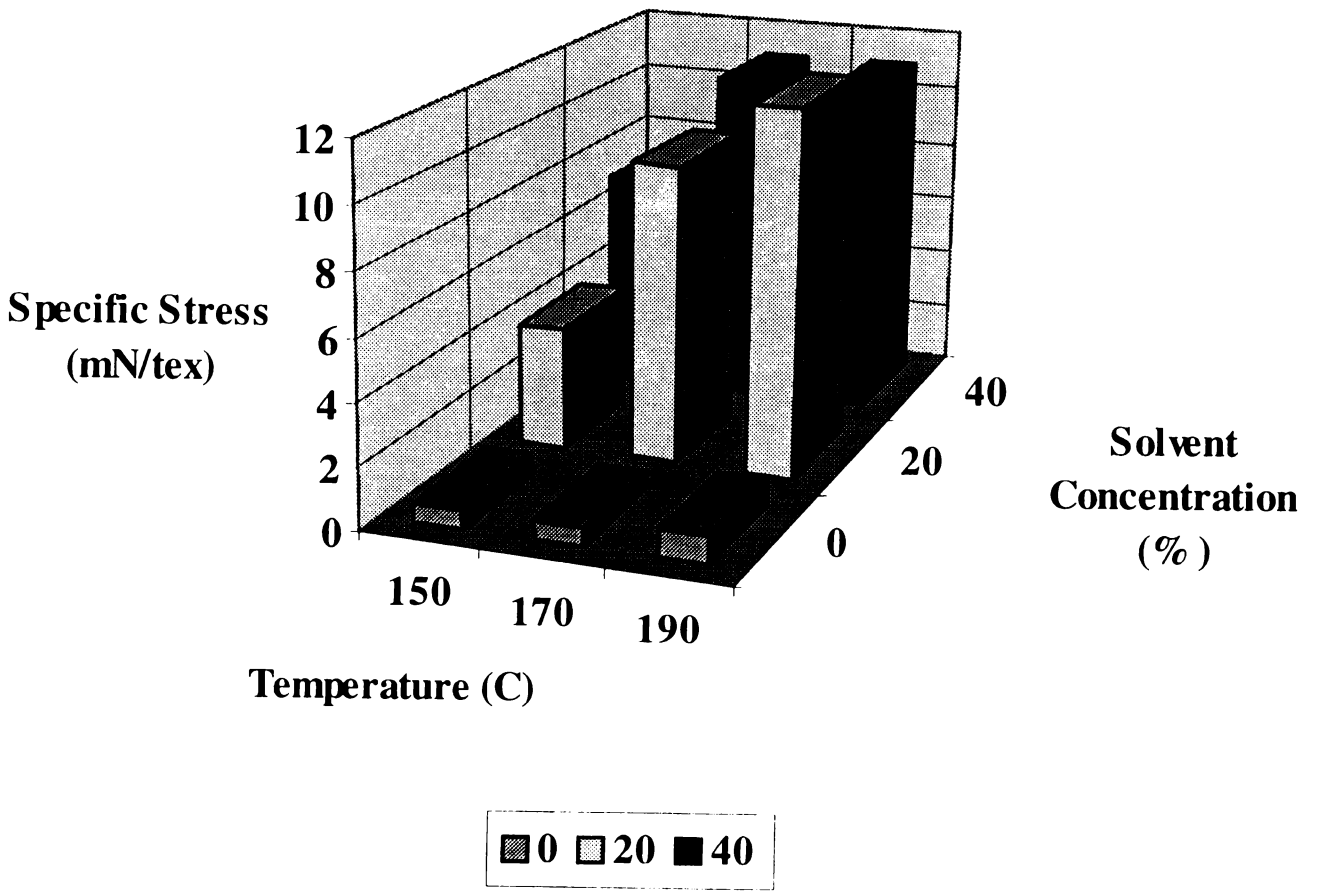

Figure 13: Temperature Effects on Fabric Specific Stress for 60/40 Blend Systems

concentration (40%) and bonded at the midpoint (170°C) and temperature extreme (190°C) (**Figure 13**).

Fabric hand was affected by increased thermal input, as reflected by flexural rigidity calculations for a given blend-solvent concentration combination. (**Figure 12**) The increased temperature supplied more thermal input to the point of contact such that greater thermal energy was available. This added presence of thermal energy for thermoplastic binder enhanced melting, flow and fusion capabilities. Hence, the individual bonds became more definitive and stronger; thus, a stiffer structure emerged. However, without further statistical treatment, it is difficult to ascertain whether the diminished fabric flexibility associated with temperature elevation is significant.

Without any further statistical or microstructural consideration, two preliminary conclusions can be asserted. Given the superior mechanical integrity of those treated webs consolidated at the higher bonding temperatures (170 and 190°C) relative to similar webs consolidated at 150°C, plasticization of the amorphous cellulose acetate binder fibers did not result in the suppression of their second order transition temperature such that the sufficient thermoplastic melting and flow could be achieved at the 150°C bonding temperature. Rather, plasticization did support sufficient chain segmental mobility such that the binder glass transition temperature was depressed in the range of the 170 to 190°C consolidation temperatures. These findings agreed with the existing patent literature that held that plasticization of cellulose acetate fibers permitted fiber coalescence at lower than normal processing temperatures (177 to 191°C). Quantitative analysis of the depression of the acetate binder glass transition temperature could be

made using differential scanning calorimetry (DSC) measurement techniques. The T_g of the original, unmodified acetate fibers could be measured and compared to the T_g of the modified acetate fibers. The isolation of a numerical figure for the T_g of the modified fibers might permit the identification of a single bonding temperature at which sufficient thermal input would facilitate complete binder melting and flow given the early conclusion that no real difference in the mechanical integrity of webs consolidated at the two higher temperatures, 170 and 190°C, exists.

The effects of web saturation prior to and upon subsequent thermal calendering cannot be overlooked in the determination of the ideal fiber unification, however. The fibrous web was highly saturated following padding operations, so saturated that upon its passage through the nip, the calendar rolls served as an additional squeezing mechanism by which the liquid excess was diverged, either by its evaporation or actual physical exit in the form of back-splash. Quite obviously, this excess solution presence interrupted the heat transfer mechanism, reducing the available heat for thermoplastic melt completion. Evaporation of the effluent took precedence over thermoplastic melting. Consequently, the web thickness temperature was never permitted to ascend the temperature of the rolls and, quite probably, the heat required to produce sufficient fabric temperature elevation for complete thermoplastic melting was never achieved. Those webs bonded at the lowest selected temperature, 150°C, would have been most greatly affected by this phenomenon. These observations are in accordance with previous work in which the presence of water brought on by the washing of DMF-modified PET filaments reduced the effective heat introduced during subsequent thermal/mechanical stressing such that resultant recrystallization was limited.

These findings would suggest the evaluation of add-on effects introduced during padding operations and the possibility of treated web passage through either a drying oven or a heated oven to facilitate effluent evaporation prior to web consolidation, thereby restoring the effective temperature experienced by the thermoplastic binder fibers. The amount of add-on introduced during padding operations should be measured and reduced to some level that will not limit heat transfer, yet still retain a sufficient presence of plasticizer that will promote the necessary chain segmental motion to promote binder flow at lower bonding temperatures. Furthermore, the additional heat input combined with the chemical input may support further glass transition temperature depression and facilitate even lower temperature bonding than the preferred 170-190°C range. The acetate fibers were modified at room temperature and did facilitate bonding at lower temperatures than dry, untreated fibers. However the previously mentioned work found that the combination chemical/thermal inputs enhanced other properties such as dye diffusion and equilibrium uptake because recrystallization, noted by the presence of external/internal surface cavitation and shrinkage, was more intensive than that noted for either chemical or thermal/mechanical stressing, alone.

Consideration of the effects of additional solvent presence on fabric mechanical integrity at hand suggested the significance of interactions between blend ratio, solvent concentration and web consolidation temperature. For any 75/25 blend system and bonding temperature treated with 20% and 40% acetone, improved mechanical integrity was marginal with additional solvent (**Figure 14**). Improved fabric tenacity was more marked for those fabrics consolidated at 150°C (**Figure 15**). The enhanced solvent presence (20% to 40%) overcame the temperature limitations imposed by the 150°C

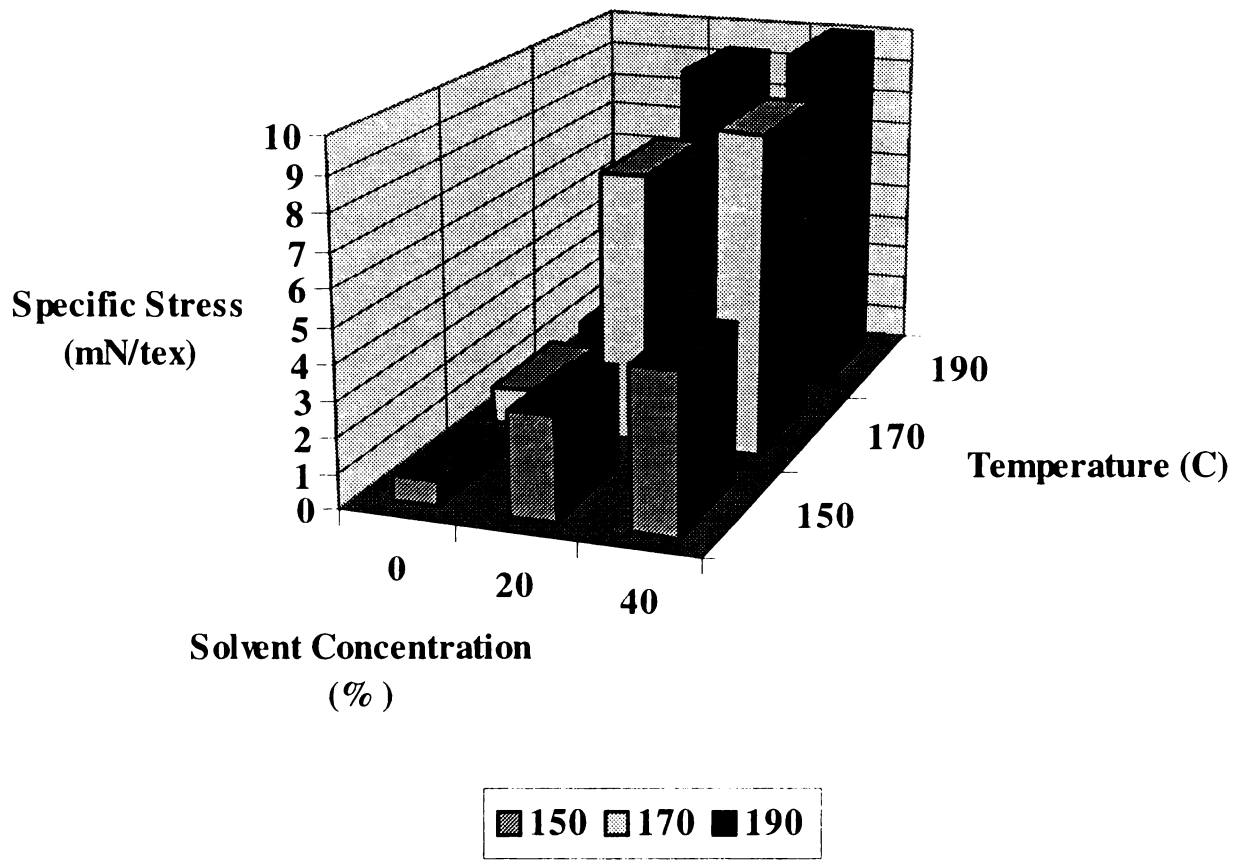

Figure 14: Solvent Concentration Effects on Fabric Specific Stress for 75/25 Blend Systems

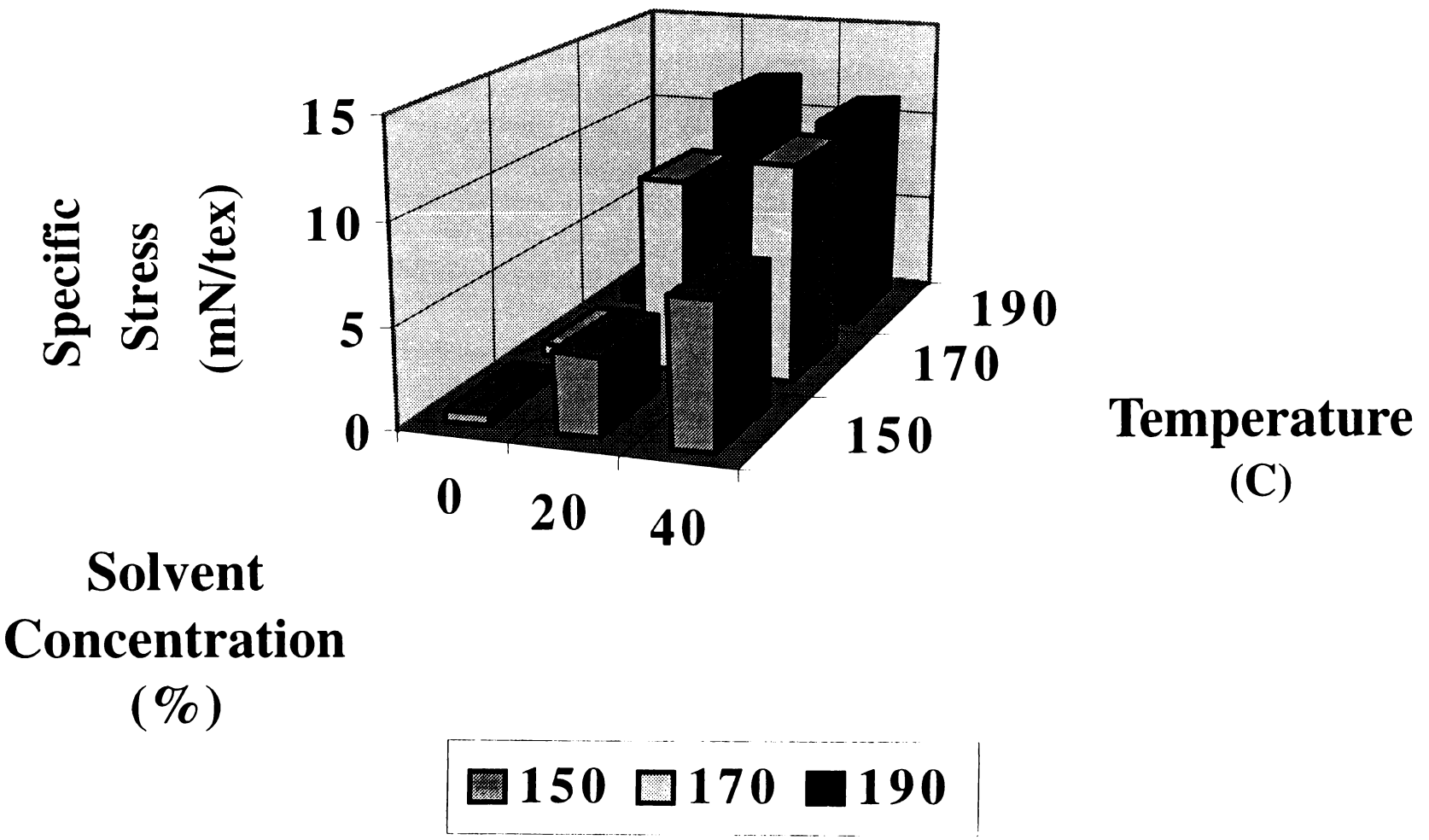

Figure 15: Solvent Concentration Effects on Fabric Specific Stress for 60/40 Blend Systems

bonding temperature, a consolidation condition far lower than the thermoplastic binder T_g. Increasing the chemical input provided additional means to overcome activation barriers to segmental motion. The additional plasticizer permitted a more thorough disruption of localized intermolecular bonds that enhanced chain mobility and ultimately permitted more complete thermoplastic binder melting. Therefore, even though the mechanical integrity of those 75/25 treated webs bonded at 150°C was very poor compared to similar fabrics consolidated at the higher temperatures, substantial improvements in the mechanical integrity of these fabrics bonded at this low temperature could be realized by increasing the solvent concentration. The mechanical integrity of 60/40 fibrous blends coalesced at 150°C were especially influenced by the addition of more solvent (**Figure 16**). This would suggest the interaction between the acetate percentage in the blend system and solvent concentration. The data once again illustrated the positive tensile performance associated with added solvent. For 60/40 blends bonded at 150°C, the specific stress for those fabrics subjected to 40% acetone almost doubled that of similar fabrics subjected to 20% acetone (7.2 mN/tex vs. 4 mN/tex). And, relative to those fabrics that contained less acetate in the blend system (75/25), the strength enhancement for 60/40 fibrous blends consolidated at 150°C and treated with 40% acetone was considerably greater (7.2 mN/tex for 60/40 vs. 4.5 mN/tex for 75/25 blends).

One can offer two explanations for the disparities in tensile performance between the two selected blend systems relative to incremental solvent concentration increase. Generally speaking, the greater the binder presence the more superior the fabric integrity, as previously noted in other thermal calendering studies. Common sense would lead one to conclude that the greater availability of binder would mean more binder flowing to

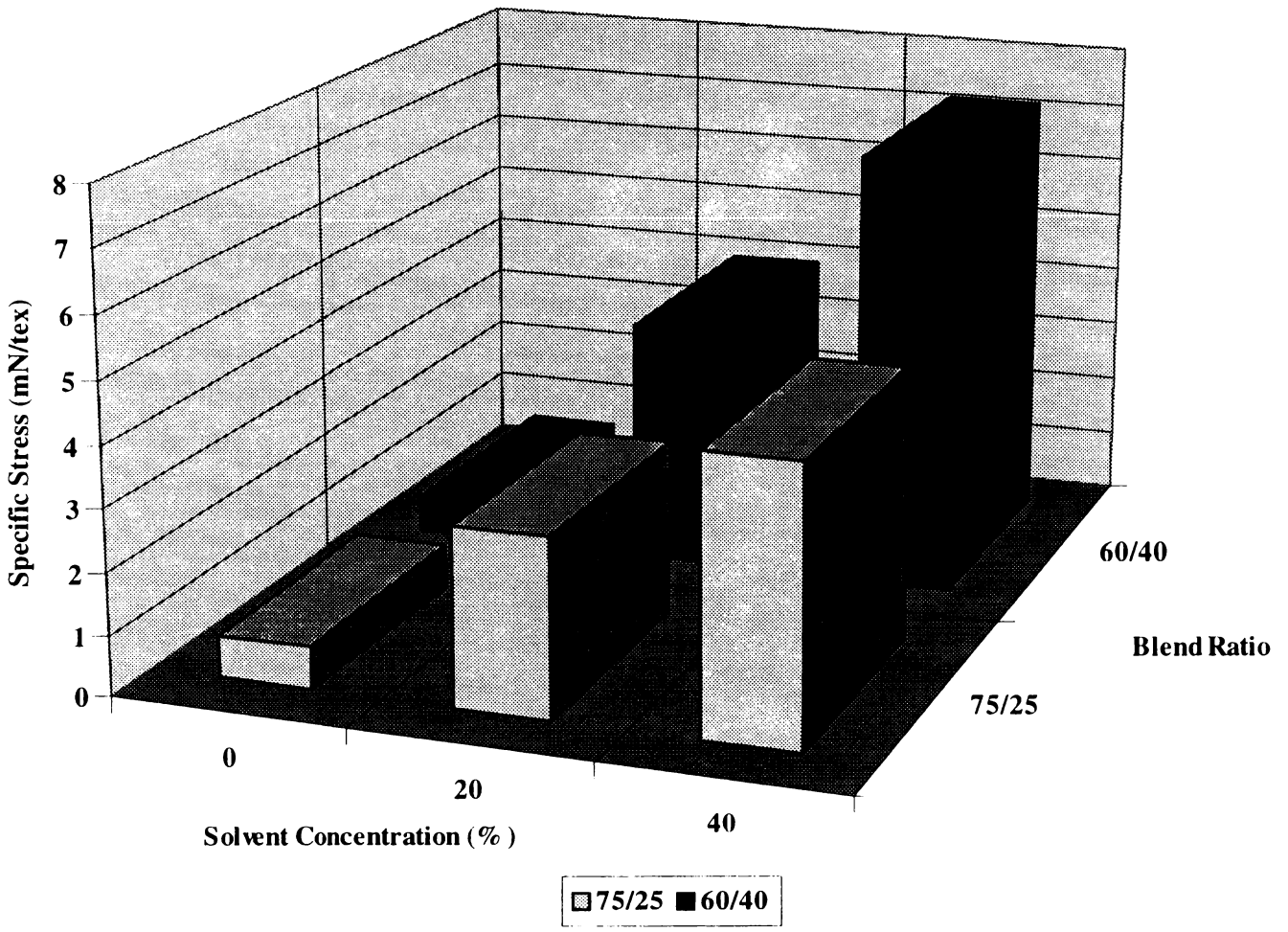

Figure 16: Blend Ratio Effects on Fabric Specific Stress for Fabrics Consolidated at 150 C

each individual bond site. Subsequent bonds become more definitive because of increased binder-binder and binder-base fiber contacts.

Again, for 60/40 webs consolidated at 150°C, marked improvements in web mechanical integrity with increased solvent modification were noted similar to the 75/25 blends bonded at the same temperature. However, the improvement for 60/40 blends was more appreciative. Increased solvent concentration for 75/25 blends unified at 150°C improved the specific stress by 1.6 mN/tex. The specific stress improvement for 60/40 blends subjected to 20% and then 40% acetone was double that figure, 3.2 mN/tex to be exact (**Figure 17**). Again, despite the thermal limitations to thermoplastic melt completion imposed by the 150°C bonding temperature, binder fusion could still be achieved in the presence of a solvent. However, the available thermal input combined with chemical modification still fell short of the heat energy required for complete thermoplastic melting. The enhanced bonding achieved with solvent modification was magnified by the larger presence of acetate binder. It is interesting to note that for all control fabrics, irrespective of bonding temperature, the specific stress for 75/25 blends always exceeded that of the 60/40 blends (**Figure 16,17,18**). Because no added chemical input was used to achieve the required chain segmental mobility for glass transition temperature suppression, only thermal input was used to facilitate thermoplastic fusion. Therefore, the available thermal energy fell short of that required for binder melt completion. Consequently, in the 75/25 blends, more thermal energy was available for each potential bond site such that more complete bonding occurred. While in the 60/40 blends, greater binder presence meant more energy consumption in the binder melt

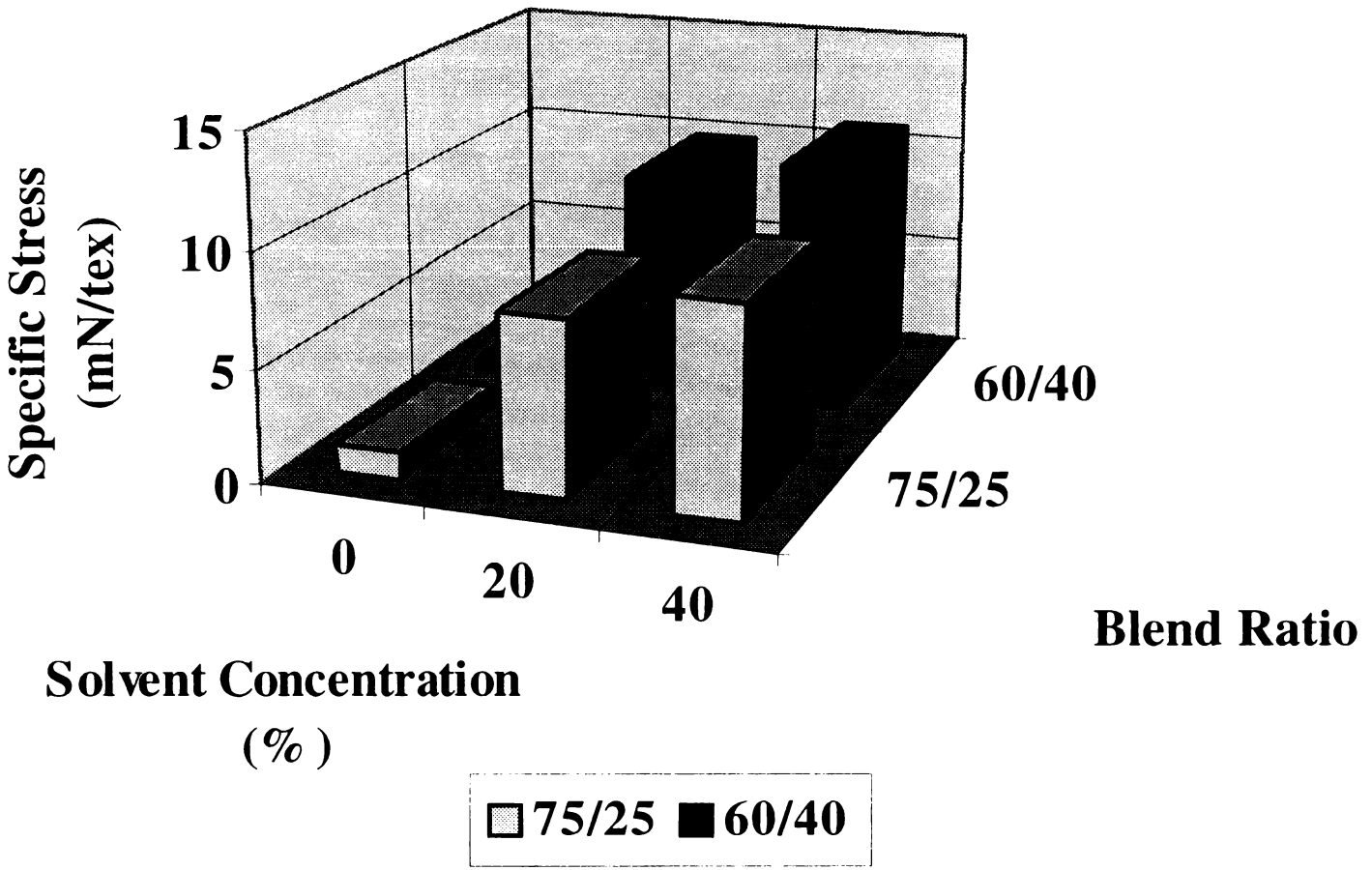

Figure 17: Blend Ratio Effects on Fabric Specific Stress for Fabrics Consolidated at 170 C

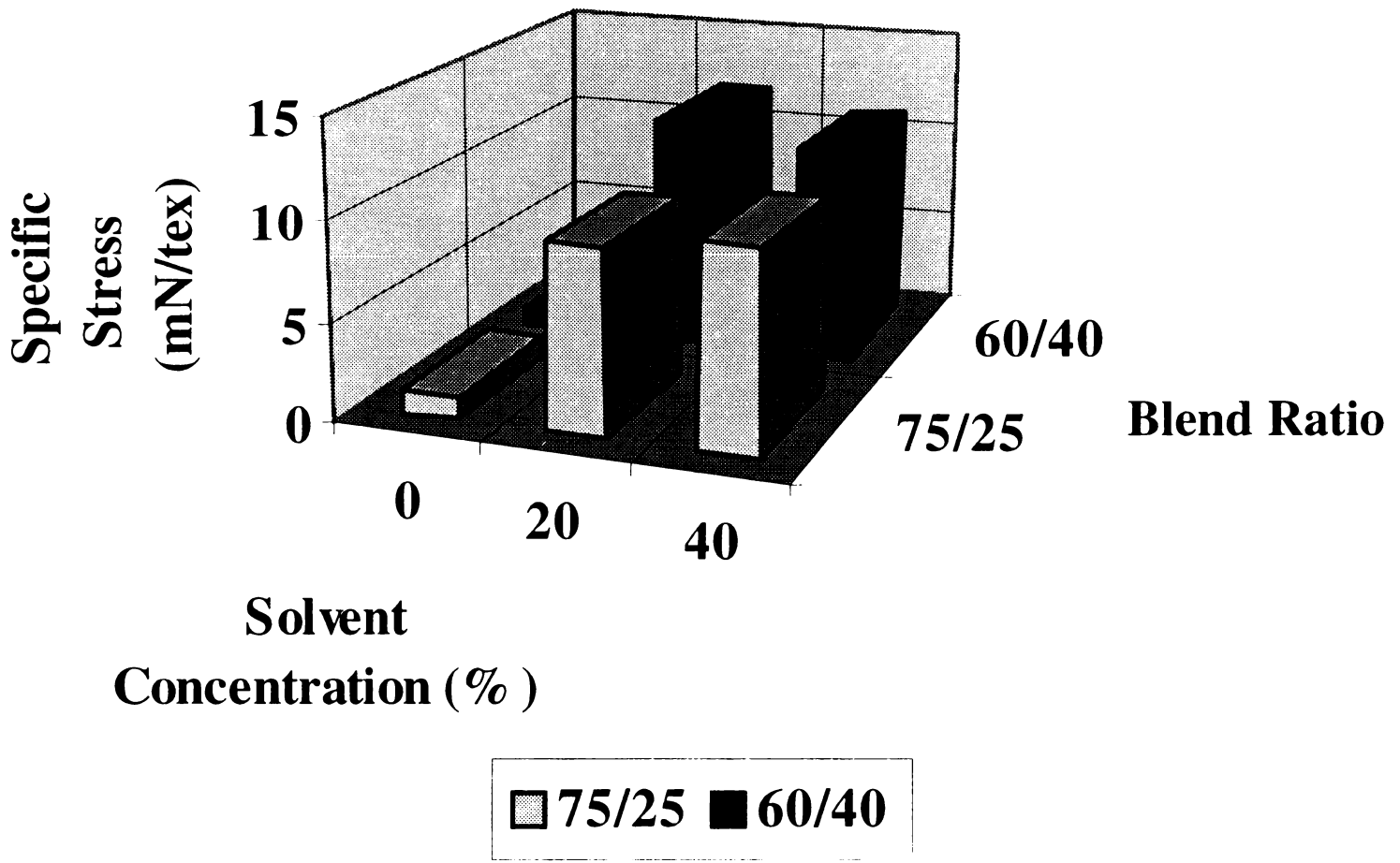

Figure 18: Blend Ratio Effects on Fabric Specific Stress for Fabrics Consolidated at 190 C

process was required; hence, less energy was supplied by the limitations of the selected 150°C temperature and there was less energy available per individual bond site.

For both blend systems, with increased web consolidation temperature, the ability to discern any added benefit with additional acetone is a challenge (**Figure 16,17,18**). This would suggest that mechanical integrity can be significantly enhanced with as little as 20% acetone. This assertion has great economic and environmental consequences for the potentially successful commercialization of this process. Aside from the mere expense of the solvent, the design and implementation of solvent recovery systems can be quite expensive, thus impeding industrial willingness to promote and accept solvent modification in textile wet processing operations.

Generally the mechanical integrity of 60/40 blends subjected to acetone plasticization superseded similar 75/25 blends. It is impossible to ascertain the significance of the relationship between blend system and mechanical integrity without further statistical evaluation. However, previously cited work identified an inverse relation between fabric tenacity and cotton content. With elevated temperature, however, less disparity between similar fabrics for both blends could be identified (**Figure 17,18**). Even though less binder in the higher cotton percentage blend meant less available binder per individual bond site, there was more unit energy per individual bond site available such that more efficient melt completion occurred.

Process variables such as bonding speed coupled with effluent evaporation may have further intensified the proposed blend system/mechanical integrity relationship, especially for the 75/25 blends. Although the speed (10 m/min) was deemed sufficient contact time for binder melt completion, the effluent evaporation depleted available

energy for binder softening. The web thickness temperature failed to ascend the effective roll temperature. Hence, even though theoretically there should be more unit energy available per individual bond site with diminished acetate presence, at this speed, in the presence of residual effluent the energy available is diminished.

Given the environmental soundness and desirable qualities associated with higher cotton content nonwovens, consideration of recent cellulose acetate microfiber technology in the role of thermoplastic binder applications is warranted. The greater surface area afforded by microfiber technology combined with the additional surface area created by the plasticization effects, i.e. surface cavitation, would provide more available bonding area per fiber. Hence, there would be increased binder/binder and binder/base thermal welding.

Fabric hand was also relatively unaffected by additional solvent; however, it was sensitive to temperature elevation, as would be expected (**Figures 19,20,21,22**). All other fabric and process variables held constant. Greater thermal energy available per individual bond site meant more complete, definitive bonding; hence, the emergence of a stiffer structure. It was somewhat surprising to observe less stiffness for 60/40 fabrics for any temperature-solvent combination compared to similar 75/25 fibrous webs. Although, without further statistical consideration, it is difficult to ascertain the significance of this observation. One explanation would be the previously offered one of the efficient energy consumption associated with less binder.

Over the course of this study the researchers considered the possibility of using the very same processing conditions and solvent modification techniques for the fabrication of ultra lightweight webs with a target basis weight of 25 to 30 g/m^2. This

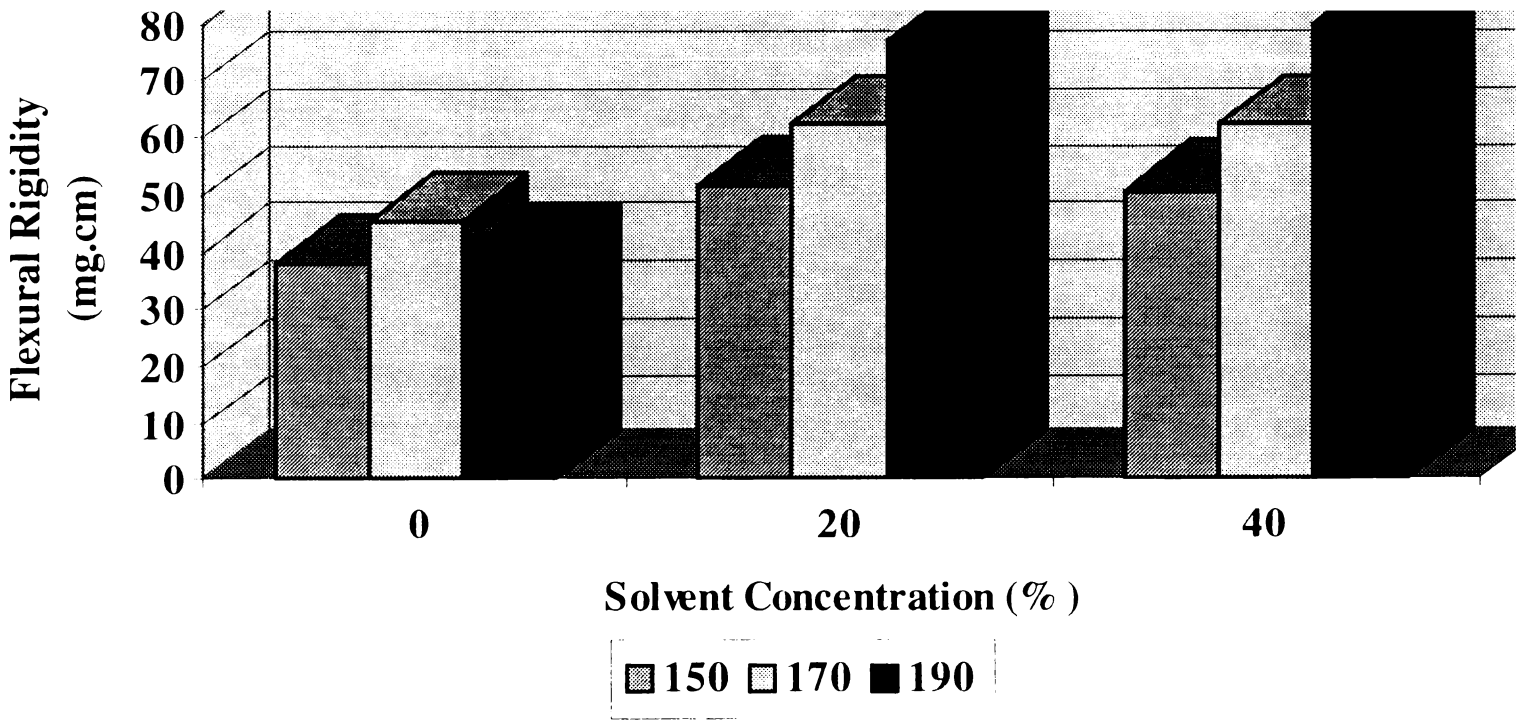

Figure 19: Solvent Concentration Effects on Fabric Flexural Rigidity for 75/25 Blends

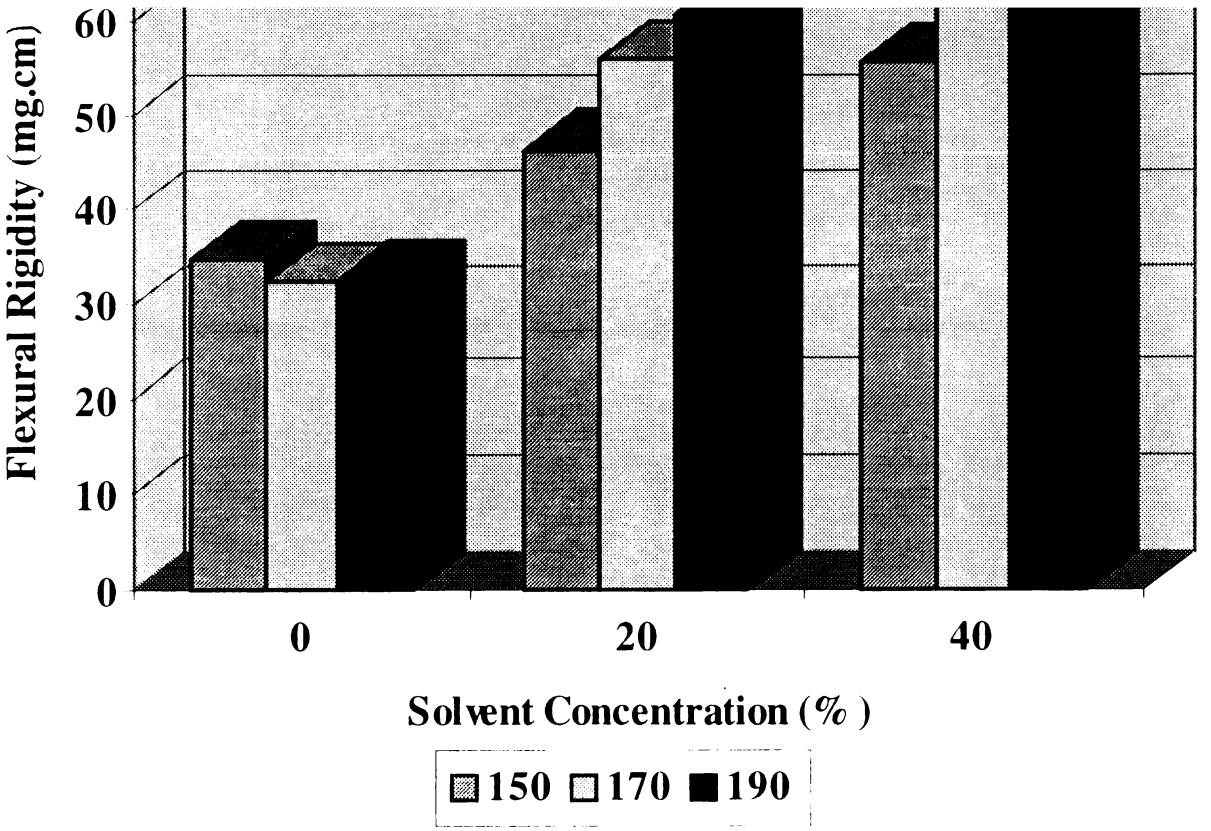

Figure 20: Solvent Concentration Effects on Fabric Flexural Rigidity for 60/40 Blends

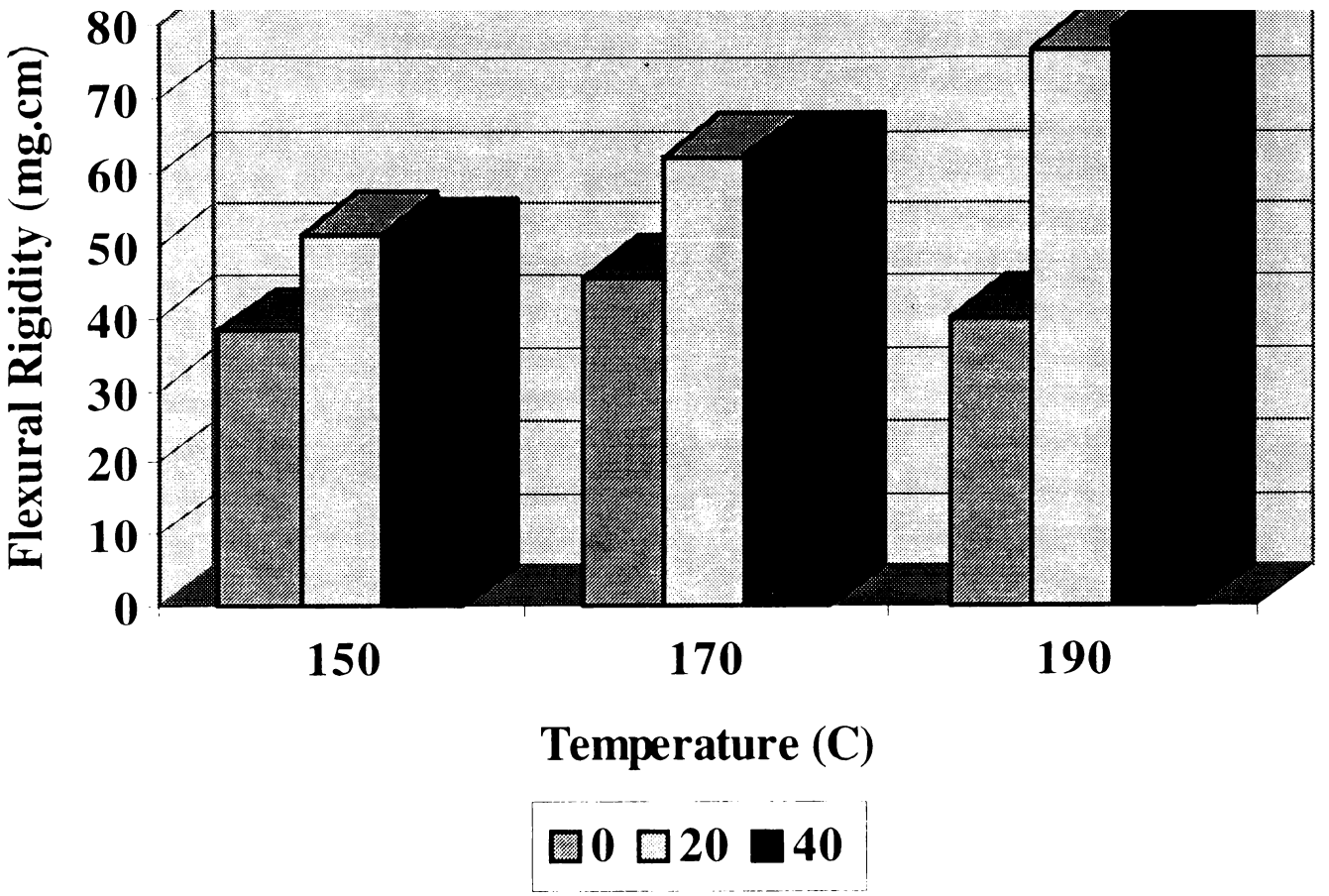

Figure 21: Temperature Effects on Fabric Flexural Rigidity for 75/25 Blends

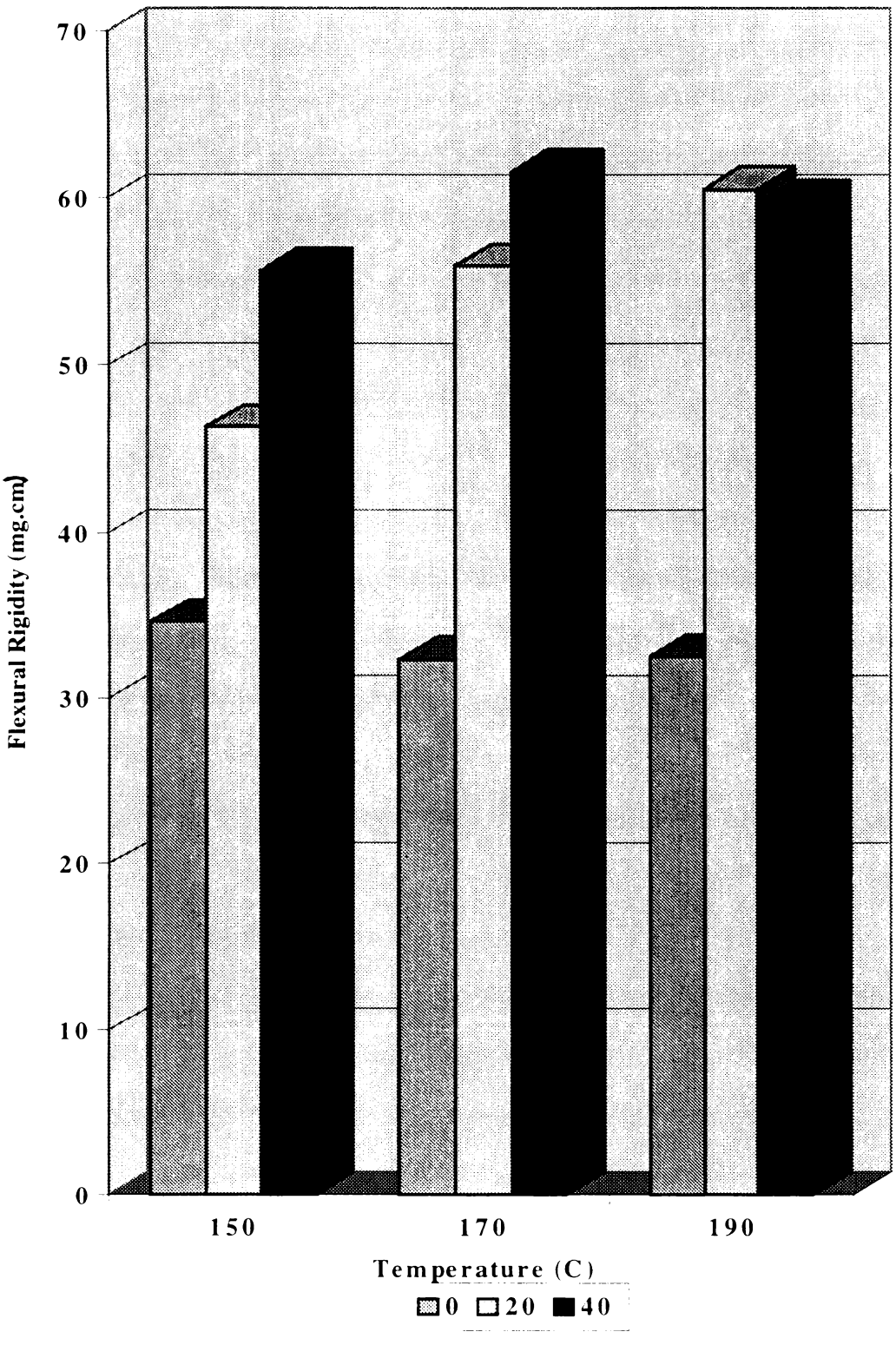

Figure 22: Temperature Effects on Fabric Flexural Rigidity for 60/40 Blends

web weight would present these fabrics as very viable baby diaper and adult incontinence coverstock materials. Because the preliminary data analysis suggested the superior mechanical integrity of 60/40 blend systems and the inadequacy of the 150°C bonding temperature, the process was applied to the 60/40 fibrous webs bonded at 170 and 190°C.

Unlike the early webs with a target 40 g/m^2 basis weight, these lighter specimens seemed to be more responsive to elevated temperature with respect to web stability. For either solvent concentration (20 and 40%), the additional thermal energy enhanced specific stress by approximately 3 mN/tex (**Figure 23,24**). The additional solvent failed to make any significant strength contribution, as was previously suggested by heavier web analysis (**Figures 25,26**). However, without any solvent modification, web stability was sacrificed at the most extreme temperature, once again suggesting the necessary glass transition suppression to impart web mechanical integrity through facilitation of bonding (**Figures 25,26**). Greater temperature sensitivity is probably attributed to the diminished web thickness. Diminished web thickness implies that the thickness of the web throughout ascends the effective calender roll temperature more thoroughly. The region of uniform temperature throughout the web equivalent to roll temperature should have also been a greater distance from the nip than the distance for thicker webs, all other bonding conditions held constant. Thus, the additional 20°C heat increment more greatly influenced the web stability of the lighter webs. Because the heavier web tenacity was largely unaffected by additional thermal input beyond 170°C, the question arises about the appropriateness of the selected bonding temperatures, speed and nip-line pressure for the application of this process for the fabrication of webs whose weights exceed 40 g/m^2.

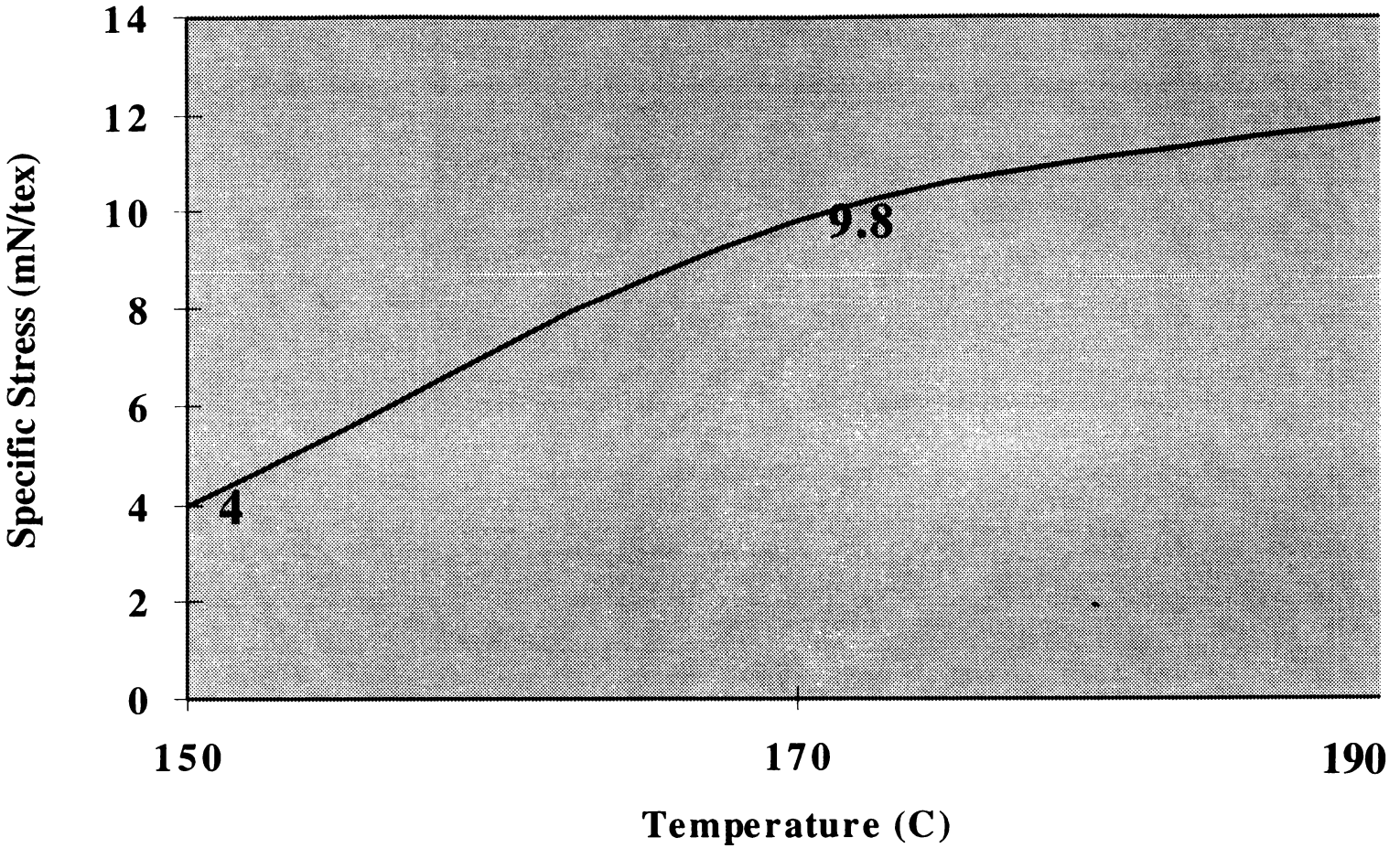

Figure 23: Temperature Effects on Fabric Specific Stress for 60/40 Blend Systems Modified with 20% Acetone

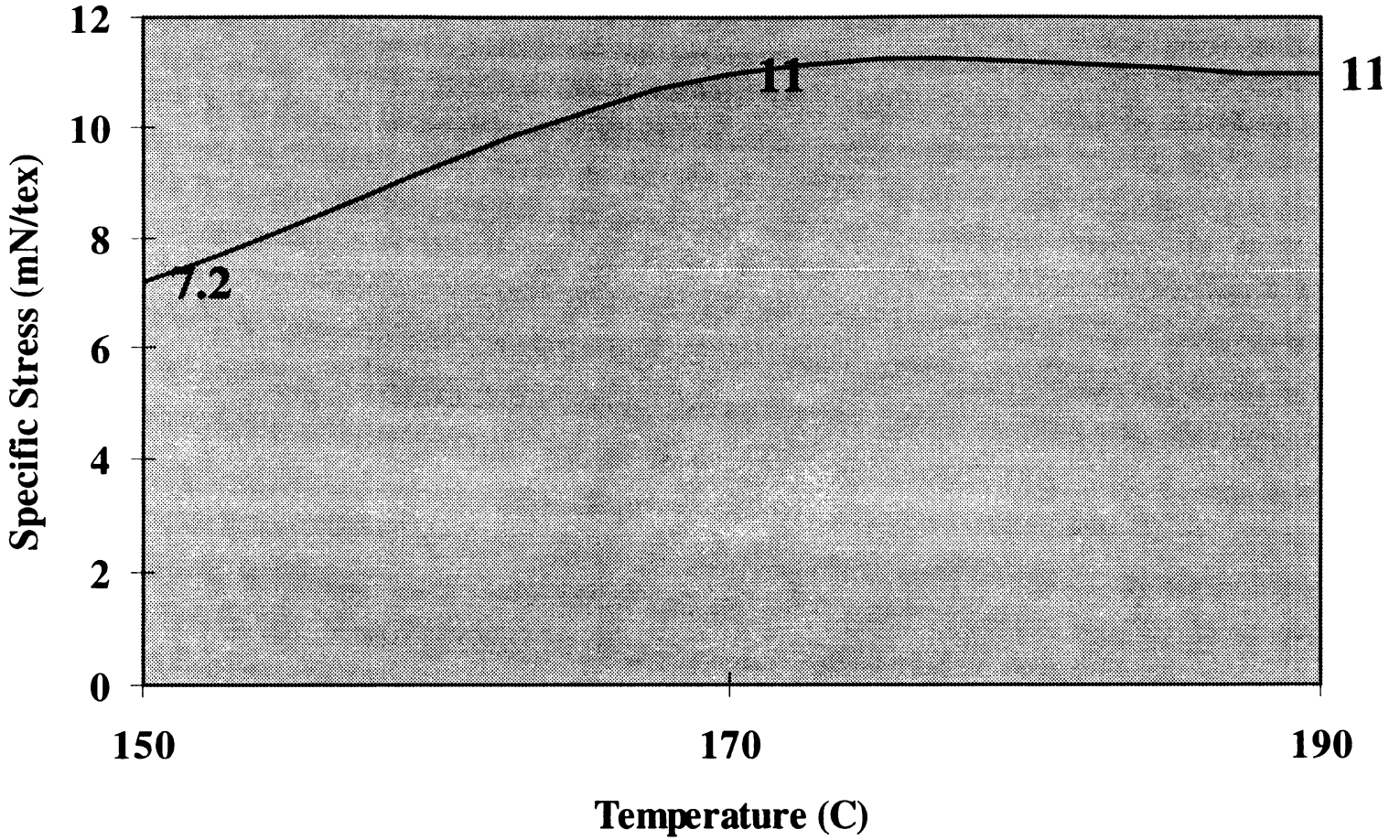

Figure 24: Temperature Effects on Fabric Specific Stress for 60/40 Blend Systems Modified with 40% Acetone

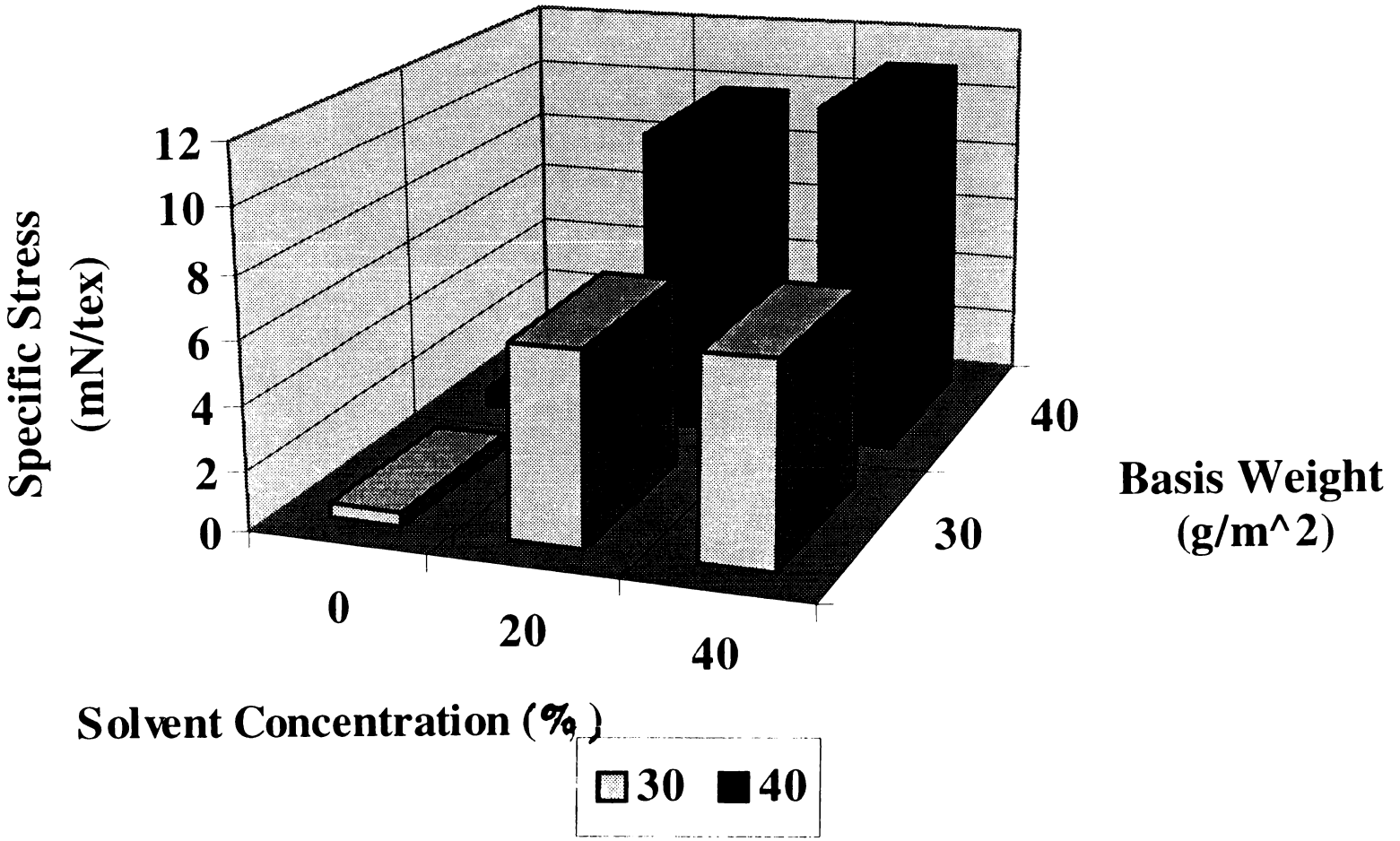

Figure 25: Basis Weight Effects on Fabric Specific Stress for 60/40 Blends Consolidated at 170 C

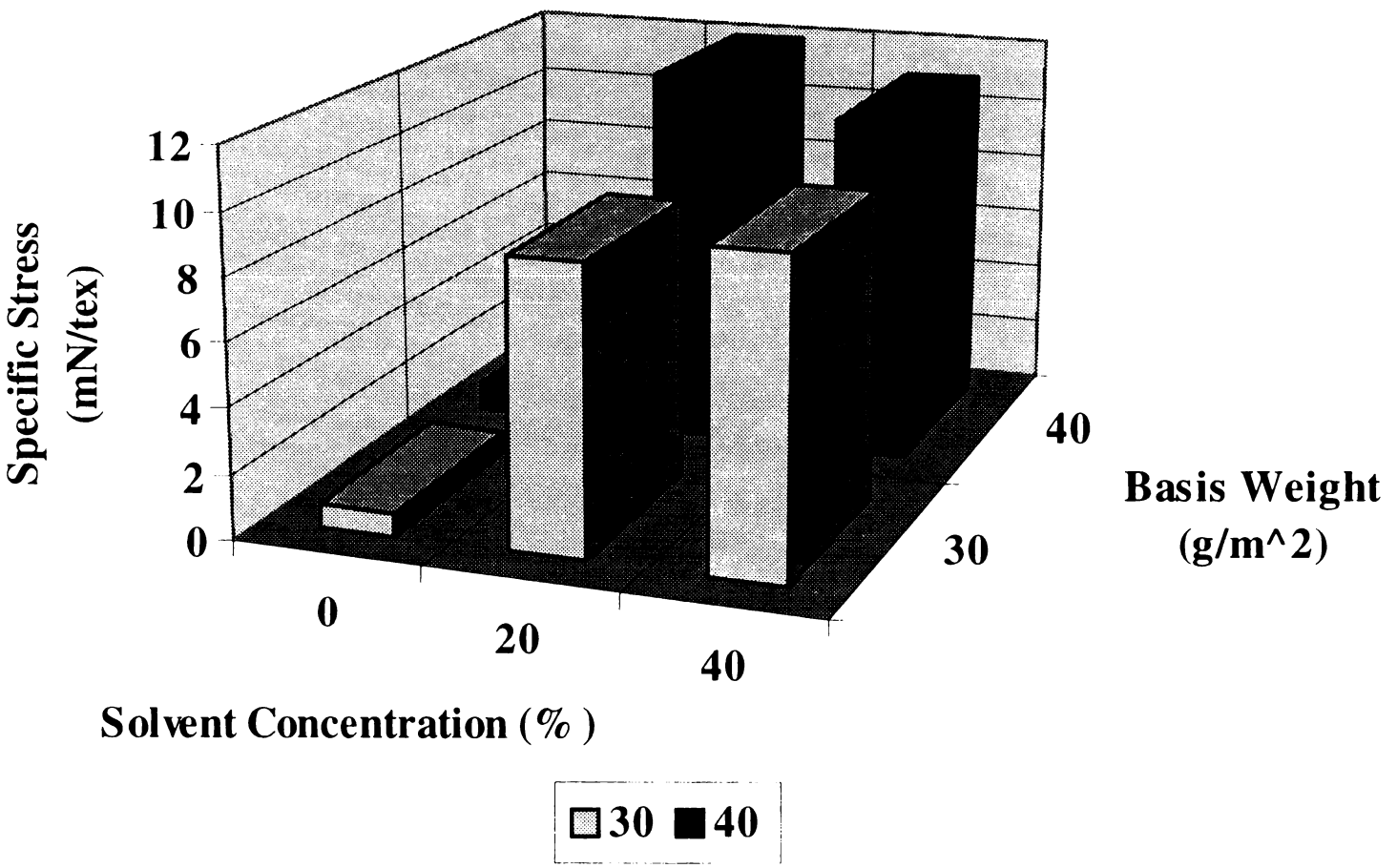

Figure 26: Basis Weight Effects on Fabric Specific Stress for 60/40 Blends Consolidated at 190 C

Given the responsiveness of the lightweight webs to added temperature and the subsequent enhanced web stability, one would expect these webs to be stiffer than the similar heavier webs. This was not the case. In fact, the lighter webs were approximately 50% more flexible than their heavier counterparts and the additional temperature and solvent appeared not to have a detrimental effect on fabric hand (**Figures 27, 28**). Instead, it would appear the greatest influence on fabric flexibility would be the diminished fiber frequency per unit area associated with diminished web weight.

Fiber frequency effects would explain the superior mechanical integrity of the heavier webs. The lighter weight webs would imply fewer fibers per unit area for distribution of tensile loading. Generally, the heavier web specific stress was 4 to 5 mN/tex greater than similar lighter webs bonded at 170°C for either solvent concentration (**Figure 25**). At 190°C, particularly with 40% acetone, the lightweight web mechanical integrity more closely resembled the heavier web integrity, with approximately 1.3 mN/tex disparity, suggesting at this temperature the diminished fiber frequency; hence, diminished binder/binder and base/binder fiber contacts created by their physical proximity was overcome by enhanced binder flow (**Figure 26**).

The effects of mechanical web formation on the mechanical integrity and dimensional stability of nonwoven fabrics cannot be overlooked in the analysis of process variables effects on fabric performance properties. Generally, the machine direction tenacity is five times greater the opposing cross direction and the results of this study were no exception. The machine direction specific stress for 60/40 fibrous blends consolidated at 170°C at both solvent quantities exceeded the opposing cross direction by

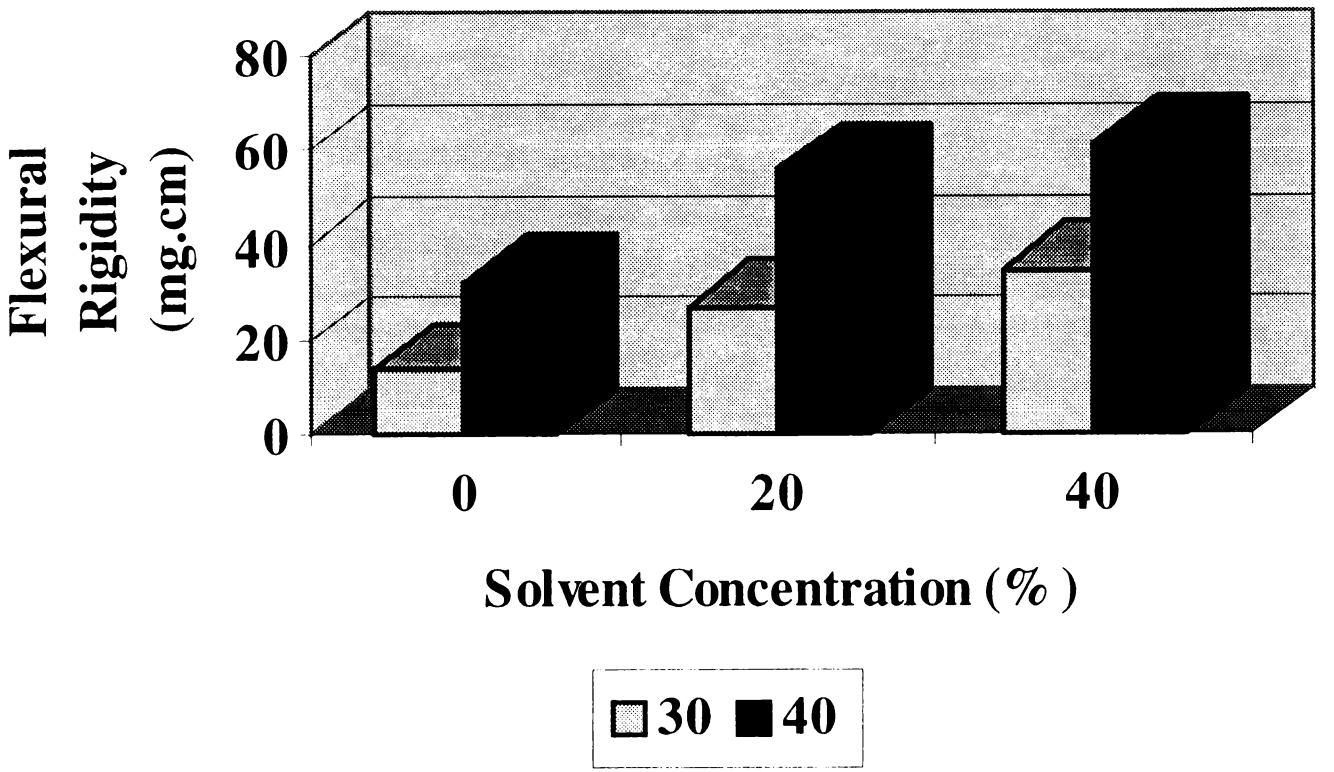

Figure 27: Basis Weight Effects on Fabric Flexural Rigidity for 60/40 Blends Consolidated at 170 C

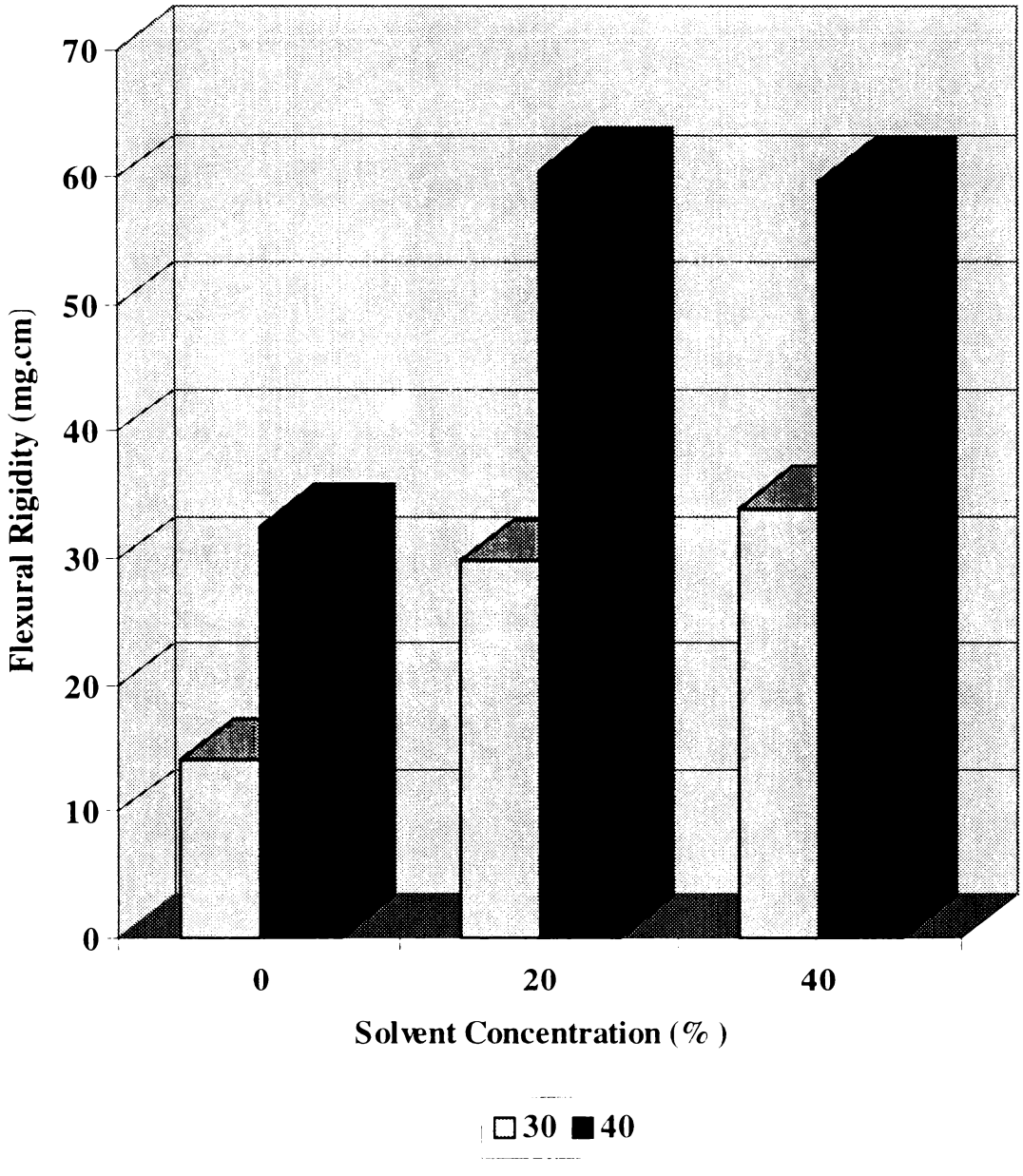

Figure 28: Basis Weight Effects on Fabric Flexural Rigidity for 60/40 Blends Consolidated at 190 C

a factor of five (**Figure 29**). The excessive machine direction fiber orientation afforded significant elongational character to the fabric cross direction. Upon tensile loading, the remaining unoriented fibers in the cross direction specimens aligned themselves parallel to the load direction, thus allowing the cross direction extension to double the machine direction elongation (**Figure 30**).

The significance of orientation effects becomes obvious when the mechanical integrity of these webs formed and consolidated using this solvent modification process were compared to random and cross-laid 60/40 webs consolidated under the exact same conditions. The specific stress values of the latter webs were considerably lower than those webs with the excessive machine direction fiber orientation introduced during the mechanical web formation (**Figure 31**). These findings demonstrate the significance of mechanical web formation effects and their influence on web stability. The results also suggest the limitations of the solvent process in the achievement of ultimate web tenacity. Perhaps the observed tensile strengths previously thought to be the outcome of the process alone, were enhanced by the significant number of load-bearing fibers in the machine direction. One must also consider the end-use application of these fabrics when giving consideration to the selection of web mechanical formation machinery. If one desires greater balance in properties between the two fabric directions, then random air-laying or cross-lapping web formation systems are mandated. However, if greater priority is given to machine direction performance, then the successive layering of parallelized fibers on a revolving collector drum is appropriate.

Bursting strength and tear resistance are also evaluative measures of web mechanical integrity and dimensional stability; however, little attention is given to the

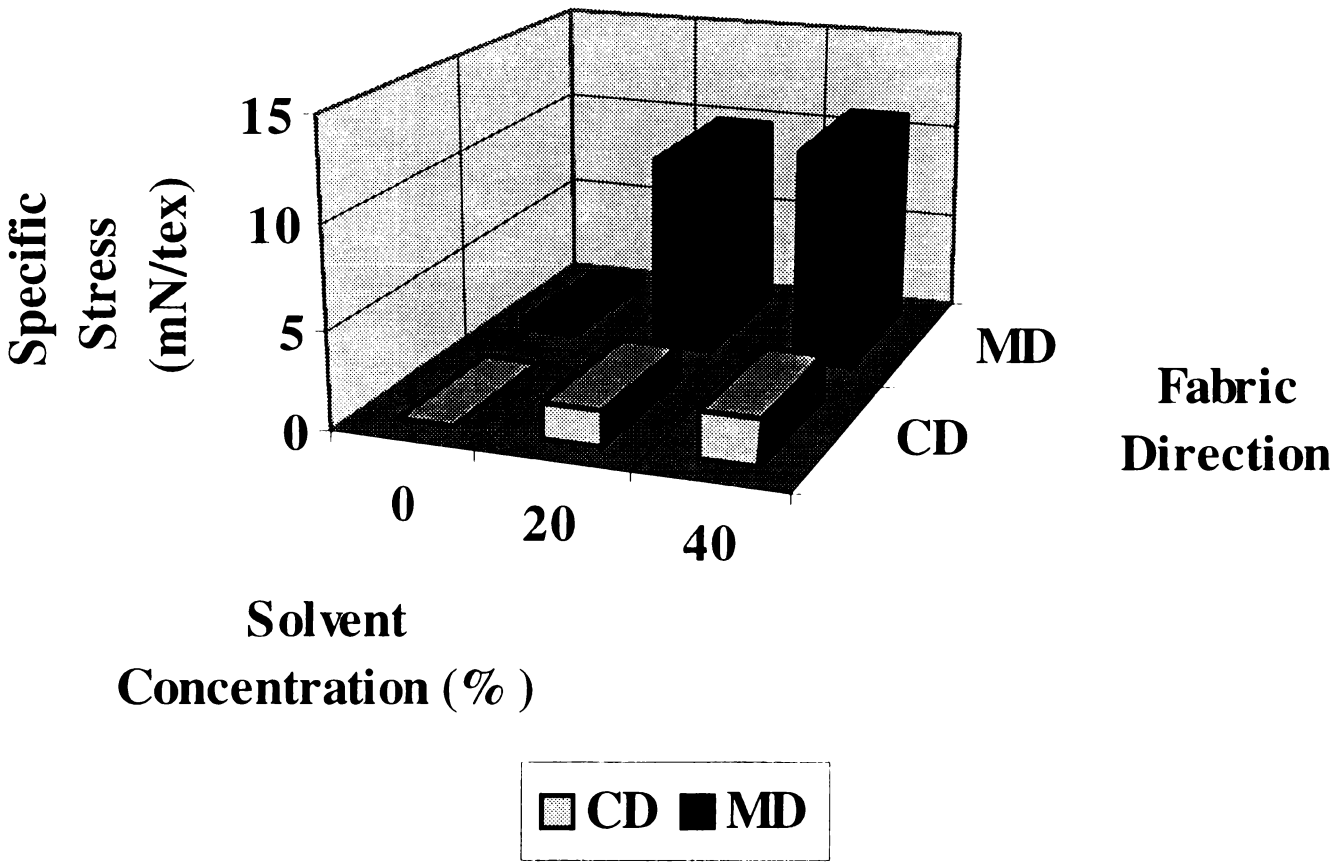

Figure 29: Directional Effects on Fabric Specific Stress for 60/40 Blends Consolidated at 170 C

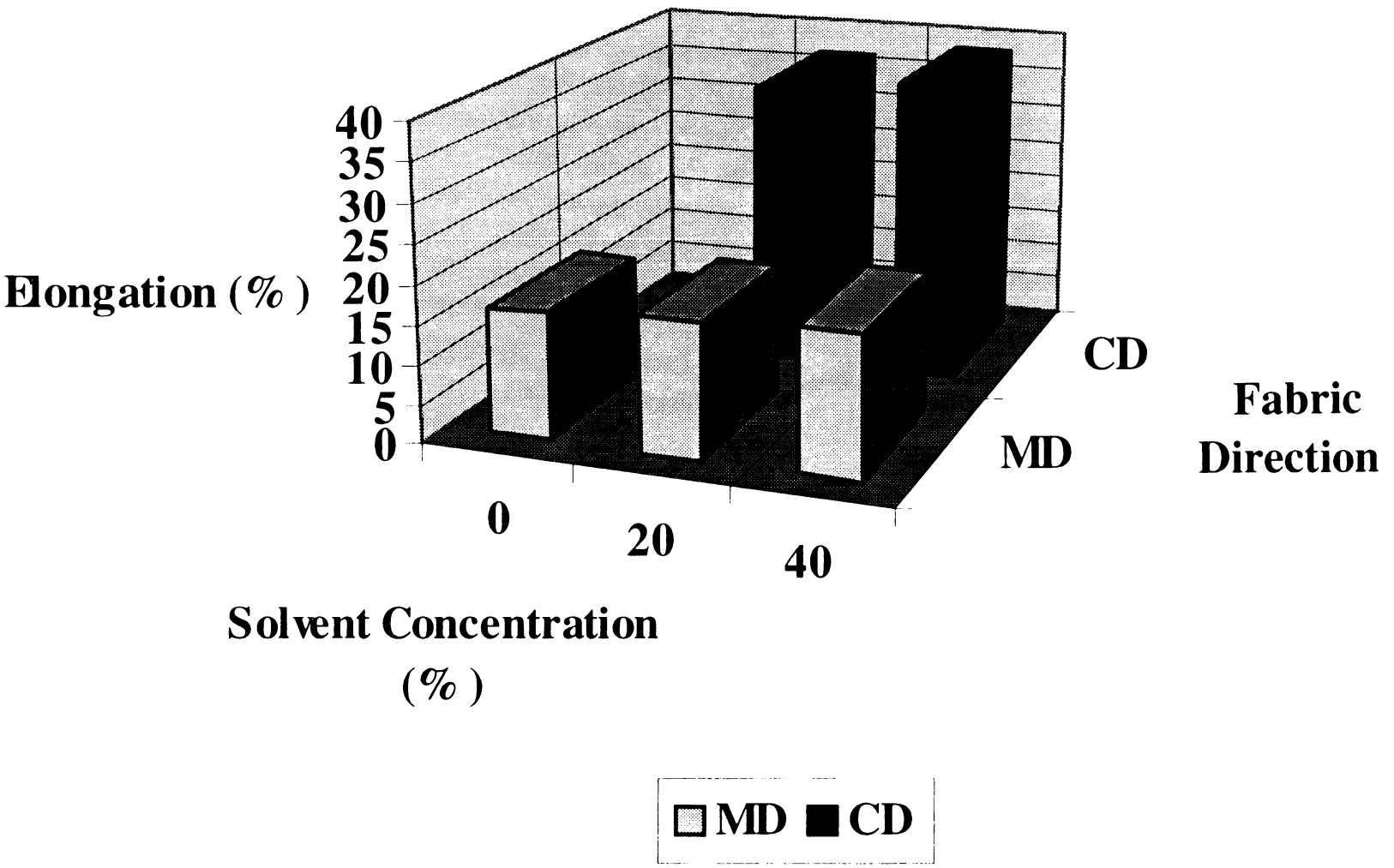

Fig Figure 30: Directional Effects on Fabric Elongational er-Properties for 60/40 Blends Consolidated at 170 C

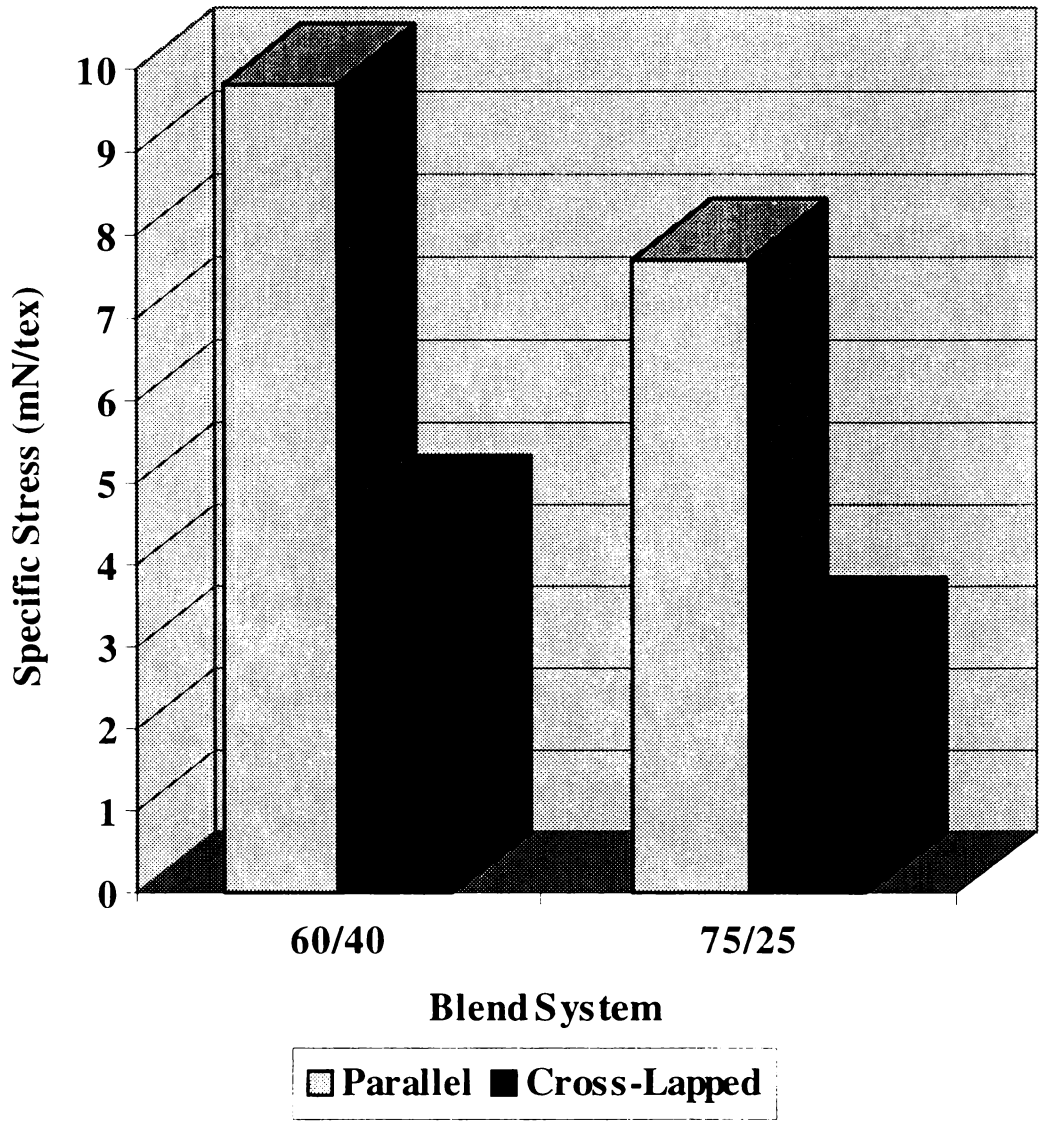

Figure 31: Card Formation Effects on Fabric Specific Stress Modified with 20% Acetone and Consolidated at 170 C

tear force results because of the inability to measure tear force in the web machine direction. Again, this behavior confirmed the excessive machine direction fiber orientation that caused the tear force to propagate perpendicular to the original tear. The weaker cross direction fiber system tearing, instead.

The bursting strength results also confirmed the excessive machine direction fiber orientation, as the slit propagation was perpendicular to the weaker cross direction fiber system, indicating cross direction fiber failure. For both blend systems, particularly the 75/25 blends consolidated at 150°C, web bursting strength remained virtually unchanged with additional solvent, substantiating earlier claims that asserted that insufficient thermal input still overcame the additional chain segmental mobility introduced with added solvent. Therefore, it could once again be concluded that although suppression of the glass transition temperature occurred with the solvent presence, additional solvent did not overcome the limitations set forth by such a low consolidation temperature and that, most definitely, the second order transition temperature was not suppressed in the vicinity of 150°C consolidation temperature. However, webs consolidated at 170 and 190°C and treated with 20% solvent had substantially higher bursting strengths than their untreated counterparts, especially 60/40 blends coalesced at 190°C. The web bursting strengths of these webs exceeded their untreated counterparts by a factor of nearly 2.2. These findings would again suggest that the suppression of the second order transition temperature in the swollen state occurred in the vicinity of 170 to 190°C, and that probably the greater sensitivity to the additional solvent for the 60/40 blends, indicated that the greater binder presence made available more binder for more definitive thermal welding. However, for both blend ratios, it was difficult to identify any additional

benefits with added thermal input in the presence of solvent, and additional solvent input also appeared to make a significant contribution to this aspect of web mechanical integrity and dimensional stability.

A secondary measure of fabric hand and comfort is fabric air permeability. Those webs in which fiber unification occurred at 150°C were more breathable; however, additional thermal and chemical inputs did not appear to have any profound negative effects on fabric breathability. However, the significant role of chemical input in facilitating web consolidation was once again demonstrated with as little as 20% solvent. For all bonding temperatures, the additional chemical input reduced fabric air permeability by at least $40cm^3/cm^2s$. However, additional chemical input failed to significantly negate fabric breathability.

Although fabric thickness measurements were made, little importance is attached to them given the inability to clearly identify any trends. One would expect that with enhanced web consolidation achieved with solvent modification of the acetate fibers, a more dense, hence, thicker structure would emerge. This was not observed at all with the 60/40 blends and was the case for 75/25 blends consolidated at 150 and 170°C. However, web thickness was diminished for those fibers unified at 190°C. One explanation for such disparity in the data may be the variation introduced during web formation because of the card machinery limitations that produced thick and thin lanes in the card; and, given that thickness measurements are taken randomly across and along the card, the measurements include these variation localities. The hypothesis that web thickness should be enhanced with improved web consolidation is supported by the fabric basis weight data which illustrates the increased mass per unit area with additional

thermal welding. The web shrinks upon web consolidation to produce a more dense structure.

STATISTICAL TREATMENT

Confirmation of the preliminary conclusions required more detailed statistical analysis using the multiple regression General Linear Model. A detailed explanation of simple and multiple linear regression methods is provided in the appendix.

FABRIC BASIS WEIGHT

As previously stated, the enhanced fiber unification and web consolidation achieved with the various solvent/temperature combinations increased the subsequent fabric basis weight; hence, a more dense, compact structure emerged. The model, including three independent variables, **blend (2), temperature (3) and concentration (3)**, was very appropriate for explaining any variation in the observed fabric response, that being the fabric basis weight. The model sum of squares, otherwise referred to as the sum of squares due to regression, **SSR** was **43.96442222,** while the sum of squares due to error, **SSE** was **0.67195556**. The **corrected total sum of squares** was **44.96442222**. Two conclusions could be made based on these figures. First, the model was very effective in predicting the fabric basis weight response, and nearly all of the variation in the responses could be attributed to regression; that is, the independent variables and not error. This was confirmed by an **R-square**, $\mathbf{R^2}$ value of **0.984946**. This figure was the ratio of the **model sum of squares** to the **corrected total sum of squares**. Only **1.5%** of the response variation could be attributed to error **($1-R^2$) x 100%.** Further affirmation of the model appropriateness was provided by the **F Value** of **20.13** with a probability that this figure, or a larger one, was achieved by chance alone of **0.00523**. The **F Value**

corresponds to the ratio of the **model mean sum of squares** to the **error mean sum of squares**. The **mean sum of squares** for each term is the **sum of squares** divided by the respective degrees of freedom, **DF**. The respective degrees of freedom, **DF,** associated with the model sum of squares is **13**; hence, the mean square is determined by the division of the model sum of squares, **43.964422** by **13** and is **3.38187863**. The **DF** associated with the error sum of squares is **four**. Thus, the error mean square is equal to the error sum of squares, **0.67195556**, divided by the **4 DF**, or **0.16798889**. The observation of all of the model sum of squares for regression including all independent variables and those interactions deemed potentially significant, solvent concentration most greatly influenced the fabric basis weight, as it dominated the model sum of squares for regression at **23.09471111** (**Table 2**).

TABLE 2. FABRIC BASIS WEIGHT SUM OF SQUARES FOR REGRESSION

SOURCE	DF	TYPE III SS	MEAN SQUARE	F VALUE	PR > F
Blend	1	1.20642222	1.20642222	7.18	0.05524
Temperature	2	7.17071111	3.58535556	21.34	0.00734
Blend * Temp	2	6.98164444	3.49082222	20.78	0.00771
Concentration	2	23.09471111	11.54735556	68.74	0.00080
Blend * Conc	2	1.92297778	0.96148889	5.72	0.06705
Temp * Conc	4	3.58795556	0.89698889	5.34	0.06680

This assertion can be made with great confidence given the extreme **F value (68.74)** with a very small probability **(0.00080)** that this value occurred by chance. The control fabrics that did not receive any acetone treatment were statistically different from those fabrics that were subjected to 20% and 40% acetone with respect to fabric density as indicated by the basis weight measurements. The mean basis weight for the control fabrics was **41 g/m^2**, while all fabrics subjected to either acetone concentration were more compact - their mean basis weight was **43 g/m^2**. The fabric basis weight was also sensitive to temperature; however, considerably less than solvent concentration, as its contribution to the overall model sum of squares was just **(7.17071111)**. The interaction between blend system and temperature was also important in determining the fabric basis weight response. Quite obviously, the absence of solvent limits web consolidation and a more open structure results. The addition of solvent facilitates acetate binder flow that promotes fiber unification and web consolidation; hence a more dense, compact structure emerges. Furthermore, additional thermal input will enhance binder latent adhesive properties. However, blend composition influences binder flow for a given consolidation temperature. The mean basis weight for 60/40 blends bonded at the low temperature 150°C was higher than similar 75/25 fabrics because, however insufficient this thermal input is at to facilitate chain segmental motion, binder flow is overcome by the effects of additional chemical input provided by the additional solvent. Hence, more binder was affected by the additional solvent in the 60/40 blends at this lowest bonding temperature. However, for the two blend systems, consolidation at the two higher temperatures revealed disparities in the subsequent fabric basis weight, which would indicate less efficient thermal welding in the higher percentage acetate blends. For all 60/40 blends

consolidated at 190°C, the mean fabric basis weight was approximately **42 g/m^2**, while the mean basis weight for all 75/25 blends receiving the exact same thermal input was **44 g/m^2**. Although less binder was available for chemical modification in the 75/25 blend systems, the additional thermal input overcame the limited binder availability such that more efficient thermal welding occurred at each individual bond site because of the greater availability of heat energy per weld due to the diminished binder presence. This assertion can be verified by the mean basis weight comparison between 60/40 and 75/25 blends consolidated at the low 150°C bonding temperature. For 60/40 systems, the mean fabric basis weight was **42 g/m^2**, approximately **1 g/m^2** greater than the 75/25 blends consolidated at the same temperature. Thus, the difference in the fabric response - that being fabric basis weight to varied solvent presence - is statistically significant. Furthermore, temperature and the interaction between blend composition and web consolidation temperature also play a statistically significant role in the determination of fabric basis weight.

FABRIC TENSILE PROPERTIES

SPECIFIC STRESS

Several independent variables and their influence on subsequent fabric specific stress were examined. In addition to the three process variables and their levels - **Blend System (2)**, **Solvent Concentration (3)**, and **Web Consolidation Temperature (3)**- other process variables including **Weight (2)**, **Card Number (3)**, and **Fabric Direction (2)**, were included in the model for the design of a straight line prediction equation for the fabric specific stress. Again, the model was very appropriate in the prediction of the response to the manipulation of the independent variables, and linear regression largely

accounted for response variation. The **Model Sum of Squares** was **3188.76401326** compared to the **error sum of squares** of **440.93651088**. Therefore approximately **88%** of the variation in fabric specific stress could be attributed to the independent variables **(R^2 = 0.878520)**, while only **12%** of the response variation was due to error **(1 - 0.878520) x 100%**. The inclusion of more independent variables in the model might be responsible for the larger error term; however, it still is considerably less than the model sum of squares term. The **model mean square** was **212.58426755** with **15 DF**, while the **error mean square** with **187 DF** was **2.35794926.** The ratio of these two figures gave a large **F value = 90.16** with an extremely small chance of realizing a value this large by chance **(5.E - 77)**.

Once again, the importance of solvent concentration in determining the fabric mechanical integrity remained insurmountable. **Table 3** illustrates the significant contribution of solvent concentration to the overall model sum of squares for regression, approximately 32%. The solvent concentration contribution to the model sum of squares for regression was **1157.33469568**, quite obviously a substantial contribution to the overall model sum of squares for regression value of **3188.76401326**. The disparity between the mean square for concentration **(578.66734784)** and the mean square for error in the model **(2.35794926)** produced an extreme **F value** of **245.41** with an extremely unlikely probability that this value was realized by chance alone **(Pr > F = 5.E - 53)**. There is a statistical difference in fabric mechanical integrity with respect to the level of solvent concentration; although, based on initial examination of the data, one would not have predicted this outcome. Of course, the chemical input is required in addition to the thermal input to permit

TABLE 3. FABRIC SPECIFIC STRESS SUM OF SQUARES FOR REGRESSION

SOURCE	DF	TYPE III SS	MEAN SQUARE	F Value	Pr > F
Concentration	2	1157.33469568	578.66734784	245.41	5.E – 53
Card (Conc)	4	69.31910985	17.32977746	7.35	2.E – 05
Blend	1	63.26022287	63.26022287	26.83	6.E – 07
Blend * Conc	2	38.89029087	19.44514544	8.25	0.00037
Temperature	2	510.79317284	255.39658642	108.31	6.E – 32
Blend * Temperature	2	1.60353855	0.80176928	0.34	0.71219
Direction	1	78.37405810	78.37405810	33.24	3.E - 08
Weight	1	0.15183341	0.15183341	0.06	0.79996

adequate second order transition temperature suppression so that acetate binder flow is permitted at the selected bonding temperatures. However, even though the mechanical integrity of webs treated with 40% acetone is significantly greater than those treated with less acetone (20%), statistically speaking, on a practical note, the use of 20% acetone is more conducive to industrial acceptance of this process (**Table 4**).

The amount of thermal input significantly influenced the fabric specific stress response, as evidenced by the large contribution of the independent temperature variable to the model sum of squares for regression, **510.79317284**, out of the total model sum of squares for regression, **3188.76401326**. The **F value** for the thermal input variable was also quite large, **108.31**, with a very small probability of being so large by mere chance, **6.E - 32**.

TABLE 4. LEAST SQUARES MEANS FOR FABRIC SPECIFIC STRESS (SOLVENT CONCENTRATION)

CONCENTRATION	STRESS LS MEAN	STD ERROR LS MEAN	T VALUE	PR > |T| HO:L S MEAN = 0
0	-0.91125557	0.45194813	-2.0163	0.04520
20	4.75410032	0.35781826	13.2864	8.E - 29
40	5.81879052	0.35791819	16.2573	1.E - 37

Although the initial examination of the data did support the statistical assertion that fabric specific stress of those webs consolidated at 150°C were significantly weaker than those webs consolidated at the two higher temperatures, the initial data did not appear to support the statistical assertion that those fabrics consolidated at 190°C were significantly stronger than the 170°C consolidated fabrics; however, examination of the results listed in **Table 5** would prove otherwise.

TABLE 5. LEAST SQUARES MEANS FOR FABRIC SPECIFIC STRESS (TEMPERATURE)

TEMPERATURE	STRESS LS MEAN	STD ERROR LS MEAN	T VALUE	PR > |T| HO:LS MEAN = 0
150	0.92640	0.39343	2.3547	0.01958
170	3.94096	0.36706	10.7365	3.E - 21
190	4.79427	0.37237	12.8750	1.E - 27

It comes as no surprise that the effects of excessive machine direction fiber orientation introduced using the rotating collector drum card formation system produced

great disparity in directional fabric mechanical integrity. According to **Table 6**, the disparity in mechanical integrity between the two fabric directions is statistically significant. As previously stated, the directional strength ratio is typically 5:1; that is, the machine direction strength generally exceeds that of the cross direction by a factor of five. This knowledge, in addition to the card formation system employed, forces one to recognize the strength enhancement introduced merely by the mechanical web formation technique. Because when the mechanical web integrity of webs formed using the rotating collector drum were compared with other card formation technology-random and cross-lap, there was a significant disparity in the strengths realized by the latter two processes, even though they were treated with the exact amount of acetone and subjected to the same web consolidation temperature as those produced at the University of Tennessee. Consequently, the improved mechanical integrity of webs subjected to acetone modification must not be overstated with respect to the solvent modification benefits. One cannot overlook the role of excessive fiber orientation in the improved mechanical properties of these fabrics.

TABLE 6. LEAST SQUARES MEANS FOR FABRIC SPECIFIC STRESS (FABRIC DIRECTION)

FABRIC DIRECTION	STRESS LS MEAN	STD ERROR LS MEAN	T VALUE	PR > |T| HO:LS MEAN = 0
CD	1.50798683	0.60249515	2.5029	0.01317
MD	4.93310335	0.22445005	21.9786	1.E - 53

As an aside, the researcher chose to identify the halved card lengths as those that went through the aqueous acetone solution first, and those that went through the solution second, and then their mechanical properties were compared to identify any possible differences that could be attributed to preferential absorption of the acetone molecules from the aqueous solution by the acetate fibers, or the redeposition of dissolved acetate onto the latter card half length passing through the solution after the first card half length had passed through, and the solution had been recycled. The statistics show that the mechanical response of the card half lengths treated with 20% acetone were statistically equivalent (**Table 7**).

TABLE 7. LEAST SQUARES MEANS FOR FABRIC SPECIFIC STRESS (CARD ORDER)

CARD ORDER (CONC)	STRESS LS MEAN	STD ERROR LS MEAN	T VALUE	PR > |T| HO:LS MEAN = 0
#1 20%	5.88582	0.53751	10.9503	0.0000
#2 20%	5.60299	0.54223	10.3333	0.0000
#1 40%	7.49794	0.54455	13.7691	0.0000
#2 40%	6.68316	0.53499	12.4922	0.0000

However, at 40%, those card half lengths that passed through the solution first were statistically different than those card halves that followed through the solution, meaning the first card halves were mechanically superior to the subsequent card halves. These findings would suggest that preferential absorption of the acetone molecules may in fact occur. They also support the statistical difference in overall mechanical properties

between fabrics treated with 20% and 40% acetone. Confirmation of this proposed preferential acetone absorption could be confirmed with simple gas chromatography injection techniques in which solution prior to card immersion could be evaluated for the initial acetone concentration and compared to the acetone concentration of the solution following the first card immersion, and again following the second card immersion.

As was predicted by initial examination of the data, blend ratio did have significant predictive power over the mechanical response of the fabrics. Furthermore, the mechanical response of the two blend systems was statistically different, the higher acetate blend composition (60/40) had superior mechanical properties (**Table 8**).

TABLE 8. LEAST SQUARES MEANS FOR FABRIC SPECIFIC STRESS (BLEND SYSTEM)

BLEND SYSTEM	STRESS LS MEAN	STD ERROR LS MEAN	T VALUE	PR > |T| HO:LS MEAN = 0
60/40	3.81371015	0.33819876	11.2765	8.E - 23
75/25	2.62738003	0.38568662	6.8122	1.E - 10

The superiority of the 60/40 blends is compounded by the evaluation of the interaction between blend system and solvent concentration (**Table 9**). It comes as no great surprise that the mechanical performance of either blend system not subjected to any solvent modification is statistically equivalent. Only when solvent is present, can the beneficial effects of additional binder presence be realized. The 60/40 blends treated with 20% and 40% acetone outperformed similar 75/25 fabrics and were mechanically superior, statistically speaking. Even more interesting is that even those 75/25 blends

subjected to the harshest acetone treatment, were statistically equivalent to 60/40 blends immersed in only 20% acetone. These findings provide sufficient evidence for the decision to select 60/40 as the blend system of choice, because less acetone can be employed and the mechanical properties equal those of the 75/25 blend at the higher solvent concentration. This assertion supports preliminary conclusions that suggested the superior mechanical integrity of the higher acetate percentage blend at all bonding temperatures and solvent concentrations. These findings support the existing literature that also suggests the superior mechanical integrity of higher acetate composition blend systems and also negates any beneficial heat transfer effects associated with less binder presence.

TABLE 9. LEAST SQUARES MEANS FOR FABRIC SPECIFIC STRESS (BLEND SYSTEM/SOLVENT CONCENTRATION INTERACTIONS)

BLEND SYSTEM * CONCENTRATE	STRESS LS MEAN	STD ERROR LS MEAN	T VALUE	PR > |T| HO:LS MEAN = 0
60/40 * 0	-0.96981578	0.44186740	-2.1948	0.02941
75/25 * 0	-0.85269537	0.53790824	-1.5852	0.11461
60/40 * 20	5.69624027	0.37478825	15.1986	2.E - 34
75/25 * 20	3.81196038	0.44228250	8.6188	3.E - 15
60/40 * 40	6.71470595	0.37493217	17.9091	2.E - 42
75/25 * 40	4.92287509	0.442311460	11.1298	2.E - 22

Examination of the interaction between blend system and web consolidation temperature substantiates the proposed mechanical superiority of 60/40 blend systems (**Table 10**).

TABLE 10. LEAST SQUARES MEANS FOR FABRIC SPECIFIC STRESS (BLEND SYSTEM/TEMPERATURE INTERACTIONS)

BLEND SYSTEM * TEMPERATURE	STRESS LS MEAN	STD ERROR LS MEAN	T VALUE	PR > |T| HO:LS MEAN = 0
60/40 * 150	1.65162223	0.42875499	3.8521	0.00016
75/25 * 150	0.20118496	0.45104424	0.4460	0.65608
60/40 * 170	4.47223422	0.37662123	11.8746	1.E - 24
75/25 * 170	3.40968249	0.44810848	7.6091	1.E - 12
60/40 * 190	5.31727399	0.38423842	13.8385	2.E - 30
75/25 * 190	4.27127265	0.45182061	9.4535	1.E - 17

The 60/40 blends outperformed the 75/25 systems at all bonding temperatures. Even at the lowest web consolidation temperature, any thermal efficiency associated with less binder presence was overcome, and the 60/40 blends consolidated at 170°C were statistically equivalent to 75/25 blends consolidated at the higher 190°C bonding temperature. Thus, more thermal input is required for 75/25 blends to achieve the same mechanical response as 60/40 blends consolidated with less thermal energy. These findings would also negate any proposed benefits as far as weld efficiency associated with less binder; for if this were truly the case, the 75/25 blends bonded at 190°C should have been significantly stronger than similar 60/40 fabrics bonded at 190°C. Therefore, the positive outcome associated with

greater binder presence in the blend composition prevails over any proposed thermal bonding efficiency associated with less binder present in the fiber system.

Lastly, the mechanical performance of the two fabric weights was statistically equivalent (**Table 11**). Based on this finding, two conclusions can be drawn. Any beneficial effects associated with the diminished web thickness with regard to more efficient heat transfer and subsequent enhanced mechanical performance were not realized. However, with regard to the desired end-use application of this fabric - that being diaper coverstock - the lighter fabric is preferred. And, since the effects of diminished fibers per unit area did not seem to negatively influence the mechanical integrity of the lighter fabrics compared to the heavier fabrics with their greater number of fibers per unit area, the lighter fabrics may be a more commercially-viable alternative.

TABLE 11. LEAST SQUARES MEANS FOR FABRIC SPECIFIC STRESS (BASIS WEIGHT)

BASIS WEIGHT	STRESS LS MEAN	STD ERROR LS MEAN	T VALUE	PR > |T| HO:LS MEAN = 0
30	3.14907465	0.57931007	5.4359	2.E - 07
40	3.29201553	0.24486088	13.4444	3.E - 29

FABRIC ELONGATION

The same independent variables used in the regression model to predict the fabric specific stress were used in the regression model to predict the fabric elongational properties, and once again had significant predictive power over the fabric response. The **model sum of squares for regression** was **3941.35507120** compared to the **error sum**

of squares of **500.30172880**. Thus, the model was very effective in accounting for the variation in the elongation response of the fabrics - **89%** to be exact. The **model mean sum of squares for regression (15 DF)** was **262.75700475**, and the **mean sum of squares for error (159)** was **3.14655175**. The ratio of these two numbers, the **F value** was quite large, **83.51** to be exact, with almost no possibility of being so large by chance alone (**Pr > F = 3.E - 67**).

The variation in fabric elongational response was most greatly influenced by the fabric direction, machine or cross (**Table 12**).

TABLE 12. FABRIC ELONGATION SUM OF SQUARES FOR REGRESSION

SOURCE	DF	TYPE III SS	MEAN SQUARE	F VALUE	PR > F
Concentration	2	39.95927708	19.97963854	6.35	0.00222
Card (Conc)	4	23.62113298	5.90528325	1.88	0.11707
Blend	1	11.39499959	11.39499959	3.62	0.05885
Blend * Conc	2	0.55575634	0.27787817	0.09	0.91552
Temperature	2	58.88749833	29.44374917	9.36	0.00014
Blend * Temperature	2	21.95056528	10.97528264	3.49	0.03292
Direction	1	1050.72666667	1050.72666667	333.93	7.E - 41
Weight	1	6.26379239	6.26379239	1.99	0.16022

The **model sum of squares for regression pertaining to fabric direction** was **1050.72666667**; **23%** of the **total model sum of squares for regression**. Consequently, an exorbitant **F value** of **333.93** with no possibility of being so large by chance alone (**7.E - 41**) was obtained. Ultimately, the disparity in fabric direction elongation is attributed to the excessive machine direction fiber orientation introduced during mechanical web formation. The cross direction specimens were significantly more extensible than the machine direction fibers because of the relatively unoriented nature of the fabric cross direction (**Table 13**). Once again, other card formation techniques may be more desirable for a better balance in the elongational properties of the two fabric directions, depending upon the end-use requirements of the ultimate end product.

TABLE 13. LEAST SQUARES MEANS FOR FABRIC ELONGATION (FABRIC DIRECTION)

FABRIC DIRECTION	ELONGATION LS MEAN	STD ERROR LS MEAN	T VALUE	PR > |T| HO:LS MEAN = 0
CD	36.9296	1.2629966	29.2397	7.E – 66
MD	17.0796	0.3911403	43.6662	2.E – 90

FABRIC YIELD STRESS

Yield stress is a very important measure of web mechanical integrity and dimensional stability because, ultimately, the observed yield stress indicates the separation between elastic and plastic deformation, that is, deformation that is reversible and that which remains irreversible. Therefore, the higher the yield stress the more

elastic deformation the material undergoes before the onset of permanent deformation, hence, failure. A "tougher" material emerges.

Once again, the independent variables included in the regression model to predict the fabric yield stress had significant predictive power. **Ninety-five percent** of the data variation was attributed to regression-$\mathbf{R^2 = 0.945443}$. The large **F value (183.69)** with no chance of being realized by mere chance **(4.E - 92)** further supported the efficiency of the regression model in predicting the fabric response. Only **5%** of the variation in the data could be attributed to error terms in the model.

It comes as no surprise that the solvent concentration and web consolidation temperature had the greatest predictive power over the fabric yield strength (**Table 14**). Concentration accounted for **29%** of the **regression model sum of squares (782.78293837/2688.87451629)**, while temperature contributed **27%** of the **model sum of squares for regression (732.36136872/2688.87451629)**. Blend effects and blend-concentration interactions could not be ignored either. Again, the 60/40 blends were superior to the lower acetate blend system in that they were "tougher" and more likely to undergo a significant amount of elastic deformation prior to failure than the 75/25 blend system. Again, without any solvent modification, the fabric yield strength of the two blend systems was statistically identical (**Table 15**).

TABLE 14. FABRIC YIELD STRESS SUM OF SQUARES FOR REGRESSION

SOURCE	DF	TYPE III SS	MEAN SQUARE	F VALUE	PR > F
Concentration	2	782.78293837	391.39146918	401.07	8.E – 63
Card (Conc)	4	12.61196704	3.15299176	3.23	0.01398
Blend	1	45.92571116	45.92571116	47.06	1.E – 10
Blend * Conc	2	26.96919314	13.48459657	13.82	3.E – 06
Temperature	2	732.36136872	366.18068436	375.24	6.E – 61
Blend * Temperature	2	0.94077326	0.47038663	0.48	0.61843
Direction	1	107.95041667	107.95041667	110.62	6.E – 20
Weight	1	6.19713503	6.19713503	6.35	0.01272

TABLE 15. LEAST SQUARES MEANS FOR FABRIC YIELD STRESS (BLEND SYSTEM)

BLEND SYSTEM	YIELD STRESS LS MEAN	STD ERROR LS MEAN	T VALUE	PR > |T| HO:LS MEAN = 0
60/40	1.33282832	0.42992137	3.10017	0.00229
75/25	0.19664967	0.43367469	0.45345	0.65084

For either blend system, the fabric toughness was statistically different between those treated with 20% and 40 % acetone. The 60/40 blends were tougher than the 75/25 blends for both solvent concentrations; and the 75/25 blends required treatment with 40% acetone to achieve the same fabric toughness as those 60/40 blends treated with only 20% acetone (**Table 16**).

TABLE 16. LEAST SQUARES MEANS FOR FABRIC YIELD STRESS (BLEND SYSTEM/SOLVENT CONCENTRATION INTERACTIONS)

BLEND SYSTEM * CONCENTRATION	YIELD STRESS LS MEAN	STD ERROR LS MEAN	T VALUE	PR > |T| HO:LS MEAN = 0
60/40 * 0	-4.99979	0.62087196	-8.0528	2.E - 13
75/25 * 0	-4.79299	0.61788295	-7.7571	1.E - 12
60/40 * 20	3.93993	0.37239135	10.5801	4.E - 20
75/25 * 20	2.13338	0.40189094	5.3084	4.E - 07
60/40 * 40	5.05834	0.37507966	13.4860	4.E - 28
75/25 * 40	3.24956	0.40433636	8.0368	2.E - 13

Although the blend-temperature interaction did not have any significant influence over fabric yield strength, it is interesting to note the statistical identity of 75/25 blends bonded at the highest temperature (190°) to the 60/40 blends bonded at only 170°C (**Table 17**). The proposed thermal efficiency associated with less acetate binder was once again negated by the observation of the statistical identity of the two blend systems, the 75/25

blends requiring more thermal input to achieve the same results as 60/40 blends consolidated with less thermal input.

TABLE 17. LEAST SQUARES MEANS FOR FABRIC YIELD STRESS (BLEND SYSTEM/TEMPERATURE INTERACTIONS)

BLEND SYSTEM * TEMPERATURE	YIELD STRESS LS MEAN	STD ERROR LS MEAN	T VALUE	PR > |T| HO:LS MEAN = 0
60/40 * 150	-1.96508	0.48797932	-4.02697	9.E - 05
75/25 * 150	-3.35167	0.48368893	-6.92938	1.E - 10
60/40 * 170	2.49872	0.44089902	5.66733	7.E - 08
75/25 * 170	1.50061	0.45474101	3.29991	0.00119
60/40 * 190	3.46485	0.44092267	7.85817	6.E - 13
75/25 * 190	2.44101	0.45630441	5.34952	3.E - 07

FABRIC BURSTING STRENGTH

Fabric bursting strength is a secondary measure of the mechanical integrity and dimensional stability of the fabrics. The proposed regression model was very effective in explaining the variation in fabric bursting strength, almost **98%** of the variation could be explained by the independent variables ($\mathbf{R^2 = 0.978269}$). Thus only **2%** of the variation could be explained by the **error terms** in the proposed model. The **model sum of squares for regression** was **76.91516806 (17 DF)**, while the **sum of squares for error** was only **1.70854340 (6 DF)**. The **model mean square for regression** was thus **4.52442165**, while the error mean square was **0.28475723**. The **F value**, the ratio of

these two values was **15.89**, with a very small probability of being so large by chance alone **(0.00128)**.

Once again, web consolidation temperature, solvent concentration, blend and, interestingly, weight, had significant influence over the bursting strength outcome of the fabrics (**Table 18**). The superiority of the **60/40** blends was reiterated, as the **mean bursting strength** for these blends was **5.04 Kpa** while the **75/25** blends had a **mean bursting strength** of **4.33055556 Kpa**.

TABLE 18. FABRIC BURSTING STRENGTH SUM OF SQUARES FOR REGRESSION

SOURCE	DF	TYPE III SS	MEAN SQUARE	F VALUE	PR > F
Blend	1	5.65040139	5.65040139	19.84	0.00431
Temperature	2	16.71177708	8.35588854	29.34	0.00080
Blend * Temperature	2	0.29423403	0.14711701	0.52	0.62084
Concentration	2	11.97997730	5.989988565	21.04	0.00194
Blend * Concentration	2	1.59087986	0.79543993	2.79	0.13886
Temperature * Concentration	4	6.77175799	1.69293950	5.95	0.02777
Weight	1	9.13507500	9.13507500	32.08	0.00130
Temperature * Weight	1	4.40440833	4.40440833	15.47	0.00769
Concentration * Weight	2	1.45153640	0.72576820	2.55	0.15805

FABRIC HAND AND COMFORT PROPERTIES

FABRIC FLEXIBILITY

An evaluative measure of fabric hand is to observe its flexibility or, in quantitative terms, its flexural rigidity. Thus, a more flexible fabric will have a lower rigidity in bending value than a more rigid structure. The proposed model to describe the equation of a straight line for multiple linear regression was adequate in describing the flexural rigidity response variation among the fabric test specimens. However, only **77%** of the variation could be attributed to **regression**; that is, the independent variables included in the model (**$R^2 = 0.779691$**). This meant that a **22%** variation in the observations was caused by **error**. Still the variation was predominantly caused by regression, as evidenced by the large **F value = 20.69** with no chance of being realized by chance alone (**Pr > F = 8.E - 20**).

The substantial predictive power that solvent concentration had on subsequent fabric flexibility comes as no great surprise (**Table 19**). The control fabrics that did not receive any solvent treatment were very limp and pliable. The addition of solvent made the fabrics substantially stiffer; however, tactile manipulation of them still deemed them acceptable to the consumer. The heat transfer effects associated with less acetate binder present were finally realized with respect to fabric hand (**Table 20**). The 75/25 blends were significantly more rigid than their 60/40 counterparts. This supports the notion that less binder present means more complete thermal welding of individual bond sites in the 75/25 blends because more heat energy is delivered to less acetate binder.

TABLE 19. FABRIC FLEXURAL RIGIDITY SUM OF SQUARES FOR REGRESSION

SOURCE	DF	TYPE III SS	MEAN SQUARE	F VALUE	PR > F
Blend	1	1294.28544444	1294.28544444	21.49	1.E - 25
Temperature	2	2213.83488889	1106.91744444	18.38	3.E - 07
Blend * Temperature	2	678.19622222	339.09811111	5.63	0.00525
Concentration	2	10781.90822222	5390.95411111	89.51	1.E - 20
Blend * Concentration	2	60.58288889	30.29144444	0.50	0.60676
Temperature * Concentration	4	1171.24444444	292.81111111	4.86	0.00152

TABLE 20. LEAST SQUARES MEANS FOR FABRIC FLEXURAL RIGIDITY (BLEND SYSTEM)

BLEND SYSTEM	FLEXURAL RIGIDITY LS MEAN	STD ERROR LS MEAN	PR > |T| HO:LS MEAN = 0
60/40	48.7400000	1.1569122	2.E - 54
75/25	56.3244444	1.1569122	5.E - 59

Furthermore, the additional thermal input significantly reduced the fabric pliability. More interesting is the interaction between blend composition and temperature (**Table 21**). The 75/25 blends were more sensitive to the additional thermal input than were their 60/40 counterparts. Although the flexibility of the two blends were nearly identical at the lowest bonding temperature, 150°C- indicating the effects of different acetate percentage were overcome by the limitations of the consolidation temperature that was insufficient. Even under the conditions of solvent modification, at the two higher temperatures, the 75/25 blends were significantly stiffer. These observations would lend further support to the election to use the 60/40 blends in the commercialization of this fabric product because of the superior mechanical integrity, yet the preservation of fabric hand is allowed with this particular blend composition.

TABLE 21. LEAST SQUARES MEANS FOR FABRIC FLEXURAL RIGIDITY (BLEND SYSTEM/TEMPERATURE INTERACTIONS)

BLEND SYSTEM * TEMPERATURE	FLEXURAL RIGIDITY LS MEAN	STD ERROR LS MEAN	PR > |T| HO:LS MEAN = 0
60/40 * 150	45.4666667	2.0038306	1.E – 35
75/25 * 150	46.7733333	2.0038306	2.E – 36
60/40 * 170	49.8933333	2.0038306	3.E – 38
75/25 * 170	56.6600000	2.0038306	4.E – 32
60/40 * 190	50.8600000	2.0038306	7.E – 39
75/25 * 190	65.5400000	2.0038306	2.E – 46

The heat transfer effects associated with the 75/25 blends with respect to solvent concentration were also observed (**Table 22**). Unlike the previously mentioned physical properties, in which the responses were nearly identical for all control fabrics, those 60/40 fabrics that did not receive the solvent treatment were significantly more pliable than their 75/25 counterparts. Once again, the additional thermal input available to each thermal weld site in the 75/25 blends was the proposed explanation for the observed diminishment in pliability of these fabrics that contained less acetate binder.

TABLE 22. LEAST SQUARES MEANS FOR FABRIC FLEXURAL RIGIDITY (BLEND SYSTEM/SOLVENT CONCENTRATION INTERACTIONS)

BLEND SYSTEM * CONCENTRATION	FLEXURAL RIGIDITY LS MEAN	STD ERROR LS MEAN	PR > |T| HO:LS MEAN = 0
60/40 * 0	33.0933333	2.0038306	7.E - 27
75/25 * 0	41.1733333	2.0038306	9.E - 33
60/40 * 20	54.2200000	2.0038306	9.E - 41
75/25 * 20	63.5200000	2.0038306	1.E - 45
60/40 * 40	58.9066667	2.0038306	3.E - 43
75/25 * 40	64.2800000	2.0038306	6.E - 46

This disparity in fabric pliability between the two blend systems was magnified by the addition of solvent. As was previously observed with other physical properties, the fabric properties of those fabrics consolidated at 150°C were considerably improved with the addition of solvent (**Table 23**). The limitations imposed by the consolidation

temperature (150°C) far below the acetate binder glass transition temperature were overcome by the addition and subsequent addition of solvent. The additional transition temperature suppression brought forth with the presence of additional solvent facilitate enhanced bonding; hence, a stiffer structure emerged. The fabrics bonded at the higher temperatures were less sensitive to additional solvent, especially those bonded at the harshest temperature, because the chosen web consolidation temperatures were already in the vicinity of the second order transition temperature suppression achieved with the lower solvent concentration.

TABLE 23. LEAST SQUARES MEANS FOR FABRIC FLEXURAL RIGIDITY (TEMPERATURE/CONCENTRATION INTERACTIONS)

TEMPERATURE * CONCENTRATION	FLEXURAL RIGIDITY LS MEAN	STD ERROR LS MEAN	PR > |T| HO:LS MEAN = 0
150 * 0	36.3200000	2.4541813	4.E – 24
170 * 0	38.9100000	2.4541813	8.E – 26
190 * 0	36.1700000	2.4541813	6.E – 24
150 * 20	48.9200000	2.4541813	6.E – 32
170 * 20	58.9900000	2.4541813	3.E – 37
190 * 20	68.7000000	2.4541813	9.E – 42
150 * 40	53.1200000	2.4541813	3.E – 34
170 * 40	61.9300000	2.4541813	1.E – 38
190 * 40	69.7300000	2.4541813	3.E – 42

FABRIC AIR PERMEABILITY

Another aspect of fabric hand and comfort is the rate at which air flows through a material - otherwise known as the air permeability of a fabric. Regression was responsible for **96%** of the variation in the data (**R^2 = 0.963829**). The **model sum of squares (13 DF)** was **13002.95679012**, significantly larger than the **sum of squares for error (4 DF)** equal to **487.98765432**. The ratio of the two subsequent mean squares for the model and error terms was an **F value** of **8.20** with a very small probability of being so large by chance alone (**Pr > F = 0.02791**).

By far, solvent concentration had the greatest predictive power over the fabric air transmission, the **sum of squares for regression** was **10938.77777778** (Table 24).

TABLE 24. FABRIC AIR PERMEABILITY SUM OF SQUARES FOR REGRESSION

SOURCE	DF	TYPE III SS	MEAN SQUARE	F VALUE	PR > F
Blend	1	87.41358025	87.41358025	0.72	0.44496
Temperature	2	1093.81481481	546.90740741	4.48	0.09517
Blend * Temperature	2	334.82716049	167.41358025	1.37	0.35173
Concentration	2	10938.77777778	5469.38888889	44.83	0.00182
Blend * Concentration	2	328.38271605	164.19135802	1.35	0.35731
Temperature * Concentration	4	219.74074074	54.93518519	0.45	0.77066

The **F value** for solvent concentration was **44.83** with the most minute possibility of being so large by chance alone (**Pr > F = 0.00182**). Thus, solvent concentration was significantly responsible for the response variation. Coming in a distant second, was bonding temperature **SSR = 1093.81481481** and a much smaller **F value** of **4.48** with a higher probability of being realized by chance (**Pr > F = 0.09517**). Fabric air permeability was less sensitive to blend composition. However, some interesting interactions between blend and temperature and blend and solvent concentration were noted. Given the previous findings establishing the mechanical superiority and hand of the 60/40 blends, it is no surprise that the superior bonding would diminish the air flow of these higher acetate composition blends. This was observed by comparison of the two blend systems bonded at the lowest bonding temperature, the 75/25 blends permitted more air transmission because the superior welding of the 60/40 blend system would diminish the air pathways available for air flow by means of fiber compression and binder flow. However, the average air flow for the two blend systems consolidated at 170°C were statistically identical. And, at the highest 190°C, the 60/40 blends were actually more permeable than the 75/25 blends. This behavior was unexpected given that the 60/40 blends, exhibited superior unification and consolidation, especially with the additional thermal input supplied by the 170 and 190°C bonding temperature.

5. CONCLUSIONS

- This study sought to fabricate cotton/cellulose acetate blends using lower than normal web consolidation temperatures, achieved only with the assistance of the industrial solvent, acetone. The acetone was used to develop the latent adhesive properties of the acetate binder fibers. The acetone penetrated the acetate amorphic proximities, swelling the fibers so that microstructural alteration of the acetate polymeric molecular chains occurred in the solvated state. The chemical input followed by additional thermal input, facilitated chain segmental mobility that ultimately resulted in the suppression of the second order glass transition temperature and acetate adhesive properties emerging at lower than normal temperatures.
- It is very apparent that solvent-assisted suppression of the glass transition temperature occurred between 170 and 190°C, as the mechanical integrity and web dimensional stability of fabrics consolidated at these two temperatures was far superior to those webs consolidated at 150°C. Therefore for the selected processing conditions, web consolidation at 150°C is not to be considered because the glass transition temperature was not suppressed in the proximity of such a low bonding temperature.
- The mechanical integrity of those webs consolidated at 170 and 190°C was statistically different, regardless of solvent concentration. Those webs consolidated at the higher of the two temperatures were mechanically superior, yet statistically speaking, there was a significant reduction in fabric flexibility associated with the greater thermal input.

- The use of solvent modification to develop the latent adhesive properties of the acetate binder fibers had a significant influence on subsequent fabric mechanical properties. For without solvent modification, the latent adhesive properties of the acetate binder fibers were not allowed to develop, even at the highest bonding temperature. The fabrics modified with 40% acetone were statistically superior to those treated with only 20% acetone, with respect to tensile, tear and bursting strengths. However, given the environmental and economic concerns associated with the selection of acetone as a modifying agent, the commercial acceptability of this particular process is more favorable using less acetone, overshadowing the enhanced strengths realized with the addition of more solvent. Quite frankly, given the earliest preliminary data that illustrated the significant fabric tenacity improvement associated with just 10% acetone compared to no acetone treatment, one should consider the possibility of using the most minimal amount of solvent that is considered an insult to the environment and costly to recover for repeated use.
- Both producers and public relations groups supporting the cotton industry are seeking to expand the presence of cotton fibers in the nonwovens sector of the textiles industry. Of course these special interest groups would prefer to use high percentage cotton blend systems in the fabrication of nonwoven fabrics intended for the absorbents market because of the environmental friendliness of cotton fibers. But it is known that the most prevalent means of web consolidation in this sector is thermal calendering, and cotton fibers require very high temperatures to accomplish fiber unification, the end result is a very stiff, harsh fabric because of the subsequent cotton fiber brittleness. Therefore a binder is necessary to promote the low temperature coalescence and

unification of the cotton fibers to each other and to the binder fibers. Although cellulose acetate is not thought of as being prone to degradation by the environment, research has proved otherwise. And, when acetate is blended with cotton, a synergistic effect is introduced in which the combination of these two fibers promotes greater degradation, than the two fibers, alone. Although the greater presence of cotton such as that found in a 75/25 blend system would suggest the evolution of about 55% CO_2, the evolution of carbon dioxide for the 60/40 blend would still probably be in the range of 45 to 50%, given that CO_2 evolution in 50/50 blends has been demonstrated to be approximately 45%.

- Statistically speaking, the 60/40 blends were superior with respect to fabric mechanical integrity and fabric hand compared to the 75/25 blends. These findings support previous research which identified a negative inverse relationship between cotton content and strength; that is, the greater cotton presence had a negative impact on the fabric tenacity, suggesting that greater binder availability meant more effective welding at each individual bond site. However on the same note, other researchers suggested that 75/25 blends would be stronger because less binder meant more heat energy was available for each individual weld site so that for a fixed thermal input and contact time, more units of heat would be available per unit of binder at each weld site. For this study, no benefits associated with greater heat efficiency with respect to less binder were identified.
- Furthermore, the 75/25 blends required the harshest processing conditions with respect to solvent concentration and consolidation temperature, that is 40% acetone with

consolidation at 190°C for their tenacities to approach those of the 60/40 blends treated with only 20% acetone and bonded at 170°C.

- The 75/25 blend fabrics were significantly stiffer than 60/40 fabrics, regardless of solvent concentration and temperature combination. These findings would support the proposed heat efficiency associated with less acetate binder; that, is more heat energy inputs would be available per unit binder with the smaller binder presence. Hence more efficient bonding at each individual bond site would promote the emergence of a stiffer structure in blend systems containing less acetate binder fibers. Even when those 60/40 blends were subjected to the harshest possible processing conditions, those being 40% acetone followed by consolidation at 190°C, they still were significantly softer and more flexible than their 75/25 counterparts. With respect to temperature, the fabric flexibility of 60/40 blends seemed to be insensitive to increased thermal input, remaining nearly the same for 150 and 170°C, and fabric hand of those 60/40 blends consolidated at 190°C was not that adversely affected, from a practical standpoint.
- Given the above arguments, from the standpoint of process optimization with the ultimate intent being the commercialization of this fabrication process for cotton-based absorbent materials for baby and adult diaper coverstock, the optimum process variable combination would be the selection of a 60/40 cotton/cellulose acetate blend system treated with 20% acetone followed by web consolidation at 190°C.
- If one seeks an end-product with a better balance of properties between the two fabric directions, machine and cross, then one should consider alternate methods of web formation than the one selected for this study, including random and cross-laying mechanical web formation techniques. Furthermore, the effects of excessive fiber

orientation on fabric mechanical properties can not afford to be understated. That is the strength enhancement associated with the solvent modification has an upper limit, especially given that webs conlidated using the exact same processing conditions that differed only in the technique by which the web was formed failed to ascertain the same strengths as those fabrics characterized by excessive fiber orientation in the machine direction.

- To increase processing efficiency and to promote the ascension of the web thickness temperature to that of the effective roll temperature, the web should be dried to a known level of wet pickup so that there is less solution present to interfere with the transfer of heat, the ultimate result will be improved fabric tenacity.
- The use of microstructural analysis techniques including x-ray diffraction, SEM, density measurements and DSC can be used to confirm proposed microstructural alteration of the acetate binder fibers, including increased crystallinity, therefore an accompanying increase in fiber density, surface and internal cavitation and finally, fiber shrinkage in response to the chain relaxation and reorganization into a more perfect, crystalline arrangement. Finally, DSC measurements can allow one to get a better handle on just how effective the solvent is in the suppression of the second order glass transition temperature of the acetate binder fibers.

REFERENCES

REFERENCES

1. Wijns, P., Nonwovens for Consumer Disposables, *Nonwovens Industry*. **27(12)**, 70 (1996).

2. Franke, I.M., Approach of a Multinational Company to Assist Management of Solid Waste-A Research Program for Baby Diapers, *INDA JNR*, **3(1),** 41-43 (1991).

3. Characterization of Municipal Solid Waste in the United States. Executive Summary. Prepared for U.S. Environmental Protection Agency, Municipal and Industrial Solid Waste Division, Office of Solid Waste, The Office, Washington, D.C., 1994.

4. Cotton in Nonwovens, *Nonwovens Industry*. **27(6)**, 40,42 (1996).

5. Noonan, E., Cotton and Cost: Nonwovens Issues, *Nonwovens Industry*. **26(6)**, 61-62,64 (1995).

6. Morton, G.P., and Rearick, W.A., Bleaching Cotton for Nonwovens Utilization, *INDA JNR*. **2(1)**, 37-42 (1990).

7. Domestic Fiber Prices, *ATI*. 19 (January 1997).

8. "Nonwovens: Theory, Process, Performance, and Testing", A.F. Turbak, Ed., TAPPI, Atlanta, GA, 1993.

9. Moreau, J.P., Properties of Thermally Bonded Cotton/Polypropylene Nonwovens, *INDA JNR*. **2(2)**, 14-22 (1990).

10. Goynes, W.R., Moreau, J.P., DeLucca, A.J., and Ingber,B.F., Biodeterioration of Nonwoven Fabrics, *Textile Res. J.* **65(8)**, 489-494 (1995).

11. Suh, H., Duckett, K., and Bhat, G., Biodegradable and Tensile Properties of Cotton/Cellulose Acetate Nonwovens, *Textile Res. J.* **66(4)**, 230-237 (1996).

12. Suh, H., Preliminary Investigation of the Specific Stress Properties of Cotton/Cellulose Acetate Nonwovens Thermal Calendered with Solvent Assistance, (December 1995).

13. Suh, H., and Heismeyer, G., Optimization of Process Variables for Cotton/Cellulose Acetate Nonwovens Thermal Calendered with Solvent Assistance, (February 1996).

14. Suh, H., Solubility of Cellulose Acetate Fibers in Acetone Solution, (May 1993).

15. Reed, R.E., U.S. Patent, 2 277 049, 1942.

16. Reed, R.E., and Ryan, J.F., U.S. Patent, 2 277 050, 1942.

17. Mathews, C.K., and van Holde, K.E., "Biochemistry", Benjamin/Cummings, Redwood City, CA, 1990.

18. Kadolph, S.J., Langford, A.L., Hollen, N., and Saddler, J., "Textiles", Macmillan, NY, 1993.

19. Carter, M.E., "Essential Fiber Chemistry", Marcel Dekker, NY, 1971.

20. Peters, R.H., "Textile Chemistry: The Chemistry of Fibres", Elsevier, NY, 1963.

21. Wagner, J.R., Effect of Variables in Textile Fibers Utilized in Carded Nonwovens, in "Proc. 6th TANDEC Conference", University of Tennessee, Knoxville, TN, 1996.

22. Hoyle, A.G., Bonding as a Nonwoven Design Tool, *Tappi Journal.* 109-112 (April 1989).

23. Narayanan, V., Gosavi, N., and Duckett, K., Nonwovens Technology Primer, *Nonwovens Industry.* **25(3)**, 50,52,54-55,57-58 (1994).

24. Wagner, J.R., Problems Encountered When Carding, in "Proc. 6th TANDEC Conference", University of Tennessee, Knoxville, TN, 1996.

25. Wagner, J.R., Relative Card Settings, Speed, and Actions, in "Proc. 6th TANDEC Conference", University of Tennessee, Knoxville, TN, 1996.

26. Muller, D., Modern Carding Technology-New Developments of Cards and Carding Lines, in "Proc. 6th TANDEC Conference", University of Tennessee, Knoxville, TN, 1996.

27. Dharmadhikary, R.K., Gilmore, T.F., Davis, H.A., and Batra, S.K., Thermal Bonding of Nonwoven Fabrics, *Textile Progress.* **26(2)**, 1-39 (1995).

28. Wrotnowski, A.C., Some Properties of Thermoplastic Fiber-Bonded Fabrics, *Textile Res. J.* **22(7)**, 480-486 (1952).

29. Duckett, K., and Ranganathan, S., The Effect of Pre-Processing Treatments on the Tensile Behavior of Cotton Nonwoven Fabrics, in "Proc. 1989 TAPPI Nonwovens Conference", TAPPI Press, Atlanta, GA, 1989, pp. 165-172.

30. Duckett, K., and Baker, A.J., The Computational Characterization of Heat Transfer Behavior in Continuous Two-Roll Thermal Calendering, in "Proc. 1990 TAPPI Nonwovens Conference", TAPPI Press, Atlanta, GA, 1990, pp. 193-199.

31. Duckett, K., and Cain, J., Finite Element Methods Applied to Thermal Calendering, in "Proc. 1991 TAPPI Nonwovens Conference", TAPPI Press, Atlanta, GA, 1991, pp. 383-391.

32. Duckett, K., and Wadsworth, L.C., Tensile Properties of Cotton/Polyester Staple Fiber Nonwovens, in "Proc. 1987 TAPPI Nonwovens Conference", TAPPI Press, Atlanta, GA, 1987, 121-127.

33. Duckett, K., and Wadsworth, L.C., Physical Characterization of Thermally Point-Bonded Cotton/Polyester Nonwovens, in Proc. 1988 TAPPI Nonwovens Conference", TAPPI Press, Atlanta, GA, 1988, 99-107.

34. Weigmann, H.D., Interactions Between Fibers and Organic Solvents, in "Handbook of Fiber Science and Technology: Vol. I Chemical Processing of Fibers and Fabrics", M.Lewin and S.B. Sello, Eds., Marcel Dekker, NY, 1983, pp. 1-49.

35. Seymour, R.B., and Carraher Jr., C.E., Polymer Chemistry: An Introduction, Marcel Dekker, NY, 1988.

36. McQuarrie, D.A., and Rock, P.A., General Chemistry, W.H. Freeman, NY, 1987.

37. Smith, W.F., Principles of Materials Science and Engineering, McGraw-Hill, NY, 1990.

38. Weigmann, H.-D., Scott, M.G., Ribnick, A.S., and Rebenfeld, L., Interactions of Nonaqueous Solvents with Textile Fibers. Part VII: Dyeability of Polyester Yarns After Heat and Solvent-Induced Structural Modifications, *Textile Res. J.* **46**, 574-587 (1976).

39. Gerold, E.A., Rebenfeld, L., Scott, M.G., and Weigmann, H.-D., PET Filaments with Radially-Differentiated Structure, *Textile Res. J.* **49**, 652-661 (1979).

40 Ribnick, A.S., Weigmann, H.-D., and Rebenfeld, L., Interactions of Nonaqeuous Solvents with Textile Fibers. Part II: Isothermal Shrinkage Kinetics of a Polyester Yarn, *Textile Res. J.* **43**, 176-183 (1973).

41. Ribnick, A.S., Weigmann, H.-D., and Rebenfeld, L., Interactions of Nonaqueous Solvents with Textile Fibers. Part I: Effects of Solvents on the Mechanical Properties of a Polyester Yarn, *Textile Res. J.* **42**, 720-726 (1972).

42. Weigmann, H.-D., and Ribnick, A.S., Interactions of Nonaqueous Solvents with Textile Fibers. Part IV: Effects of Solvents on the Mechanical Properties of Various Textile Yarns, *Textile Res. J.* **44**, 165-173 (1974).

43. Merkel, R.S., Textile Product Serviceability, Macmillan, NY, 1991.

44. Annual Book of ASTM Standards, Textiles, Vol. 7.01 and 7.02, American Society for Testing and Materials , Philadelphia, PA, 1991.

45. INDA Standard Test Procedures, Association of the Nonwoven Fabrics Industry, Cary, NC.

46. Ott, R.L., An Introduction to Statistical Methods and Data Analysis, Wadsworth, Belmont, CA, 1993.

APPENDIX

APPENDIX

STATISTICAL ANALYSIS

REVIEW OF SIMPLE LINEAR REGRESSION AND CORRELATION

The performance properties of interest in this study included specific stress, elongation, flexural rigidity and air permeability to name a few. Each of these properties alone, would be considered the dependent variable, y. The variable of interest, for instance specific stress is affected by one or more additional variables and their interactions, thereof called independent variables. Independent variables can have different levels. One of the independent variables largely responsible for the resultant fabric specific stress was the web consolidation temperature, which had three levels, 150, 170 and 190°C, respectively.

The simplest type of model relating the outcome, or dependent variable **y** to a single quantitative independent variable **x** is given by the equation of a straight line [46]:

$$Y = \beta_0 + \beta_{1x}$$

where β_0 = **y-intercept (value of y when x = 0)** and β_1 =**slope of a straight line (change in y for a unit change in x)**

therefore β_0 and β_1 are considered constants.

Therefore,

$$\text{SPECIFIC STRESS} = \beta_0 + \beta_1(\text{WEB CONSOLIDATION TEMPERATURE})$$

where this deterministic model uses a straight line with slope β_1 and intercept β_0 to represent the relationship between mean specific stress and web consolidation temperature over the range from 150 to 190°C. If there exists a true linear relationship between this aspect of fabric mechanical integrity and temperature, then the constant β_1

measures the rate at which specific stress changes. The constant β_0 has questionable application since the fabric specific stress corresponding to no thermal input is 0 mN/tex. Therefore this straight line offers at best a good approximation for temperatures within the 150 to 190°C range, and may be limited at temperatures below or in excess of the two ends of the continuum [46].

This model is unrealistic in that it does not include for the possibility that the experimental observations do not lie on a straight line. That is the variation in observed specific stresses for the same web consolidation temperature , *i.e.* 150°C. Therefore a model is required that allows for this random variation [46]:

$$Y = \beta_0 + \beta_{1x} + \varepsilon$$

where ε is a random error term that represents the difference between an observation **y** and a point on the line $\beta_0 + \beta_{1x}$. The term ε is comprised of unforeseen and unknown factors not already included in the model that are responsible for the observed specific stress deviations from the predicted observation, *i.e.* 150°C. Fiber variation, web nonuniformity, inconsistent solvent penetration, test apparatus limitations and operator error effects introduced during physical testing are all examples of factors that can give rise to observations deviating from the expected value for a specific condition. The assumption exists that the random error average value for a given value of **x** is **0**.

The average expected value of **y** for a given value of **x** is given by the expression [46]:

$$E(Y) = \beta_0 + \beta_{1x}$$

As a result estimates of β_0 and β_1 are constructed and are $\hat{\beta}_0$ and $\hat{\beta}_1$ and the estimated value of **y** based on these parameters is $\hat{y}$. Therefore,

$$\hat{Y} = \hat{\beta}_0 + \hat{\beta}_{1x}$$

[46]

One way to determine the prediction equation is to plot the experimental observations on a scatter diagram and then use a straight edge to draw a straight line through the individual data points, illustrating the linear relationship between the independent variable and the response. However, given the same set of data, many different prediction equations may result [46].

LINEAR REGRESSION AND THE METHOD OF LEAST SQUARES

If $\hat{y}$ is the anticipated value of **y** for a given value of **x,** then the error of prediction called the residual is the disparity, hence the difference between the observed value of **y** and the predicted value of $\hat{y}$, $(y-\hat{y})$. The Least Squares Method chooses the prediction line $\hat{y} = \hat{\beta}_0 + \hat{\beta}_{1x}$ that minimizes the sum of the squared errors of prediction $\Sigma(y-\hat{y})^2$ for all observations. Therefore, the sum of squared errors of prediction for the linear model $y = \beta_0 + \beta_{1x} + \varepsilon$ is given by the expression [46]:

$$\Sigma (Y-\hat{Y})^2 = \Sigma (Y - \hat{\beta}_0 - \hat{\beta}_{1x})^2$$

Thus the least squares method finds those estimates $\hat{\beta}_0$ and $\hat{\beta}_1$ that minimize $\Sigma (y-\hat{y})^2$. The estimates are called least squares estimates [46].

The least squares estimate of $\hat{\beta}_1$, the slope of a straight line is defined as [46]:

$$\hat{\beta}_1 = S_{xy}/S_{xx}$$

and the estimate of β_0, the y-intercept is [46]:

$$\hat{\beta}_0 = \bar{Y} - \hat{\beta}_1 \bar{X}$$

where

$$S_{XX} = \sum(X-\bar{X})^2 = \sum X^2 - (\sum X)^2/N$$

$$S_{XY} = \sum(X-\bar{X})(Y-\bar{Y}) = \sum XY - (\sum X)(\sum Y)/N$$

The distance between an observation **y** and the sample mean $\bar{y}$ can be expressed as the sum of two components, $(\hat{y}-\bar{y})$ and $(y-\hat{y})$. The quantity $(\hat{y}-\bar{y})$ represents that portion of the distance between observation **y** and the sample mean that can be attributed to the independent variable **x**. The quantity $(y-\hat{y})$ represents that portion that cannot be attributed to the independent variable **x** and is the outcome of error.

For all sample observations, the total variability in the sample observations about the sample mean, $\sum(y-\bar{y})^2$, called the sum of squares about the mean can be expressed as the sum of squares due to regression, $\sum(\hat{y}-\bar{y})^2$, and the sum of squared errors of prediction, $\sum(y-\hat{y})^2$, called the sum of squares for error [46]. Thus,

SUM OF SQUARES ABOUT THE MEAN = SUM OF SQUARES DUE TO REGRESSION + SUM OF SQUARE FOR ERROR

And, total variability in y-values is broken into two components, that explained by the model and that variability that is unexplained [46]:

$$\sum (Y-\bar{Y})^2 = \sum (\hat{Y}-\bar{Y})^2 + \sum (Y-\hat{Y})^2$$

TOTAL VARIABILITY IN Y-VALUES = VARIABILITY EXPLAINED BY MODEL + UNEXPLAINED VARIABILITY

In the quest to ascertain a value for **y** for a given value of the independent variable **x**, the model that best "fits" the data is the one in which a larger portion of the variability is explained by the model rather than the unexplained [46].

CORRELATION

A measure of the strength of a relationship between the variable of interest **y** and one or more independent variables is expressed with a correlation coefficient, **r**. The sample correlation coefficient **r** can be calculated using the expression [46]:

$$R = S_{XY}/(S_{XX}S_{XY})^{1/2}$$

where $S_{yy} = \Sigma y^2 - (\Sigma y)^2/n$ and **r** is similar to the slope of the least squares equation [46]:

$$\hat{\beta}_1 = S_{XY}/S_{XX}$$

$$R = \hat{\beta}_1 (S_{XY}/S_{XX})^{1/2}$$

The value of **r** lies between **-1** and **+1**. When **r** exceeds **0** ($r > 0$), a positive linear relationship is indicated between **x** and **y**. That is **y** is increasing with additional unit **x** increase. When the value of **r** is negative ($r < 0$), a linear relationship between **x** and **y** that is negative is indicated. That is with each unit increase in **x** there is a corresponding diminishment in **y**. When $r = 0$, assertion can be made that the data fails to support the existence of a linear relationship between **x** and **y**. The sample correlation coefficient **r**, when raised to the second power (r^2) indicates that proportion of the total variability in the y-values that can be accounted for by the regression model, that is the independent variable, **x**. Furthermore, $1 - r^2$ represents that proportion of the total variability in the y-values that cannot be attributed to the variable x. [46].

INFERENCES RELATED TO LINEAR REGRESSION AND CORRELATION

The strength of the relationship between **x** and **y** can be deduced by the conducting a statistical test of the null hypothesis H_0: $\beta_1 = 0$ versus the alternative hypothesis H_a: $\beta_1 > 0$. Recall that β_1 is the slope of the linear equation $y_i = \beta_0 + \beta_1 x_i +$

ε_1 or the change in **y** for every unit change in the independent variable **x**. The alternative hypothesis suggesting that β_1 exceeds **0** indicates a positive linear relationship between **x** and **y**. Also recall that β_0 is the y-intercept, that is the value of **y** when **x** is **0**. The parameter β_0 has questionable practical value because the true fabric specific stress corresponding to no thermal energy or web consolidation conditions would be 0 mN/tex. Also remember that least squares estimates for β_0 and β_1 are computed as follows [46]:

$$\hat{\beta}_1 = S_{XY}/S_{XX} \text{ AND } \hat{\beta}_0 = \bar{Y} - \hat{\beta}_1\bar{X}$$

Therefore substitution of $\hat{\beta}_1$ and $\hat{\beta}_0$ for β_1 and β_0 takes place.

For any conclusions about the parameters β_0 and β_1 to be made, certain assumptions concerning the random error term must be made. The error terms associated with each independent variable, ε_1, ε_2 **n** are independent of each other. And, the error term ε for a given level of the independent variable **x** has a normal distribution with an average value of **0** and a variance σ^2_ε which is constant for all settings or levels of the independent variable **x**. These assumptions allow for the assertion that each observation or response, y_i has a normal distribution with mean $\beta_0 + \beta_1 x_i$ and constant variance σ^2_ε and that each observation of **y** are independent. Therefore the parameter estimates $\hat{\beta}_0$ and $\hat{\beta}_1$ have normal sampling distributions with means called expected values and standard errors as shown [46]:

$$\mu_{\hat{\beta}0} = \beta_0 \text{ AND } \mu_{\hat{\beta}1} = \beta_1$$

$$\sigma_{\hat{\beta}0} = \sigma_\varepsilon (\sum X^2/NS_{XX})^{1/2} \text{ AND } \sigma_{\hat{\beta}1} = \sigma_\varepsilon/(S_{XX})^{1/2}$$

Efforts to compute the standard errors for the parameter estimates $\hat{\beta}_0$ and $\hat{\beta}_1$ in linear regression are complicated by the fact that we do not know the standard deviation of the

random error terms, **εs** expressed as σ_ε. We can estimate this term by first determining the variance of the **εs** by dividing the sum of squares for error **(SSE)** by **n - 2** degrees of freedom. This variance estimate σ^2_ε is designated as s^2_ε and is given by the expression [46]:

$$s^2_\varepsilon = \sum (Y - \hat{Y})^2/N - 2 = SSE/N - 2$$

The standard deviation σ_ε is thus determined by the expression [46]:

$$s_\varepsilon = (SSE/N - 2)^{1/2}$$

The calculated s_ε can be substituted for σ_ε in the formulas for determining the estimated standard errors $\sigma_{\hat{\beta}1}$ and $\sigma_{\hat{\beta}0}$ and are given the notation $\hat{\sigma}_{\hat{\beta}1}$ and $\hat{\sigma}_{\hat{\beta}0}$. They are called standard errors for $\hat{\beta}_1$ and $\hat{\beta}_0$ [46].

Confidence intervals and statistical tests for the parameters β_1 and β_0 using the parameter estimates $\hat{\beta}_1$ and $\hat{\beta}_0$ can be constructed assuming a normal distribution for ε_I from the linear regression model. The confidence intervals $100(1 - \alpha)\%$ for $\hat{\beta}_0$ and $\hat{\beta}_1$ can be specified using the **parameter (estimate) ± t (standard error)** according to the following expressions [46]:

$$\hat{\beta}_0 \pm T_{\alpha/2} S_\varepsilon (\sum X^2/N S_{XX})^{1/2}$$

$$\hat{\beta}_1 \pm T_{\alpha/2} S_\varepsilon/(S_{XX})^{1/2}$$

statistical tests for β_0 and β_1 use a **t statistic** of the form **t = estimate/standard error** or

$$\text{TEST STATISTIC, } T = \hat{\beta}_0/ S_\varepsilon (\sum X^2/N S_{XX})^{1/2}$$

$$\hat{\beta}_1/ S_\varepsilon/ (S_{XX})^{1/2}$$

Because of the limited practicality of statistical hypothesis testing of the parameter β_0 where the null hypothesis is H_0: $\beta_0 = 0$, more importance is given to the

statistical hypothesis testing of the parameter β_1, the slope of the linear regression model. That is, $\mathbf{H_0: \beta_1 = 0}$ and alternatively, $\mathbf{H_a: \beta_1 > 0}$ or $\mathbf{H_a: \beta_1 < 0}$ or $\mathbf{H_a: \beta_1 \neq 0}$. The null hypothesis is rejected in favor of the alternative hypothesis $\mathbf{H_a}$ for a given value of α and $\mathbf{df = n - 2}$ if the value of the test statistic, **t** exceeds the **t** value for a stated level of confidence α, $\mathbf{t > t_\alpha}$, **t** is less than $\mathbf{-t_\alpha}$, $\mathbf{t < -t_\alpha}$, or the absolute value of **t** exceeds $\mathbf{t_{\alpha/2}}$, $\mathbf{|t| > t_{\alpha/2}}$ [46].

Quite obviously the increased web consolidation temperature improves the web mechanical integrity as reflected by the enhanced specific stress values. Therefore, β_1 will most certainly exceed 0 and rejection of the null hypothesis $\mathbf{H_0: \beta_1 = 0}$ in favor of the alternative hypothesis $\mathbf{H_a: \beta_1 > 0}$ is mandated. Thus it is more meaningful to construct a confidence interval for β_1, allowing one to infer that at a stated degree of confidence, the specific stress will fall within a given range per unit temperature elevation, expressed in mN/tex.

The statistical test about β_1 can be restated in terms of an **F statistic** and expressed in terms of analysis of variance. As previously stated, the sum of squares (**SS**) can be partitioned into regression and error sum of squares components (**SSREG** and **SSE**). Good model fitting is achieved when the **SSREG** is considerably larger than the **SSE**. For statistical hypothesis testing where $\mathbf{H_0: \beta_1 = 0}$ and the alternative $\mathbf{H_a: \beta_1 \neq 0}$ using the **F** test statistic based on **SSREG** and **SSE** can be computed as [46]:

$$\mathbf{F = SSREG/s^2_\varepsilon}$$

under $\mathbf{H_0}$ with $\mathbf{df_1 = 1}$ and $\mathbf{df_2 = n - 2}$. The $\mathbf{df_1 = 1}$ accounts for the inclusion of one independent variable in the model. Therefore the **F test statistic** is the ratio of the

explained variation to the unexplained variation divided by the respective **df**, degrees of freedom. Therefore a large **F** value would provide sufficient evidence or cause to reject the null hypothesis in favor of the alternative, supporting the existence of a linear relationship between **x** and **y**, and for the stated level of confidence, the value of **F** is so large, that it did not occur by chance. Truly the outcome is dependent upon the level or setting of the independent variable.

MULTIPLE REGRESSION AND THE GENERAL LINEAR MODEL

The simplest type of regression model that relates the response **y** to the independent variable **x** is given by the equation [46]:

$$Y = \beta_0 + \beta_{1X} + \varepsilon$$

Recall that the average value of ε for a given value of **x** is **0**, also called the expected value of ε, $E(\varepsilon) = 0$. Therefore this model indicates that the expected value of **y** for a given value of **x** can be described by the straight line [46]:

$$E(Y) = \beta_0 + \beta_{1X}$$

For this particular study, the fabric response was influenced by at least three different independent variables-blend ratio, solvent concentration and bonding temperature, for example. Each of these three independent variables had various settings which resulted in eighteen unique fabric combinations. Oversimplification would permit one to ascertain that the fabric mechanical integrity was positively enhanced by increased web consolidation temperature, all other process variables held constant. However it was difficult to discern any further improvements in web mechanical integrity between fabrics bonded at 170 and 190°C. This would suggest interaction between other process variables and the web consolidation temperature.

The inclusion of more than one independent variable in the regression model that relates the response **y** to these several independent variables is a direct extension of a polynomial regression model and is called the multiple regression model. The multiple regression model is written as [46]:

$$Y = \beta_0 + \beta_1 X_1 + \beta_2 X_2 + \ldots + \beta_K X_K + \varepsilon$$

Each individual term is classified by its exponents. The degree of each term is given by the sum of the exponents for the independent variables in the term. A model can be identified by the types of terms it contains. First-order models contain all possible first-degree terms in the independent variables. Second-order models contain all possible first and second-degree terms in the independent variables. Higher-order models are extensions of first and second-order models [46].

FIRST-ORDER MODEL [46]:

$$Y = \beta_0 + \beta_1 X_1 + \beta_2 X_2 + \beta_3 X_3 + \varepsilon$$

where **y** is related to three independent variables, x_1, x_2, x_3. Each independent variable appears, no cross-product terms or terms in powers of the independent variables are included.

SECOND-ORDER EQUATION [46]:

$$Y = \beta_0 + \beta_1 X_1 + \beta_2 X_2 + \beta_3 X_3 + \beta_4 X_1^2 + \beta_5 X_2^2 + \beta_6 X_3^2 + \beta_7 X_1 X_2 + \beta_8 X_1 X_3 + \beta_9 X_2 X_3 + \varepsilon$$

where **y** is related to the independent variables x_1, x_2, x_3, the independent variables raised to a power of 2, and their cross-product terms.

Again little emphasis is given to the importance of β_0 in the prediction equation, rather more is given to the other parameters, β_1, β_2, β_3 ... and are commonly called

partial slopes [46]. In simple linear regression the parameter β_1 is the slope of the regression line and represents the expected change in **y** for a unit increase in **x**. In a first-order multiple regression model, β_1 represents the expected change in **y** for a unit increase in x_1 when all other x_s are held constant. Thus the effects of the independent variables are additive. The expected change in **y** for a unit change in **x** is constant, remaining insensitive to the values of any other x_s included in the model [46].

Interaction can occur between variables, x_1 and x_2 in a manner such that the expected change in **y** for a unit change in x_1 now depends on the level of x_2 [46].

The simplest model allowing for interaction between x_1 and x_2 is [46]:

$$Y = \beta_0 + \beta_1 X_1 + \beta_2 X_2 + \beta_3 X_1 X_2 + \varepsilon$$

A single general model can be used for multiple regression models in which a response is related to a set of quantitative independent variables called the general linear model [46]:

$$Y = \beta_0 + \beta_1 X_1 + \beta_2 X_2 + \ldots \beta_K X_K + \varepsilon$$

The x_s in these multiple regression models represent independent variables, independent variables raised to powers, and cross-product terms involving the independent variables [46]:

$$Y_I = \beta_0 + \beta_1 X_{I1} + \beta_2 X_{I2} + \ldots + \beta_K X_{IK} + \varepsilon_I$$

where **i** is the number of observations, **n** and exceeds **k**, is the number of independent variables, $\mathbf{n > k}$.

The same procedure for finding the least squares estimates $\beta_0, \beta_1 \ldots \beta_k$ for the least squares prediction equation $\hat{y} = \hat{\beta}_0 + \hat{\beta}_1 x_1 + \ldots + \hat{\beta}_k x_k$ minimizes the **SSE**, that is the $\sum_i (y_i - \hat{y}_i)^2$. However the determination of the estimates for $\beta_0, \beta_1 \ldots \beta_k$ are more

painstakingly solved for using a set of simultaneous equations, called the normal equations [46]. More commonly, statistical software packages are enlisted to solve for these estimates [46].

That proportion of the response variation that can be attributed to the independent variables for the general linear model is called the **coefficient of determination**, $\mathbf{R^2}$ and is computed using the following expression [46]:

$$\mathbf{R^2_{Y.X1X2...XK} = S_{YY} - SSE/ S_{YY}}$$

where $\mathbf{0 \leq R^2 \leq 1}$. There is no general relationship between the coefficient of determination $\mathbf{R^2}$ and the squares of the individual correlation coefficients $\mathbf{r_{yxj}}$. If their is a lack of correlation among the independent variables , then [46]:

$$\mathbf{R^2 = R^2_{YX1} + R^2_{YX2} + \ldots + R^2_{YXK}}$$

However interaction amongst the independent variables makes the partition of $\mathbf{R^2}$ into the proposed contribution of each individual independent variable nearly impossible. This **collinearity** causes a overlapping contributions by the independent variables to the response variation [46]. Furthermore the **coefficient of determination**, $\mathbf{R^2}$ is generally less than the squares of the individual correlation coefficients, $\mathbf{r^2}$ [46]:

$$\mathbf{R^2_{Y.X1X2...XK} < R^2_{YX1} + R^2_{YX2} + \ldots + R^2_{YXK}}$$

VITA

Greta Marie Heismeyer was born on February 18, 1968 to her parents, Willard Waldo and Gail Marie Heismeyer in Estelline, South Dakota. The oldest of three children, Greta enjoyed the privileges and experiences of growing up on a four generation family farm. Greta raised and managed a commercial/show flock of Suffolk, Hampshire and Dorset sheep. A former South Dakota Hampshire Sheep Queen, Greta was very active in promoting the sheep and wool industry. It was her love of sheep that influenced the nature of her undergraduate and graduate studies. Greta graduated from South Dakota State University with honors, obtaining a degree in General Textiles and Clothing. When not studying, Greta was very active in activities and contests that supported the growth of the domestic sheep and wool industry. Greta also played college basketball and held acting and directing roles in college and community theatre productions. Greta came to the University of Tennessee in 1994 for the purpose of studying the fabrication and properties of nonwoven fabrics. Greta felt that wool fibers were ideal raw materials for the fabrication of nonwoven fabrics intended for garment and structural insulatory applications, battery separator materials, filtration media and surgical apparel and protective devices. She is a co-inventor on a patent with Dr.Charles Hassenboehler, *Wool in Meltblown Composites*. Greta's future plans are to become a large animal veterinarian and establish her own practice specializing in sheep reproductive management and genetic selection, improving the competitiveness of the domestic sheep and wool industry through the use of EPD's.